Designing Robust and Adaptive Investment Strategies for Dutch DSOs

Integrating Robust Decision Making and Adaptive Planning for Regional Distribution Networks

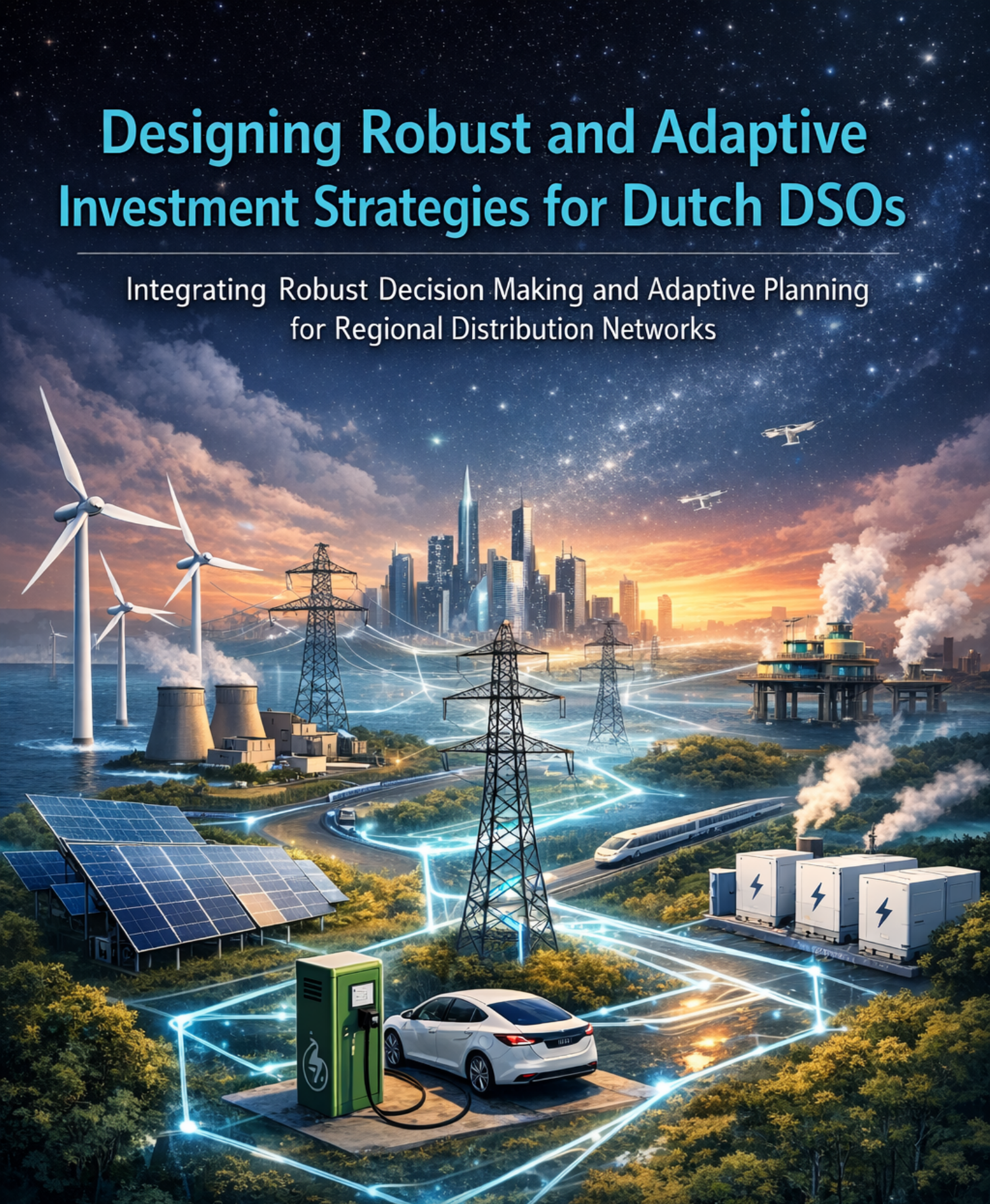

EPA2942: Master Thesis EPA

Mart Frans Christiaan Müter

Designing Robust and Adaptive Investment Strategies for Dutch DSOs

Integrating Robust Decision Making and Adaptive Planning for Regional Distribution Networks

by

Mart Frans Christiaan Müter

Master thesis submitted to Delft University of Technology in partial fulfilment of the requirements for the degree of:

Master of Science in Engineering and Policy Analysis

Faculty Technology, Policy and Management,

to be defended publicly on Monday March 23, 2026 at 15:30 PM.

The codes that have been used in this thesis are available on GitHub:
`https://github.com/MartEPA/Master-Thesis-Mart-Muter-Open`

Student number:	5035961	
MSc Programme:	Engineering & Policy Analysis	
Project duration:	September 1st, 2025 - 23th March, 2026	
Thesis committee:	Dr. ir. I. Nikolic,	TU Delft, First supervisor and Chair
	Prof. dr. ir. J.H. Kwakkel,	TU Delft, Second supervisor
	Ir. H.A.M. (Ton) Wurth,	TU Delft, External supervisor (PhD-candidate)
	Dr. ir. A.M. van Voorden,	Stedin, External supervisor

Acknowledgements

To anyone who read this thesis, have as much fun reading it as I had creating it. This thesis marks the end of my masters programme Engineering and Policy Analysis at the TU Delft. During my bachelors I enjoyed the Energy & Industry courses the most, especially the courses where modelling and programming were used to answer specific questions. During my masters, my knowledge of coding and simulation got enhanced and I got introduced to the concept of deep uncertainty. Add to that, my personality of not coping well with uncertainty and unpredictability and the choice for this thesis writes itself.

This thesis also marks the end of my time as a student. During the past seven years, I have developed both academically and personally. Studying at three different universities broadened my academic portfolio. It helped me with my internships here at Stedin as well as the Ministry of Foreign Affairs. While academic/professional accomplishments are entertaining, more important are the people that stood by me and helped me through this thesis period. I want to thank my family, friends and girlfriend for supporting and encouraging me, while also being able to take my mind of my thesis. Without all of you, I would not have been able to bring this thesis to a good conclusion.

Lastly, as demanded by the TU Delft I must incorporate an AI statement in the acknowledgements. Therefore, I have used AI tools such as Microsoft Co-Pilot to enhance and explain Python code. Furthermore, I have used it to develop LaTeX tables and sometimes for grammar and structuring sentences.

M. F. C. Müter
Delft, March 2026

Management Summary

The Dutch electricity grid is currently facing unprecedented net congestion, with a backlog of industrial connections and estimated social costs ranging from €10 to €40 billion per year. Distribution System Operators (DSOs) like Stedin must invest heavily in their infrastructure in order to mitigate net congestion. However, traditional Electricity Distribution Expansion Planning (EDEP) methods are often too deterministic and static, failing to account for deep uncertainty regarding changing energy policies, technological adaptations and different stakeholder perspectives.

This research was conducted in collaboration with Stedin, one of the largest Dutch DSOs, responsible for managing and expanding the electricity distribution network across significant parts of the Netherlands. The focus of this thesis is on Stedin's masterplan level investment planning process and its exposure to deep uncertainty. This thesis aims to bridge the gap between theory and practice by developing a Robust Decision-Making (RDM) combined with a Dynamic Adaptive Policy Pathways (DAPP) approach at a masterplan scale. A Python based object-oriented simulation model was developed to stress-test Stedin's candidate investment strategy against 10,001 plausible future scenarios generated through Latin Hypercube Sampling (LHS). The Patient Rule Induction Method (PRIM) was used to identify specific combinations of uncertainties that lead to capacity risks.

The analysis revealed that the candidate investment plan is insufficiently robust against long-term uncertainties, with some substations (i.e. facilities for voltage conversion, specifically in this study medium-voltage levels to lower-voltage distribution levels) facing capacity bottlenecks in over 80% of scenarios by 2052. Five distinct storylines were identified as primary drivers of capacity risks:

1. Medium-to-fast residential heating transition;
2. Medium-to-fast electric mobility growth;
3. Emergence of large datacenters ($>$ 30 MVA) in rural areas;
4. Residential housing expansion combined with medium-to-fast residential heating transition;
5. High electrification of industrial activities combined with medium-to-fast EV growth.

To mitigate these risks, four distinct mitigation measures were incorporated into an adaptive investment plan:

1. Reallocating industrial rings of substations S and W to substation K, which has unexploited capacity in earlier years;
2. Constructing substation H as a 21 kV substation instead of a 13 kV substation;
3. Construction of an additional 21 kV substation (Substation X) downstream, specifically triggered in scenarios with large datacenters;
4. Using diesel/gas generators as temporary measures to bridge short-term demand peaks on substation W.

By incorporating such mitigation measures, the adaptive investment plan is able to outperform the candidate investment plan in terms of robustness. Furthermore, a comparison table shows that the adaptive investment plan outperforms the worst case and candidate investment plan in balancing costs and capacity risks. Therefore management is advised to:

1. Commence construction of substation H and K immediately without delay, as the grid cannot cope with deep uncertainty without them.

2. Finalise the decision to build substation H as a 21 kV substation to ensure long-term robustness.

3. The reallocation of the industrial rings of substations S and W can significantly relieve long-term capacity bottlenecks. When the future moves towards storylines 1, 2, 4 or 5 begin to reallocate industrial rings around 2039.

4. Once the future moves towards storyline 3, begin to construct one additional substation around 2042 to relieve electricity demand on substation K.

List of Abbreviations

Abbreviation	Definition
ATP	Adaptation Tipping Point
DAPP	Dynamic Adaptive Policy Pathways
DMDU	Decision-Making under Deep Uncertainty
DSO	Distribution System Operator
EDA	Exploratory Data Analysis
EDEP	Electricity Distribution Expansion Planning
EMA	Exploratory Modelling and Analysis
EPA	Engineering and Policy Analysis
EV	Electric Vehicle
HHP	Hybrid Heat Pumps
KM	Koersvaste Middenweg
kW	Kilowatt
LHS	Latin Hypercube Sampling
MCS	Monte Carlo Sampling
MVA	Mega-Volt-Amperes
MW	Megawatt
PDF	Probability Density Function
PRIM	Patient Rule Induction Method
PV	Photovoltaic Installation
PUE	Power Usage Effectiveness
RDM	Robust Decision-Making
RES	Renewable Energy Strategy
RO	Robust Optimization
TSO	Transmission System Operator

List of Figures

1 *Capacity Map of the Dutch electricity grid (TenneT, 2025).* . . . 1
2 *Conceptual Model of Candidate Investment Plan* . . . 10
3 *Research Workflow and relationships among the sub-research questions* . . . 11
4 *Conceptual Model of Research Design* . . . 13
5 *Conceptual overview of municipal borders of this case study (a), the current catchment areas of existing substations (b), and projected catchment areas following the construction of future substations H and K (c)* . . . 20
6 *Catchment areas of different rings belonging to a substation* . . . 21
7 *XLRM Framework with additional uncertainties incorporated* . . . 24
8 *Forecast of hourly electricity demand for substation S and W* . . . 28
9 *Hourly electricity demand per ring* . . . 29
10 *Schematic simulation model layout, adjustments (yellow) no adjustments (green)* 36
11 *Demand analysis for all substations* . . . 39
12 *Demand analysis for 50 kV network* . . . 41
13 *Feature scores per substation across all simulated years* . . . 43
14 *PRIM results: (a) trade-off between coverage and density; (b) selected box 3.* . . . 45
15 *Alternative Network Configuration* . . . 49
16 *Overview of demand analysis results: (a) first simulation model, (b) second simulation model.* . . . 55
17 *Visualisation of the adaptive plan, using a DAPP MetroMap* . . . 57
A.18 *XLRM Framework adapted from (Marang, 2025)* . . . 78
C.19 *Maximum (abs) peaks per reference year of PV* . . . 83
C.20 *Consumption peaks per Energy Source* . . . 84
C.21 *Consumption peaks of Air-conditioner units (both big and small)* . . . 85
C.22 *EV Charging Demand per Ring* . . . 87
C.23 *New Building Energy mix* . . . 88
C.24 *New Industry Energy mix* . . . 89
C.25 *Greenhouse Energy Mix* . . . 90
C.26 *Solar Park Construction* . . . 91
C.27 *Shore Power connections* . . . 92
C.28 *Solar panels on large roofs (exclusively on Industrial Rings)* . . . 92
C.29 *Wind Park Generation* . . . 93
C.30 *Data Center Demand* . . . 93
C.31 *Growth of total buildings with spatial constraints* . . . 94
D.32 *Quasi UML diagram of Simulation and Adjustments made to the simulation model* 96
E.33 *Risky days per substation of 10000 simulation runs* . . . 97
F.34 *PRIM results for substation H (2052): side-by-side comparison* . . . 103
G.35 *Worst Case Investment Plan* . . . 107

List of Tables

1 *Table for source categorisation based on search query.* 5
2 *Overview of research steps necessary to answer sub-question 1* 15
3 *Overview of research steps necessary to answer sub-question 2* 17
4 *Overview of research steps necessary to answer sub-question 3* 19
5 *Input values per ring for the simulation model* 27
6 *Summary of Uncertainty Mapping for KM' Scenario* 30
7 *Example of LHS subset used as input for the simulation model* 32
8 *Summary table of risky scenarios per substation per year* ($N = 10{,}001$) 38
9 *Summary table of first simulation PRIM results* 47
10 *Categorical Adaptive Rules Implemented in Second Simulation Model* 52
11 *Changes between First and Second Simulation Model* 53
12 *Summary and Comparison table risky scenarios per substation per year* ($N = 10{,}001$) *second simulation model* 53
13 *Comparison table with multiple criteria per investment plan* 60
14 *Overview of uncertainties and scenario value meaning* 77
15 *Correspondence between simulation ring names and ring names referenced in this study* 82
16 *Total number of allowed growth of houses for one scenario* 94
17 *Coincidence counts per uncertainty value* 98
18 *Total Costs of Investment Plans* 106
19 *Decision table with multiple criteria per investment plan MCA* 108

Contents

List of Figures v

List of Tables vi

1 Introduction 1
- 1.1 Societal relevance . . . 1
- 1.2 Scientific relevance . . . 3
- 1.3 EPA perspective . . . 4

2 State of the Art 5
- 2.1 Search strategy . . . 5
- 2.2 Literature review . . . 5
  - 2.2.1 Current shortcomings in EDEP under deep uncertainty . . . 5
  - 2.2.2 Methodologies for managing deep uncertainty . . . 8
  - 2.2.3 RDM and DAPP for electricity distribution expansion planning . . . 8
- 2.3 Case Study Description . . . 9
- 2.4 Knowledge gap . . . 10
- 2.5 Main research question and sub-research questions . . . 11

3 Methods 13
- 3.1 Research Design . . . 13
- 3.2 Methods for Sub-Question 1 . . . 14
  - 3.2.1 Structuring the Problem . . . 14
- 3.3 Methods for Sub-Question 2 . . . 15
  - 3.3.1 Construction of Scenario Subset and Simulation Model . . . 15
  - 3.3.2 PRIM for Scenario Discovery . . . 16
- 3.4 Methods for Sub-Question 3 . . . 18
  - 3.4.1 Development of Adaptive Mitigation Measures . . . 18

4 Conceptualisation 20
- 4.1 Geographical Scope . . . 20
- 4.2 Long-Term Uncertainties Identification . . . 21
- 4.3 Additional Long-Term Uncertainties . . . 22
  - 4.3.1 Construction of Wind Park . . . 22
  - 4.3.2 Data Center Construction . . . 23
  - 4.3.3 Surface Constraints Uncertainties . . . 23
  - 4.3.4 XLRM Framework . . . 24

5 Data preparation 26
- 5.1 Input Parameters and Assumptions . . . 26
- 5.2 Hourly Profile Construction . . . 27
- 5.3 Construction of KM Scenario for Simulation Integration . . . 29

6 Formalisation 31
- 6.1 Generation of Scenario Subset . . . 31
- 6.2 Capacity Risks and Investment Costs Metrics . . . 32
- 6.3 Mathematical Formulations of Added Model Components . . . 33

6.3.1 Formalisation of Wind Park Component . . . 33
6.3.2 Formalisation of Datacenter Component . . . 33
6.3.3 Formalisation of Surface Constraints . . . 34
6.4 Simulation Model Components . . . 36

7 Results **38**
7.1 Exploratory Data Analysis (1st Iteration) . . . 38
7.1.1 Robustness of Candidate Investment Plan . . . 38
7.1.2 Substation Load and Capacity Analysis . . . 39
7.1.3 Substation Feature Scores . . . 42
7.2 Key Drivers of Capacity Risk (1st Iteration) . . . 44
7.2.1 General PRIM Choices and Explanations . . . 44
7.2.2 Short-Term and Long-Term Drivers of Capacity Risks . . . 45
7.2.3 Derivation of Storylines . . . 47
7.3 Construction of Robust and Adaptive Investment Plan . . . 48
7.3.1 Alternative Network Configuration . . . 48
7.3.2 Implementing Mitigation Measures . . . 49
7.3.3 Comparison of First and Second Simulation Model . . . 52
7.4 Exploratory Data Analysis (2nd Iteration) . . . 53
7.4.1 Robustness of Adaptive Investment plan . . . 53
7.4.2 Substation Load and Capacity Analysis . . . 54
7.5 Key Drivers of Capacity Risk (2nd Iteration) . . . 56
7.6 Visualisation of Adaptive Investment Pathways . . . 57
7.6.1 ATP Interpretation . . . 57
7.6.2 Pathway Structure . . . 58
7.6.3 Timing of Adaptive Measures . . . 58
7.7 Comparison of Investment Plans . . . 58
7.7.1 Worst Case Investment Plan Configuration . . . 58
7.7.2 Comparative Assessment of Investment Plans . . . 59

8 Discussion, Limitations & Recommendations **61**
8.1 Scientific Debate . . . 61
8.2 Practical Debate . . . 62
8.3 Limitations . . . 63

9 Conclusions **66**

References **68**

A Appendix Uncertainties **76**
A.1 Structuring the Decision-Making Problem . . . 77
A.2 KM' Scenario Mapping . . . 78

B Appendix Data Preparation **80**
B.1 Calculation of Input Parameters . . . 80
B.2 Construction of Hourly Electricity Profiles per Ring . . . 81

C Appendix Model Calculations and Verification **82**
C.1 Solar Profile . . . 82
C.2 Heating Transition in Existing houses . . . 83
C.3 Cooling transition existing buildings . . . 84
C.4 Electric Vehicles Charging Stations . . . 85
C.5 New buildings Energy Mix . . . 87
C.6 Industrial Expansion and Energy Mix . . . 88
C.7 Greenhouse Expansion and Energy Mix . . . 89
C.8 Solar Park Construction . . . 90
C.9 Shore Power Adoption . . . 91
C.10 Large Roof PV . . . 92
C.11 Wind Park Construction . . . 92
C.12 Data Center Construction . . . 93
C.13 Surface Constraints . . . 94

D Appendix Simulation Formalisation and Adjustments **96**

E Appendix Results **97**
E.1 Candidate Investment Plan . . . 97
E.2 Feature Scoring Unexpected Outcomes . . . 97

F Appendix PRIM Analysis **98**
F.1 Key Drivers of Capacity Risks per Substation per Year . . . 98
F.1.1 Key Drivers Substation S . . . 98
F.1.2 Key Drivers Substation W . . . 99
F.1.3 Key Drivers Substation H . . . 100
F.1.4 Key Drivers Substation K . . . 101
F.2 Deeper Understanding of PRIM Results . . . 102
F.3 Explaining Unexpected Drivers of PRIM Analysis . . . 103

G Appendix Costs of Adaptive Measures and Investment Plans **103**
G.1 Costs of Adaptive Measures . . . 103
G.2 Costs of Investment Plans . . . 104
G.3 Elaboration on Comparison of Investment Plans . . . 107
G.3.1 Worst Case Configuration . . . 107
G.3.2 Multi-Criteria Analysis Example . . . 107

H Pseudo-Code of Adaptive Measures **108**

1 Introduction

This research is carried out in collaboration with Stedin, the regional Dutch Distribution System Operator responsible for the electricity network in the study area. As part of this thesis, Stedin seeks to determine how its investment plans on a masterplan scale perform when confronted with a wide range of plausible future developments, and whether such investment plans provide sufficient network capacity under evolving conditions. The following sections introduce the broader societal and scientific background of this thesis.

1.1 Societal relevance

Electricity powers modern society. Consequently, the net production of electricity in the Netherlands has gradually increased, rising from approximately 85.000 GWh in 2000 to around 120.000 GWh in 2024 (CBS, 2025a). This growth goes hand in hand with the growth of renewable energy supply, like solar power, which has increased from 8 GWh in 2000 to 24 GWh in 2024 (CBS, 2025a). This puts significant pressure on the Dutch electricity grid in terms of congestion (Hennig, De Vries, & Tindemans, 2024). This is further underscored by the electricity capacity map produced by TenneT, see Figure *1*. It shows nearly all regions of the Netherlands in red, indicating a capacity shortage of the electricity grid and a backlog of industrial connections awaiting integration into the electricity grid.

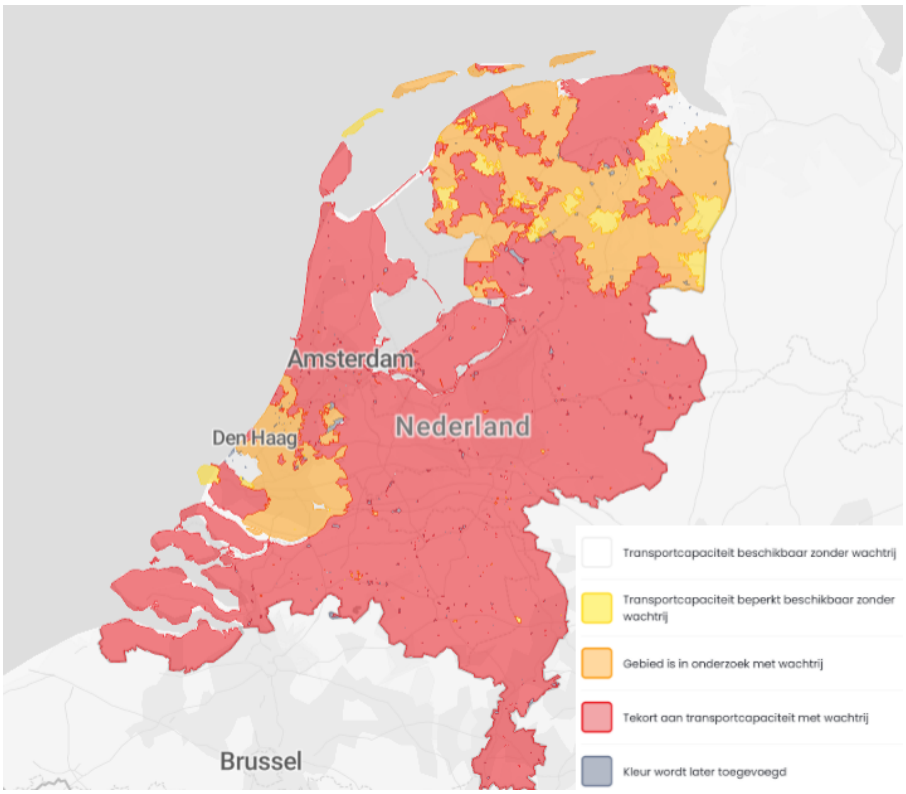

Figure 1: *Capacity Map of the Dutch electricity grid (TenneT, 2025).*

A recent interdepartmental policy research by the Dutch government stated that: "longstanding focus on electricity supply and demand often overlooked whether the grid was actually capable of accommodating such rapid growth" (Ministerie van Klimaat en Groene Groei, 2025). Partly due to this lack of focus, Distribution System Operators (DSOs) in the Netherlands are now faced with significant challenges in timely upgrading the grid infrastructure, with an estimated 200 billion euros required to address the issues of the electricity grid (PWC, 2025). When assessed over time and assuming the current net congestion levels are main-

tained, the estimated social costs range between €10 and €40 billion per year (Venema, van Swieten, van den Boogaard, Bieze, & Group, 2024). Given the long-term nature of these planning investments and the fact that the future is deeply uncertain, DSOs like Stedin must adopt a decision-making strategy that accounts for a wide range of possible and plausible futures.

The challenge of timely and cost effectively upgrading the grid under an uncertain future is a long-term infrastructure investment problem. Electricity Distribution Expansion Planning (EDEP), is the discipline that addresses such problems, and provides ways to make infrastructure investment decisions in order to meet future electricity demand (Vahidinasab et al., 2020a). However, current EDEP practice relies predominantly on deterministic, short-term planning forecasting methods that consider only a limited number of scenarios as demonstrated by (Keen et al., 2022), making it ill-equipped to handle deep uncertainty. As a result, EDEP is a planning problem under deep uncertainty. This classification is supported by both academic literature and the contents of Stedin's investment plan (Stedin, 2024). According to Marchau, Walker, Bloemen, and Popper (2019a) deep uncertainty exists when experts or parties cannot agree on:

1. *The external context of the system.*
   Stedin acknowledges, in section 8.5 (pp. 72-77), that the external context of the investments planning, like energy policies, subsidies, available space, permits and customer requests, has a significant influence on the expansion planning of the grid. It is stated that as a result of this Stedin cannot say with certainty which projects will be delayed. Thus the external context has significant influence on the EDEP of Stedin.

2. *The probabilities of future outcomes are unknown or unstable.*
   The investment plan explains, in Chapter 4 (pp. 25-30), that each scenario leads to a different energy infrastructure. Gaining insights into the effects of all transition paths is favourable to Stedin, as it shows that different "futures" can lead to different system structures. The fact that there are multiple plausible future outcomes shows that there is no consensus on a stable or known future. As a consequence, the probabilities (or probability density function) of these future energy infrastructure states are unknown.

3. *The preferences of involved actors about outcomes are unstable or ambiguous.*
   Section 9.9 of Stedin's annual report highlights the different perspectives among involved actors regarding the electricity distribution expansion planning. The influence of multiple layers of government and stakeholders with different ambitions and preferences, points to the lack of stable and unambiguous outcomes of the EDEP.

What factors and trends drive the deep uncertainty? Deep uncertainty in the planning of distribution networks is primarily driven by a complex interplay of technical and economic factors as highlighted by Ehsan and Yang (2019). Technical factors consist of the growing capacity of Photovoltaic (PV) and wind generation, load demand, rise in electric vehicle (EV) charging station demand etc. These developments introduce significant variability and unpredictability in grid operations. Moreover, economic uncertainties are cost of electricity production, electricity market prices, taxes, economic growth, energy policies etc. These factors add extra variability and uncertainty to the grid since they are influenced by highly changeable variables like human behaviour, policy interventions and market developments. Current EDEP methods, which will be discussed in more detail in Section *2.2.1*, described in literature fail to properly incorporate these long-term uncertainties into simulation models, often because of challenges associated with the acquisition of data and expert knowledge over a long-term planning horizon, solely

focusing on worst-case scenarios or fit-and-forget methods (Hemmati, Hooshmand, & Taheri, 2015; Petřík, 2024).

Consequently, the continued reliance on such traditional deterministic expansion planning approaches has contributed to the emergence of network congestion across the Dutch electricity grid. Recent cases in the Netherlands illustrate the societal consequences of the traditional paradigm, with numerous companies being unable to secure grid connections due to capacity constraints (Kieviet & Dietvorst, 2025; Roerdink, 2025). This not only disrupts business operations of those involved businesses but also poses a broader threat to national economic growth of the Netherlands (RVO, 2025). These developments underscore the urgent need to transition away from the traditional deterministic models towards planning methods for DSOs that can provide robust and adaptive investment strategies.

1.2 Scientific relevance

Current state-of-art network planning methodologies like stochastic programming and Robust Optimisation (RO) have shortcomings in terms of computational burden, a need for probability density functions and a lack of effectively incorporating active stakeholder engagement, which will be discussed in more detail in Section *2.2.1*. To illustrate these shortcomings more concretely, this section highlights two studies. First, Wurth (2022) mentions several shortcomings. Currently, the investment planning of DSOs considers too few scenarios to comprehensively encompass long-term uncertainty, limiting the insights into potential transport evolution pathways, while also focusing too heavily on the end state of scenarios rather than transient scenarios. Furthermore, DSOs use a static rather than an adaptive investment plan thinking approach and current methodologies often ineffectively deal with active multi-stakeholder engagement in the decision-making process, especially by limiting the number of scenarios that can be used in the planning process. As a result of these shortcomings, the current investment planning approach is insufficient for handling deep uncertainty of the energy system. Second, Marang (2025) used a RDM based simulation model to identify which rings beneath a substation contributed to capacity risks. The analysis demonstrated that, given the long-term uncertainties considered, the investment plan remained insufficiently robust to possible future developments in these rings. Such insights could not have been discovered using traditional network planning approaches, as these methods consider too few scenarios to expose specific combinations of long-term uncertainties that drive capacity risks.

Given that traditional EDEP methods consider too few scenarios, more suitable methods are needed. Robust Decision-Making (RDM) serves as an essential tool within the family of approaches of Decision-Making under Deep Uncertainty (DMDU), to ensure robust future investments in the electricity grid. RDM enables stress-testing of investment strategies against a variety of future scenarios to help decision makers identify and frame difficult trade-offs (Wurth, 2022). Furthermore, the investment plans must become adaptive rather than static, because the uncertainties driving capacity risks do not have to materialise all at once but can unfold gradually over time. A static investment plan, designed for a single projected future, cannot be adjusted as new information emerges or when the future deviates from the original projection. As such, the Dynamic Adaptive Policy Pathways (DAPP) is a convenient framework for designing and visualising adaptive investment plans, while accommodating handling vulnerabilities identified through RDM (Kwakkel, Haasnoot, & Walker, 2016). However, RDM is a generic method and not directly applicable to the distribution expansion planning problem of Stedin. The *Gridmaster* project represents an advancement in operationalising RDM principles into EDEP. The method was applied in the Rotterdam Harbour Cluster, where it stress-tested a candidate

network expansion plan, based on scenarios, to identify vulnerabilities. Unlike current practices, which consider four cornerstone scenarios, the Gridmaster method explored 10,000 potential scenarios to capture the deep uncertainty of the energy system evolution. Stress-testing provided detailed insights into overload developments over time. While this method proved effective for the Rotterdam Harbour Cluster, it is not yet applied to a DSO context of expansion planning in the built environment. Next to this, visualising adaptive expansion planning policies through metro-maps using DAPP has also never been done. This master thesis aims to address this gap by applying the expansion planning method developed in the Gridmaster project, to the distribution expansion planning of Stedin while also visualising a to be developed adaptive investment plan through DAPP techniques.

1.3 EPA perspective

The challenge of managing deep uncertainty in electricity grid investment planning exhibits the core characteristics of a wicked problem. It involves multiple stakeholders at various levels, including DSOs, provinces, municipalities, energy producers and regulatory bodies, each with different objectives and interests. Next to the increasing complexity of stakeholder involvement, the European Green Deal has shifted the focus of energy generation in the Netherlands towards more renewable sources, which are inherently more variable than fossil-based energy systems (Painuly & Wohlgemuth, 2020). This adds extra complexity as these renewable sources introduce additional uncertainty about the magnitude of future electricity demand and supply, further adding difficulty in reaching consensus on long-term investment decisions. Addressing such a wicked problem requires an approach that spans multiple domains, including engineering, economics, and public energy policies. This is precisely the domain of Engineering and Policy Analysis (EPA).

By integrating exploratory modelling with simulation-based scenario analysis, this research translates a complex socio-technical EDEP problem into interpretable policy narratives that support robust and adaptive investment decisions. In doing so, it exemplifies the multidisciplinary approach that EPA brings to network expansion planning challenges.

2 State of the Art

This section details the search strategy used to structure the literature review, and subsequently presents the key insights derived from this review. It also introduces the company-specific research objective by introducing the investment plans and identifies the knowledge gap that this thesis seeks to address.

2.1 Search strategy

In order to find relevant scientific literature the following search queries have been used, see table *1*. All search queries were executed by Google Scholar.

Search Query	**N**
("electricity grid" OR "energy systems") AND ("Robust Decision Making" OR "RDM") AND ("investment") AND ("Decision-Making under Deep Uncertainty" OR "DMDU") AND ("Dutch" OR "Netherlands")	56
("characteristics") AND ("deep uncertainty") AND ("network planning")	85
("Exploratory Modeling and Analysis" or "EMA") AND ("XLRM") AND ("PRIM")	26
("EMA Workbench") AND ("DAPP") OR ("RDM") AND ("Energy")	42
("RDM" OR "DMDU") AND ("distribution planning") AND ("energy")	42
("distribution network") AND ("uncertainties" OR "planning methods") AND ("stakeholder engagement") AND ("Robust optimization")	64

Table 1: *Table for source categorisation based on search query.*

Apart from the search queries, the scientific literature was narrowed down by reading papers cited by the *Gridmaster* report of my supervisor and the report of a former graduate that worked for Stedin. Moreover, I took some inspiration from the RAND organisation website, which extensively discuss RDM. Moreover, the BrightSpace page of Model-Based Decision-Making (EPA141A) was used to acquire knowledge. Furthermore, interesting articles about current practices in EDEP were provided by this thesis supervisors, their references are displayed below.

- (Vahidinasab et al., 2020a)
- (Borozan, Giannelos, & Strbac, 2021)
- (Wu et al., 2020)
- (De Lima, Lezama, Soares, Franco, & Vale, 2024)
- (Rahim & Siano, 2022)
- (Ehsan & Yang, 2019)

2.2 Literature review

The literature review is divided into three sections. First, the current shortcomings of EDEP will be discussed. Second, methodologies for managing deep uncertainty are discussed. Third, two promising approaches for EDEP will be discussed.

2.2.1 Current shortcomings in EDEP under deep uncertainty

Electricity grids and energy systems in general are complex systems, as stated by Kremers (2013), which is a label that also applies to the Dutch electricity grid. As mentioned by Kwakkel and

Haasnoot (2019) decision-making in complex systems is characterised by irreducible uncertainty, stemming from a multitude of stakeholders, inherent unpredictability of the complex system and the fact that complex systems are never fully understood. Furthermore, uncertainties have been growing over the last couple of years regarding the energy infrastructure. For example, the unbundling of the energy market has increased uncertainty due to separation of responsibilities between grid operators and generation companies. This division means that decisions made by the generation companies are not in-line with the planning efforts (including investment strategies) of TSOs and DSOs, creating extra uncertainty about how future grid expansions will match energy production (Spyrou, Hobbs, Chattopadhyay, & Mukhi, 2024).

Historically, the Dutch electricity network was centrally organised, with power flows going from electricity provider to end-user (EZK, 2023). However, currently due to growing generation of renewable energy sources like PV and wind energy, the grid now produces both centrally as well as decentrally. This introduces bidirectional power flows and enhanced peaks in both supply and demand side which, in turn, increase network congestion (Hennig, De Vries, & Tindemans, 2023). The grid was never designed for such a rapid emergence of decentralised generation. Moreover, additional sources of uncertainties, like AI-related electricity consumption, have recently emerged that were similarly unforeseen by traditional EDEP. As highlighted by Arciniegas Rueda, Gill, and van Soest (2025), planners risk significant underestimation of future electricity demand when such non-traditional, rapidly scaling demand drivers are not incorporated into EDEP. Noting this, traditional EDEP methods fall short due to a multitude of reasons.

Traditional planning methods are deterministic and static, which fail to provide robust and adaptive investment strategies over time. In a static planning approach, the input variables are assumed constant over time. Such an approach typically involves designing a plan for one or more scenarios at a single point in time. This assumption introduces two limitations: first, it fails to indicate the appropriate timing for implementing specific measures, second, the static plan does not account for changes in system configuration (Vahidinasab et al., 2020a). As a result, static planning approaches do not provide insights into how the investment plan should develop over time.

Several modelling techniques for multi-stage network planning under uncertainty have been proposed in academic literature, of which stochastic programming and Robust Optimisation are currently considered state-of-art (Borozan et al., 2021). Stochastic programming has widely been used to model uncertain parameters in network planning approaches. And while it bases its decisions on an objective function representing an expected value (like minimising cost or maximising profit), the first issue with this technique is that it comes with high computational burden which can make it unscalable for problems with large scenario sets (De Lima et al., 2024). In addition to the computational burden there is another issue with how stochastic programming models the future. A study by Wu et al. (2020) shows this by using a pre-defined, multi-stage scenario tree to represent long-term uncertainties in load demand and distributed generation. This scenario tree maps out a set of possible future paths and their corresponding probabilities. Moving through the trees goes sequentially, meaning that as the future unfolds along one specific path, other branches of the tree become irrelevant. However, by predefining the scenario tree, they assume that they already know the critical system states over time that influence transport capacity. In energy systems characterised by deep uncertainty, such critical system states over time cannot be reliably identified in advance. Instead, they can only be uncovered through exploratory modelling, in which a simulation model is run across thousands

of scenarios to map the uncertainty space and identify which combinations of conditions lead to capacity risks. Lastly, stochastic programming needs probability distribution functions (PDFs) to describe the uncertain input parameter space. While Ehsan and Yang (2019) states that it is possible to extract probability density functions based on historical data using k-means clustering algorithms, they also acknowledge that the availability of massive and precise historical data of uncertain parameters is essential for extracting the PDF. This presents a fundamental limitation, in cases where no historical data is present, constructing meaningful PDFs becomes infeasible. Knowing that the EDEP problem of this thesis suffers from deep uncertainty, where probabilities of future outcomes are inherently unknown, stochastic programming is inadequate as a method for managing deep uncertainty.

In addition to stochastic programming, Robust Optimisation has emerged as a prominent technique for addressing uncertainty in EDEP. Unlike stochastic programming, RO does not require probability density functions of input parameters, instead, it deals with uncertain parameters using bounded intervals (Vahidinasab et al., 2020a). This enables robust decisions to remain feasible for all realisations of uncertain inputs and provides solutions that remain feasible under worst-case realisations (Rahim & Siano, 2022). In many RO formulations, the uncertain parameter space is transformed to a deterministic tractable form, thereby facilitating computational efficiency. However, because RO optimises for the worst-case realisation of uncertainty, it tends to produce over-dimensioned investment plans that incur unnecessarily high costs when the worst case does not materialise (De Lima et al., 2024). Furthermore, because RO treats uncertainty as a fixed set of bounds rather than a dynamic process, it fails to capture the path dependency of evolution pathways. The omission of path dependency is especially problematic in the long-term planning contexts, such as EDEP, where uncertainty evolves over time and decisions must adapt accordingly. As a result, RO does not adequately support long-term EDEP, where the ability to adjust decisions in response to evolving and path-dependent uncertainties is essential.

In addition, both stochastic programming and RO fail to effectively incorporate multi-stakeholder engagement. In stochastic programming, too few scenarios are taken into account indicating that not all interests and objectives of important stakeholders are considered. A study by Silvestro et al. (2019) showed that current planning studies of DSOs worldwide still suffer from a lack of transparency and standards to exchange information with other stakeholders. This issue is further underscored by recent evaluations from the Dutch Authority for Consumers and Markets (ACM), which found that several DSOs, were unable to sufficiently demonstrate the traceability of their investment prioritisation (Ministerie van Klimaat en Groene Groei, 2024). Regardless of whether this reflects a managerial or a modelling issue, it highlights a fundamental requirement: planning methods must be capable of generating transparent, traceable investment decisions that can be discussed with stakeholders. Methods such as stochastic programming and RO, which either rely on too few scenarios or focus too heavily on worst-case realisations, do not produce outputs that enable meaningful stakeholder engagement. A planning approach that cannot facilitate such engagement therefore does little to improve the traceability of the investment decisions.

In conclusion, contemporary state-of-art techniques for managing uncertainty fail to tackle the challenges of the modern-day network expansion planning. Stochastic programming and RO either rely on too few scenarios or focus too heavily on the worst-case scenario. Furthermore, both methods fail to incorporate stakeholder engagement.

2.2.2 Methodologies for managing deep uncertainty

There are methods capable of addressing the inherent complexity of the grid, while also considering a wide range of plausible future scenarios and diverse objectives. While the traditional decision making models take limited consideration regarding long-term uncertainties, a study by Maier et al. (2016) proposes a more robust approach to decision-making, underscoring the need for RDM and adaptive investment strategies to manage deep uncertainty. The scientific literature on Decision Making Under Deep Uncertainty offers a range of methodologies for handling deep uncertainty. As discussed by Kwakkel et al. (2016), the combined use of RDM and DAPP can offer a promising methodological approach. RDM is a technique that considers a multiplicity of plausible futures to seek robust rather than optimal strategies (Marchau, Walker, Bloemen, & Popper, 2019b). In other words, the RDM approach seeks investment strategies that perform well over a wide range of plausible futures rather than an investment strategy that performs optimal in only one future. To do this, the RDM approach stress-tests these strategies over a myriad of plausible future policy paths (Lempert, 2019). This will provide so-called Adaptation Tipping Points (ATPs), which showcases the vulnerabilities of the investment strategy. Knowing these ATPs allows for the creation of mitigating measures, which may enhance the robustness and adaptiveness of an investment strategy.

While RDM is an appropriate method to detect vulnerabilities of a system, it does not offer a framework in which these stress-tested strategies can be visualised and serve as input for stakeholder engagement (Kwakkel et al., 2016). This gap is addressed by the DAPP approach. The DAPP methodology follows a stepwise framework that helps identify the decision context, assess vulnerabilities and opportunities, design policy pathways, and ultimately develop adaptive strategies (Haasnoot, Warren, & Kwakkel, 2019). By applying the DAPP methodology, DSOs can identify appropriate defensive or corrective actions to be incorporated in the expansion plan. Integrating the insights of both RDM and DAPP enables the development of investment strategies that are not only robust to deep uncertainty but also adaptive to future developments in the energy system.

2.2.3 RDM and DAPP for electricity distribution expansion planning

Given that RDM and DAPP provide valuable frameworks for developing investment strategies that remain effective across evolving futures, it is imperative to examine whether and how these methods have been applied within EDEP. While there is little literature on the integration of adaptive investment strategies in the Dutch electricity grid, several studies have investigated the uses of RDM and DAPP within other energy systems. For example, Jiang, Vogt-Schilb, Spyrou, and Hobbs (2025) show that, across all performance metrics to which the energy system in Bangladesh is measured, the RDM based model with adaptive investment strategies outperforms the static strategy. In addition, Aji, Goyal, Pfenninger, and Nikolic (2025) propose a DAPP approach for Indonesia's national power grid to manage deep uncertainty regarding climate change. By employing the XLRM framework to define exogenous factors and performance metrics, they demonstrate how adaptive pathways can prevent decision makers from taking future paths that lead to suboptimal outcomes. Both papers showcase that using RDM and DAPP can be effective to create robust and adaptive investment strategies.

Moreover, Wurth (2022) provides two main benefits of using RDM for EDEP. First, it supports multi-stakeholder decision making. By accommodating a large number of scenarios, RDM provides space to incorporate many different stakeholder visions about the future, ensuring that

interests and objectives of different parties are represented in the planning process. Second, exploratory modelling investigates the impact of a vast scenario space on the investment plans for grid expansion. Tools like the EMA Workbench offers a suitable and open toolkit for exploratory modelling studies (Kwakkel, 2017) & (Bartholomew & Kwakkel, 2020). The Gridmaster study demonstrates the practical applicability of RDM techniques for EDEP, specifically within the Dutch electricity grid, using the EMA Workbench to support their analysis under deep uncertainty. The Gridmaster study shows that this new approach is a promising method to investigate investment strategies for energy infrastructure expansion. One of its key conclusions is that adaptive investment strategies not only reduce the risk of stranded assets but also increases robustness against a wide future scenario space. However, applying the Gridmaster-method to a masterplan scale of a DSO has never been done. Furthermore, the combination of DAPP within a RDM-based network expansion planning method remains unexplored. In the context of energy infrastructure expansion planning, these gaps represent a window of opportunity for this research. This research aims to develop a RDM based EDEP method at a masterplan scale and develop adaptive plans to manage long-term uncertainties. Furthermore, to enhance the communicability and the practical relevance of these adaptive plans, this research integrates DAPP visualisation techniques for informed decision-making among stakeholders.

2.3 Case Study Description

This research applies a real-world case study conducted in collaboration with Stedin. Stedin seeks to determine whether its investment plan on a master-plan scale remains robust across a wide range of plausible futures. Figure *2* presents the candidate investment plan, consisting of four voltage levels connected through transformers which reduce voltages from higher to lower levels. Each transformer has a capacity expressed in MVA. Because this study assumes a power factor of 1, reactive power is not modelled, and MVA is treated as equivalent to active power (MW). The candidate investment plan consists of four substations: S, W, H and K. Substations are key points in the electricity grid where power is routed and controlled (Atwa, 2019). Substation S and W are already operational, whereas substation H and K are planned to be constructed in the near future. Substation K is planned as a 21 kV substation, providing an estimated upper transport capacity of approximately 70 MVA. In comparison, substation H operates at 13 kV voltage levels with an upper transport capacity of approximately 45 MVA.

Keeping the focus on substation H, it has a transport capacity of 2×45 MVA. However, this does not imply that 90 MVA of electricity loads can be transported. In accordance with the N-1 criterion, stating that the unexpected outage of a single system component may not result in loss of load (Ovaere & Proost, 2016), only one of the two transformers can be relied upon for secure transport of electricity loads. Consequently, the upper capacity limit of substation H is 45 MVA. This restriction does not apply to reverse power flows, like solar or wind generation, for which the full 90 MVA transport capacity can be used. This means that the lower capacity limit of substation H is -90 MVA. The same logic applies to all substations within the candidate investment plan.

To evaluate the robustness of this candidate investment plan, a simulation model is developed that reproduces the network topology and generates the electricity demand and generation profiles of substation S, W, H and K. In this context, Stedin seeks to assess whether, in light of long-term uncertainties that drive deep uncertainty, the candidate investment plan remains sufficiently robust across a wide range of plausible futures.

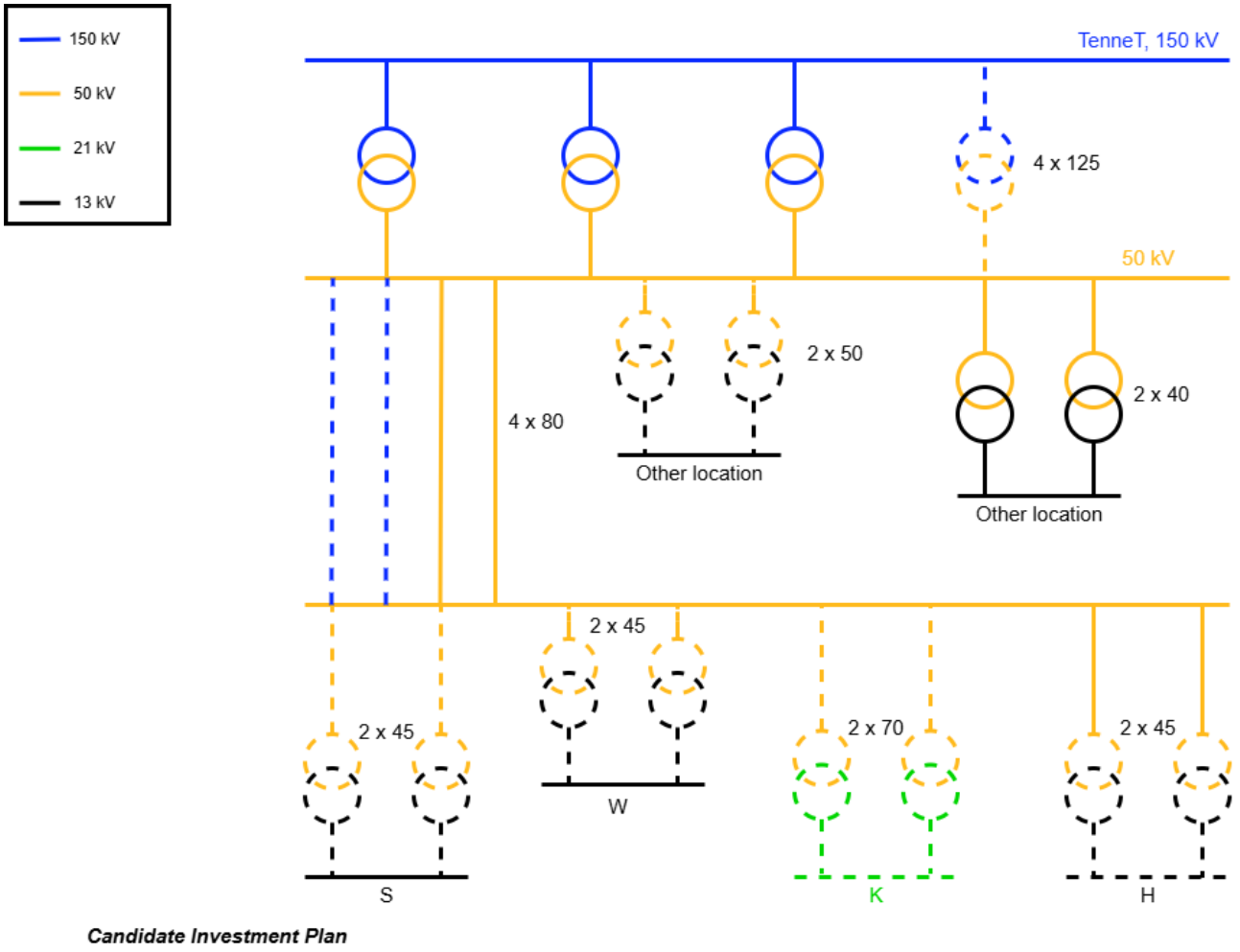

Figure 2: *Conceptual Model of Candidate Investment Plan*

2.4 Knowledge gap

This literature review provided a critical insight: traditional deterministic approaches in EDEP are inadequate for managing deep uncertainty in the energy grid. Although stochastic programming and robust optimisation offer alternatives, they remain limited: stochastic programming is data and computationally intensive and uses a limited number of prespecified scenarios, while robust optimisation produces overly conservative outcomes. In addition, this research highlights RDM and DAPP as promising methodologies to support planning under deep uncertainty. Although applied in some other contexts, these methods have not been applied for EDEP on a masterplan scale.

While an RDM based simulation model provides robust stress-testing and DAPP offers adaptive pathway visualisation, no existing study to date demonstrates how these methods can be operationalised together in an EDEP context. The simulation model is designed to simulate electricity demand and feed-in within a defined catchment area. These simulated demand and generation profiles enable the identification of capacity risks, i.e. instances where electricity demand or reverse flows exceed the capacity of substations. Furthermore, the model enables the analysis of uncertainty combinations that contribute most to capacity risks in the catchment area. This capability provides Stedin with a decision-making support tool to assess the robustness of investment strategies under multiple plausible futures, while also identifying the specific uncertainties that trigger capacity bottlenecks.

The knowledge gap therefore lies in the absence of a methodological development and empirical application of RDM and DAPP at a master-plan scale of EDEP in an unbundled energy sector. Addressing this gap is essential for DSOs like Stedin to design long-term robust and adaptive investment strategies that reduce both the risk of stranded assets and network congestion and enhances stakeholder dialogue.

2.5 Main research question and sub-research questions

To address this knowledge gap, one main research question and three sub-research questions are formulated.

Main research question:
"*What is a robust and adaptive investment strategy for electricity distribution networks on a masterplan scale?*"

Sub-questions:

1. "*What are the long-term uncertainties that influence the effectiveness of an investment strategy?*"
2. "*What are the vulnerabilities of the candidate investment plan, given the long-term uncertainties?*"
3. "*How can insights into these vulnerabilities be used to create a robust and adaptive investment strategy?*"

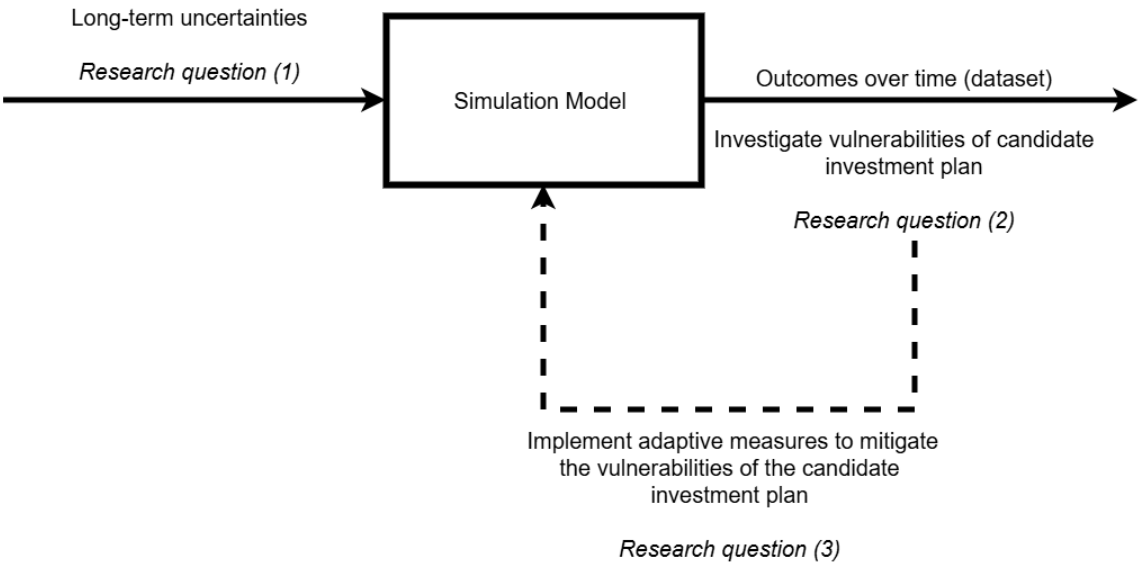

Figure 3: *Research Workflow and relationships among the sub-research questions*

Given the abstract nature of the aforementioned sub-research questions and the potentially non-obvious relations among them, the conceptualisation of Figure *3* has been developed. This conceptualisation showcases the connections between the sub-questions and provides a coherent and structured representation of the overall path of the master thesis. The research must first identify which long-term uncertainties affect the investment strategy. These uncertainties serve as input for the simulation model that will stress-test the candidate investment strategy. The output

of the simulation model will be a large dataset that can be analysed to find the vulnerabilities that have the most effect on the candidate investment plan. When the vulnerabilities are found, (adaptive) mitigation measures can be taken to handle these vulnerabilities and make the candidate investment plan more robust and adaptive.

3 Methods

This Section outlines the design of the research and methodological framework to address the main and sub-research questions. It provides a detailed description of the analytical techniques, the rationale behind the chosen methods and the sequence of steps that need to be followed in order to answer the three research questions.

3.1 Research Design

In order to get a clearer understanding of what steps were undertaken to answer the research questions, the conceptual model shown in Figure 4 has been developed. It clarifies the research steps that have been undertaken to answer each sub-question.

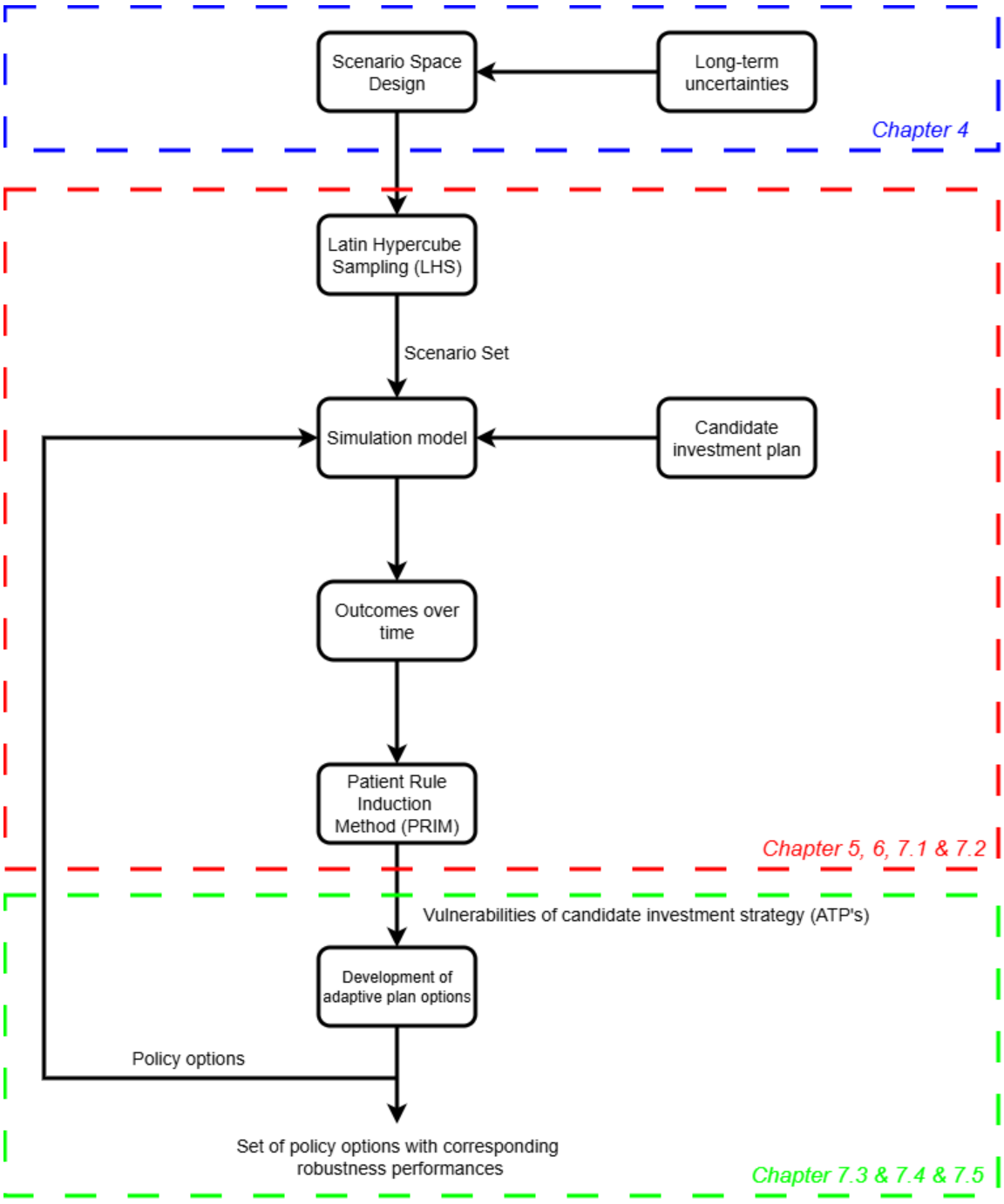

Figure 4: *Conceptual Model of Research Design*

To address the main research question and its sub-questions, this research is organised into three specific tasks. First, as shown in Figure *2*, the identification of long-term uncertainties shape the scenario space design. Based on the found scenario space, a scenario set of all the input parameters was generated using Latin Hypercube Sampling (LHS), which has been done using the EMA Workbench (Kwakkel, 2023). This scenario set captures a wide range of plausible future conditions under which the candidate investment plan is tested. Consequently, this scenario subset served as input for the simulation model.
Second, a Python based simulation model creates the demand and generation profiles impacting the energy grid on a masterplan scale. As a first step, the network configuration of the candidate investment plan was integrated into the simulation model. Hereafter, the simulation model was used to evaluate the performance of the expansion plan, using performance metrics of capacity risks and investment costs. The simulation model provided hourly electricity demand/generation per scenario per day and year. These results were analysed using the Patient Rule Induction Method (PRIM). PRIM is an algorithmic technique that identifies regions in an uncertain model input space that are highly predictive of model outcomes that are of interest (Kwakkel & Cunningham, 2016). Using PRIM enabled the identification of combinations of input variables that led to unwanted model outcomes, like high investment costs or high capacity risks.
Third, based on the vulnerabilities identified through PRIM, adaptive actions were developed to mitigate the risk of unwanted model outcomes occurring. Incorporating these adaptive measures into the candidate investment plan make an adaptive investment plan. This adaptive investment plan was incorporated into the simulation and subsequently executed. In doing so, a comparison between the candidate and adaptive investment plan could be made based on performance metrics of capacity risks and costs.

3.2 Methods for Sub-Question 1

In order to find an answer to the first sub-question: "*what are the long-term uncertainties that influence the effectiveness of an investment strategy?*" this research engaged with experts in the field, reviewed relevant academic literature and constructed an extensive XLRM diagram. Long-term uncertainties that influence energy systems are systematically outlined by Dawes et al. (2025a). The study summarises the uncertainties based on their aggregation level. There are factors that influence the system like weather, electricity prices and grid status. Next to this, there are uncertainties regarding the storage of energy, energy generation, amount of electric appliances and human behaviour. Furthermore, knowledge exchange with employees offered valuable insights into possible energy system developments affecting transport capacity demand. This research will build upon the uncertainties identified in the literature, particularly those incorporated by Marang (2025) in a previous study on EDEP within Stedin. This research adopted most of the uncertainties applied in that study, with additional uncertainties introduced to capture possible emerging factors on a masterplan scale.

3.2.1 Structuring the Problem

To structure the decision-making process under deep uncertainty, the XLRM framework was applied. The framework is widely used throughout literature to structure decision-making problems that suffer from deep uncertainty (Engholm & Kristoffersson, 2025; Groves, Molina-Perez, Bloom, & Fischbach, 2019; Vaghefi, Muccione, Van Ginkel, & Haasnoot, 2021). The XLRM framework comprises four elements:

- **Exogenous factors (X)**: are outside the control of the decision-makers. In this case study these included all identified long-term uncertainties

- **Policy levers (L)**: are instruments available to Stedin with which they can influence the system outcomes, such as relocation of rings or the construction of a new substation
- **Relationships (R)**: are the linkages between the uncertainties and policy levers, which are embedded in the simulation model to evaluate system behaviour
- **Performance metrics (M)**: are criteria by which the investment plans was evaluated. For this case study those metrics are investment costs and capacity risks. Further detail is provided in *6.2*. These metrics reflect the dual priorities of Stedin between economic efficiency and system reliability. In general, there is a trade-off between the two metrics. Investment plans that reduce capacity risks often require higher investment costs.

Once the decision-making problem was structured and the scenario set of the uncertainty space, were known, the answer to the first research question could be formulated. The table below summarises what data was needed to answer the first research question.

Method/Data Gathering	**Process with Acquired Data**	**Expected Outcome**	**Used Tools**
Expert knowledge and XLRM framework	An insightful scenario space design, with multiple long-term uncertainties, which were extensively discussed and formulated with experts of Stedin	A set of long-term uncertainties that, through stress-testing the candidate investment plan, significantly influenced the performance of the candidate investment plan	Interaction with colleagues, meetings and technical reports

Table 2: *Overview of research steps necessary to answer sub-question 1*

3.3 Methods for Sub-Question 2

In order to answer the second research question: "*what are the vulnerabilities of the candidate investment plan, given the long-term uncertainties?*" a Python based simulation model needed to be used to evaluate its performance across a range of plausible future scenarios. Some long-term uncertainties that were included in the scenario space consist of transitioning away from gas fired boilers to electric heating options, industrial electrification, share of (large) solar panels, electric mobility, wind parks and the construction of datacenters. Building upon the simulation model of a previous EDEP study by Marang (2025), this research expanded its functionality and integrated it into Stedin's internal systems. This integration offered two advantages. First, it ensured continuity beyond completion of this thesis, enabling Stedin to apply the model in future investment planning challenges. Second, it improved computational capacity by running the model on Stedin servers rather than local hardware. This integration allowed for an increased scenario testing from 1000 to 10,000 scenarios.

3.3.1 Construction of Scenario Subset and Simulation Model

The 10,000 scenarios were constructed using LHS as the sampling method, ensuring representative representation of the full uncertainty space. Further details on the generation of this scenario

set is provided in Section *6.1*. This LHS subset of the scenario space served as input for the simulation model. The model simulated for each scenario the hourly demand and generation profiles for the years 2025 to 2052 with intervals of three years. The simulation model used an objected-oriented structure to define certain critical entities in the energy system, such as substations or associated distribution rings. This approach enabled the creation of hierarchical relationships, where objects inherit attributes and behaviours from parent classes. Such an object-oriented structure in simulation modelling is an especially suitable modelling choice when modelling complex systems with multiple interacting components (Kruglov & Brodsky, 2021). An alternative approach, a multi-model approach, was also considered. While such a modelling approach offers benefits such as mitigating model bias and supporting DMDU, it presents challenges related to scalability and opaqueness to external stakeholders (Nikolic et al., 2019). Consequently, this research adopted an object-oriented structure as it facilitates code reusability, scalability and simplicity (Parmar & Parmar, 2024).

3.3.2 PRIM for Scenario Discovery

Once the simulation modelling choice and long-term uncertainties were known, it was essential to find the vulnerabilities (ATPs) of the candidate investment plan. These vulnerabilities represent conditions under which the current status quo starts to perform unacceptably (Kwakkel et al., 2016). In this research a binary classification was used where a scenario is either deemed risky or non-risky based on exceeding capacity thresholds, more on that can be found in Section *6.2*. Analytical methods such as PRIM or CART help find the scenario space in which these vulnerabilities started to exhibit themselves (Kwakkel, 2018). Both algorithms are widely used for identifying binary classifications in scenario discovery. PRIM was preferred over CART because the improved objective functions proposed by Kwakkel and Jaxa-Rozen (2015) make PRIM more effective when dealing with cases that contain integer, continuous and categorical uncertain factors. Given that the uncertainty space in this thesis is categorically structured, this improved PRIM formulation was better suited than CART. Furthermore, CART can produce too many boxes for an analyst to interpret decreasing the usefulness of CART. A second reason for preferring PRIM over CART is based on the random boxes extension proposed by Kwakkel and Cunningham (2016). This approach integrated CART principles, like random feature selection, into PRIM. In doing so, it enhances the interpretability by deciding to drop unimportant uncertainties based on feature scores. Given the emphasis on interpretability for external stakeholders in this thesis, PRIM was preferred over CART.

The execution of the simulation model provided a large CSV file with hourly demand and generation profiles of both substations and rings with corresponding risky days (i.e. days on which available capacity is insufficient to supply all demand or reverse power flows). Subsequently, the PRIM algorithm found combinations of uncertainties that showed the vulnerabilities of the candidate investment plan. It provided the answer to the second research question.

Method/Data Gathering	Process with Acquired Data	Expected Outcome	Used Tools
Use of internal Stedin data and external data sources for simulation model setup	Used internal Stedin data on the electricity grid (like hourly profiles or capacities of substations). External data also provided input parameters such as number of houses or EVs	A simulation setup with input parameters closely matching real-world values	Excel, Python and meetings with colleagues
Integrated the simulation model of a previous EDEP study internally in Stedin's modelling environment and added additional uncertainties to the model	The integration of the simulation model internally at Stedin required substantial code restructuring. Additional long-term uncertainties were added to the simulation model	A workable and appropriate simulation model that could be used to generate the hourly profiles	Python and meetings with colleagues
Creation of LHS scenario subset for model execution	Generated an LHS scenario subset that uniformly sampled the uncertainty space and served as input for 10,000 simulation runs	A representative scenario sample that enabled stress-testing of the candidate investment plan	EMA Workbench specifically `LHSSampler()`
Analysed the model outcomes of each scenario using PRIM	Conducted PRIM on the binary model outcomes, PRIM generated a peeling trajectory, after which boxes were selected based on coverage and density. For each substation, the most informative boxes were selected. PRIM identified combinations of uncertainties were the candidate investment plan was vulnerable	A set of high density and high coverage boxes describing combinations of uncertainties that produced risky scenarios. Such key drivers of capacity bottlenecks served as input for the derivation of storylines	EMA Workbench specifically PRIM
Derivation of storylines by combining the insights of the PRIM analysis	Grouped the key drivers of capacity bottlenecks into thematic clusters and translated these into interpretable storylines	Storylines that help stakeholders understand when and why the candidate investment plan becomes vulnerable	PRIM results

Table 3: *Overview of research steps necessary to answer sub-question 2*

3.4 Methods for Sub-Question 3

In order to answer the last sub-question: "*how can insights into these vulnerabilities be used to create a robust and adaptive investment strategy?*" the identified vulnerabilities had to be translated into storylines. These storylines consist of so-called *storyline drivers*. These are underlying factors that explain why the energy grid fails under certain conditions and also points towards potential mitigation measures. Based on these storyline drivers, a set of adaptive measures was formulated and implemented in scenarios that evolved towards futures characterised by emerging capacity bottlenecks.

3.4.1 Development of Adaptive Mitigation Measures

Next, these insights were used to construct alternative network configurations for the candidate investment plan. By identifying where and what types of bottlenecks presented itself in the candidate investment plan, additional model components were added. Two alternative configurations to the candidate investment plan were made. The worst case investment plan comprises network configurations in which all future scenarios were captured. In contrast, the adaptive investment plan only added certain model components if the scenario demanded it. Added network components ranged from adding additional upstream transformers to constructing an additional substation downstream. The enhanced network configuration of the adaptive investment plan was then integrated into a second simulation model. Using the same subset of 10,001 scenarios (one scenario was added in *5.3*), the second simulation model was executed and analysed using PRIM to identify remaining vulnerabilities of the alternative network configurations. The worst case network configuration was not stress-tested due to time constraints. Nevertheless, given the extent of the reinforcement implemented, it is reasonably expected to remain robust under the examined scenario subset.

Finally, the timing of the adaptive measures was operationalised through the development of a MetroMap. This visualisation technique supported the determination of when adaptive measures should be activated as the future unfolds, which is in line with the DAPP approach (Lawrence et al., 2019). DAPP structures around ATPs, which specify the conditions under which a given plan ceases to meet wanted model outcomes. By mapping the ATPs onto different policy pathways over time, the MetroMap was able to outline the sequence and timing of actions that Stedin should follow under future conditions.

Method/Data Gathering	Process with Acquired Data	Expected Outcome	Used Tools
The derived storylines were used to create adaptive measures	Adaptive measures were formulated and implemented only in scenarios that moved towards futures characterised by capacity bottlenecks	A set if adaptive measures designed to enhance the robustness of the candidate investment plan	Translation of storyline drivers into Python code
Different investment plan network configurations were mapped out	By identifying where the main bottlenecks resided in the grid, alternative network configurations were constructed, such as adding upstream transformers or additional downstream substations to the candidate investment plan	A set of investment plans that were more expensive but also more robust against a wide range of futures	Meetings with colleagues responsible for masterplan developments
Incorporated the more robust network configurations and adaptive measures in a second simulation model and executed the model using the same LHS scenario subset	The updated simulation model was run across all 10,000 scenarios, after which outcomes were analysed using PRIM to identify remaining sources of vulnerability	A more robust and adaptive investment plan	Python, EMA Workbench specifically PRIM
Developed a MetroMap	The MetroMap was used to determine when adaptive measures should be activated as future conditions unfold	A policy pathway map outlining the sequence and timing of adaptive measures for Stedin	Consultations with supervisor

Table 4: *Overview of research steps necessary to answer sub-question 3*

4 Conceptualisation

This Section focuses on defining the system boundaries and identifying the long-term uncertainties that may influence hourly electricity demand and generation within the catchment area. To achieve this, a conceptual model was developed to represent the geographical scope and some underlying assumptions of this case study. Because the geographical scope of this study contains sensitive information, all reference identifiers and URL-links have been anonymised.

4.1 Geographical Scope

The candidate investment plan belongs to a region in the Netherlands comprising of two municipalities, hereafter referred to as H and Z. Figure *5a* conceptually shows the municipal borders of this case study. Moreover, Figure *5b* presents the current catchment areas of each substation as indicated by the red and blue surfaces. A catchment area refers to the geographical region supplied by a substation. Currently, the region is served by two substations referred to as substation S and substation W. Substation W provides electricity to both municipalities H as Z, whereas substation S exclusively serves municipality Z. According to the candidate investment plan, two additional substations will be constructed to accommodate anticipated growth of hourly electricity demand and generation in the region. Figure *5c* conceptually shows the projected catchment areas following the construction of the two new substations H and K. In the projected version municipality Z will be served by three substations S, W, and K, while municipality H will be supplied solely by substation H. In doing so, the candidate investment plan aims to enhance regional capacity and ensure reliable service under increasing electricity demand and generation in the region.

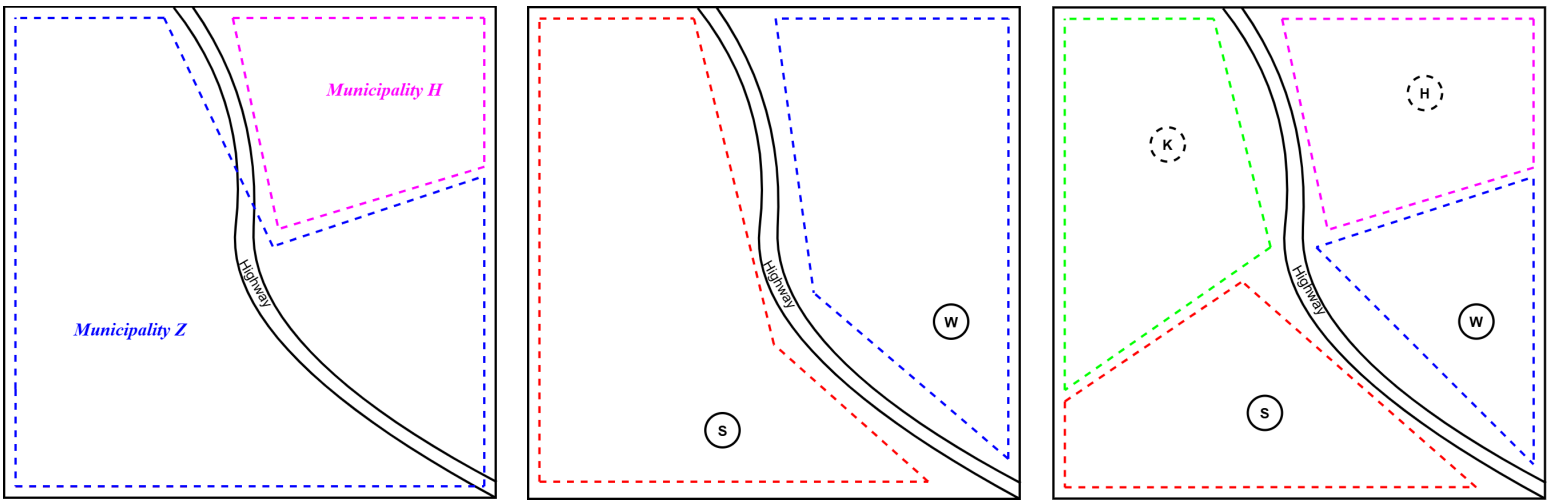

(a) *Municipal borders* **(b)** *Current catchment areas* **(c)** *Projected catchment areas*

Figure 5: *Conceptual overview of municipal borders of this case study (a), the current catchment areas of existing substations (b), and projected catchment areas following the construction of future substations H and K (c)*

Beyond the substation catchment areas, this case study identifies six distribution rings situated downstream of the substations. These rings represent network segments that can be reassigned between substations to ensure balanced load distribution. Common practice of Stedin is to assign these rings to substations that are geographically closest to them. When looking at Figure *6*, we see six rings that can be distinguished each assigned to a substation. These rings are carefully constructed using data of distribution houses internal Stedin data. The rings make up a substation, in other words the sum of the total demand per ring is the total electricity

demand of that substation. Currently, Ring I, II and III link to substation S, whereas substation W consists of Rings IV, V and VI. On average, it takes about seven years (including possible delays) to create new substations. This means that the substations K and H will be fully operational around the year 2032. After the year 2032 these substations can take over rings that are currently under the substations S and W. To make clear where those rings reside and how they look like the following conceptualisation was made:

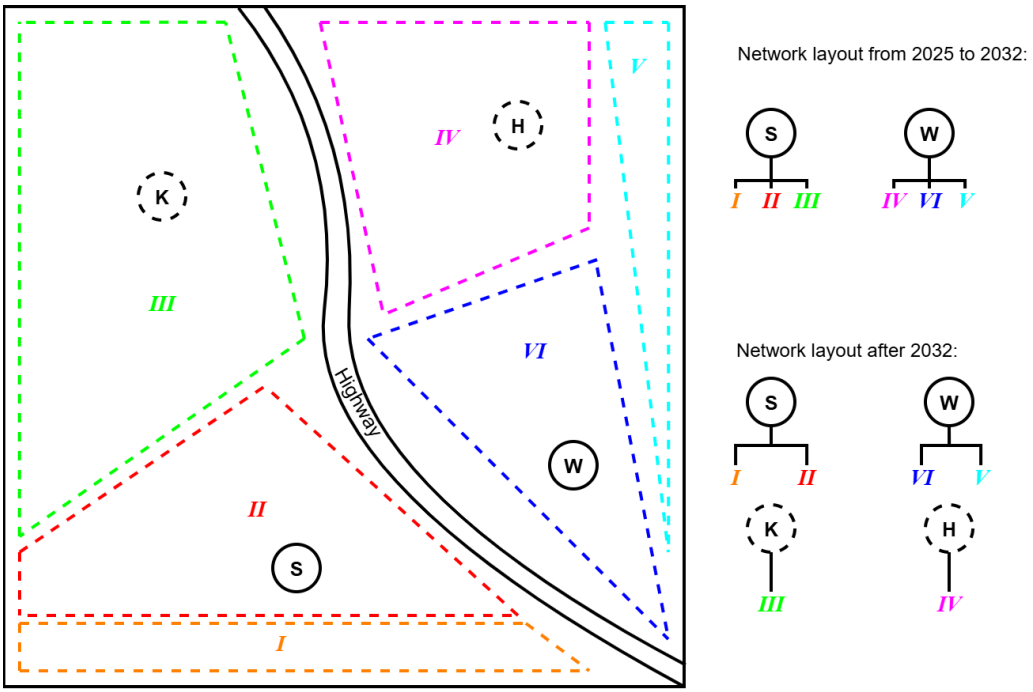

Figure 6: *Catchment areas of different rings belonging to a substation*

As illustrated in Figure *6*, the highway functions as a natural division line between the two catchment areas. While it is technically feasible to install electricity cables across the highway, this option is generally avoided by Stedin due to high costs. Nevertheless, if anticipated gains in system robustness justify the additional costs of reallocating the ring across the highway, such actions may be justifiable. However, for the first iteration of the simulation model, the highway functions as a natural division line for the electricity distribution rings. Consequently, substation S takes over Ring I and II, substation K takes over Ring III when constructed, substation H takes over IV when constructed and substation W takes over Ring V and VI. Following this reallocation, the existing substations will be left with fewer rings and thus fewer hourly demand and generation, decreasing the risk of capacity bottlenecks. The schematic network layout of the rings and substations through the simulated years is provided on the right side of Figure *6*.

The composition of each ring varies significantly. Rings II, IV and VI are predominantly residential rings, as they consist largely of residential houses. Rings I and V are primarily industrial rings, encompassing all industrial activity of both municipalities. Ring III differs from the other rings, as it is largely rural area with a limited number of residential houses. Notably, Ring III is the only ring that houses greenhouse facilities. A detailed numerical breakdown of the ring compositions is provided in Section *5.1*.

4.2 Long-Term Uncertainties Identification

The geographical scope of this case study differs from that of Marang (2025), which examined a single substation and its associated rings. In contrast, this research encompasses multiple

substations and therefore a wider spatial area. Nonetheless, several of the uncertainties identified in the single substation case study remain applicable to this case study. In short, long-term uncertainties regarding residential heating transitions, cooling demand, PV adaptation, EV charging points, behavioural charging patterns, new building development, electrification of greenhouses and horticulture, electrification of industrial activities, solar park expansion and shore power developments shape future electricity demand and generation profiles. Following consultations with Stedin experts and the thesis supervisors, it was concluded that these long-term uncertainties identified by Marang (2025) could be retained and applied to the context of this case study.

In addition, the categorical built-up of the uncertainties (A, B, C) are also adopted in this research. Such a built-up can generally be regarded as fast, medium and slow trajectories over time. For example, the lifespan of a hybrid heat pump can be ten years (A), fifteen years (B) or twenty years (C). Next to this, uncertainties can also have different growth values per year. For instance, EV growth can be 30% in 2028 to 99% in 2052 (A), 20% in 2028 to 75% in 2052 (B), and lastly 10% in 2028 to 50% in 2052 (C). For a detailed description of all categorical uncertainty values, see *Appendix Uncertainties*. The uncertainty parameter values adopted from earlier modelling work were systematically reviewed and validated (see *Uncertainty_space_for_scenario_creation.csv*). Where necessary, adjustments were made to align these parameters with real-world expectations and to improve reliability of the model outcomes.

4.3 Additional Long-Term Uncertainties

Three additional categories of uncertainties are added to the uncertainty space and will be conceptually discussed in the following sections. Furthermore, these new long-term uncertainties exclusively impact Ring III, as this ring offers the greatest available surface for facilitating such future developments.

4.3.1 Construction of Wind Park

The municipality of Z, where substation S, W and K are situated, has sufficient suitable land available for the construction of a wind park. The construction of a wind park is not a novel concept, an earlier proposal from 2016 envisioned the installation of 10 to 15 wind turbines in the region (R News, 2021). This plan was put on hold because of fierce resistance by the local populace. However, it remains plausible that it could be revived, as public attitude towards wind energy may have evolved over the past decade. Moreover, as indicated by the Regional Energy Strategy (RES) of the municipality, it is evident that the plan expresses an intention to invest in renewable energy projects and to identify suitable locations for the implementation of renewables such as solar parks or wind turbines (Gemeente, 2024). The terrain where these projects are intended have already been purchased by the municipality (Gemeente, 2023). Consequently, the potential construction of wind turbines on Ring III represents a plausible future development. Therefore, this uncertainty should be considered when simulating the electricity distribution network. The scenario dependent growth parameters vary across categorical uncertainty values. For uncertainty value A, the installed capacity increases by 100% per year until reaching a fivefold expansion by 2052 (500%). For uncertainty value B, per year growth is set at 50% until it reaches a threefold expansion (300%) by 2052. Under uncertainty value C, growth proceeds until it reaches 150% of initial size in 2052.

4.3.2 Data Center Construction

Global datacenter market demand is growing rapidly, with reported annual growth rates ranging from 10% to over 20%. This increase is primarily driven by the increasing migration of in-house data processing to centralised infrastructures ("the cloud"), which promote economies of scale and operational efficiency (Stratix, 2020). A significant additional factor is the exponential increase in demand for computing power from AI-related services. This phenomenon is initiating large-scale projects, such as the European stimulation of "AI factories", where the expected infrastructure requirements will substantially increase the need for cooling and electricity (Dialogic, 2025). The Province, to which the municipalities belong, has a policy that excludes hyperscale datacenters but anticipates growth in the mid-sized datacenter market in the region. This datacenter sector has a significant impact on grid operations, as datacenters are major consumers of electricity (Dialogic, 2025). This puts pressure on the electricity grid and can hinder economic growth due to grid congestion (Stratix, 2022). Moreover, according to Netbeheer Nederland (2025c), the Dutch DSOs and TSOs anticipate a significant increase in electricity demand from datacenters. Projections indicate that the electricity demand of datacenters increases more than fivefold, reaching 55 TWh in 2050, thereby imposing significant additional pressure on the electricity grid. Given that Ring III offers substantial available surface area and access to cooling water, the possible construction of a datacenters happens on this Ring. Therefore, this uncertainty should be taken into account when planning for the future in the region. With uncertainty growth parameters ranging from $1\frac{1}{2}$ (C) to 5 (A) times the initial size of the datacenter.

4.3.3 Surface Constraints Uncertainties

In addition to uncertainties that directly influence hourly demand profiles, this study incorporates two uncertainties related to spatial constraints within the simulation model. Without such constraints, the model could theoretically allocate multiple model components, such as wind parks or datacenters, to the same square meter, resulting in unrealistic hourly electricity demand and generation profiles. The maximum share of land available for new developments is set at 75% of total undeveloped surface area in a ring (uncertainty value A), while the lower bound is set at 25% of available land (uncertainty value C). Introducing these surface constraints ensures a more realistic simulation model by limiting growth based on available surface area of a Ring. Simulating spatial constraints this way reflects real-world planning considerations, as land-use competition between renewable energy infrastructure and other sectors (e.g., agriculture, industry) is a well-documented challenge in regional energy strategies (Koelman, Hartmann, & Spit, 2025).

Each categorical spatial uncertainty variable (A, B or C) reflects a plausible future policy focus. Uncertainty value A assumes a combined focus of renewable energy technologies and the development of a datacenter, consistent with the Paris Climate Agreement targets and their influence on Dutch climate policy (Ministerie van Algemene Zaken, 2025), as well as ongoing public debates about datacenter placements (AD, 2025b; NOS, 2025). Uncertainty value B addresses the dire housing shortage in the Netherlands, currently estimated at 396,000 houses, which was top priority in the Dutch elections of 2025 (Universiteit Leiden, 2025). Finally, uncertainty value C, considers an increased focus on greenhouse horticulture and industrial growth, motivated by historical lessons of food shortages during the World War I (Hellema, 2012) and the subsequent creation of a new agricultural province (Canon van Nederland, n.d.).

4.3.4 XLRM Framework

The additional uncertainties have been incorporated into an XLRM framework, as illustrated in Figure 7. The structural basis for this XLRM builds on earlier work from (Marang, 2025), which is included in Appendix *A.1* for transparency.

Both the construction of a solar parks and wind parks can exhibit a negative relationship with capacity risks when their generation reduces net demand at substation level. However, when combined outputs become sufficiently high, these same sources can induce reverse power flows that increases capacity risks. Consequently, their relationship to capacity risks is conceptualised with a solid orange arrow. Additionally, surface constraints have a moderating effect on all uncertainties associated with growth potential. In other words, this means that the extent to which some uncertainties can amplify capacity risks may be limited by spatial constraints, thereby tempering their overall impact in terms of capacity risks.
Two additional policy levers were identified. The first concerns the design choice of substation H: constructing it as a 21 kV rather than a 13 kV substation. In doing so, the operational range goes from 45 MVA to 70 MVA, and allows for reverse power flows a range from -90 MVA to -140 MVA, thereby reducing capacity risks. The second additional lever involves the employment of diesel and gas generators. Although these measures are temporary, they can effectively relieve substations during periods of peak electricity demand.

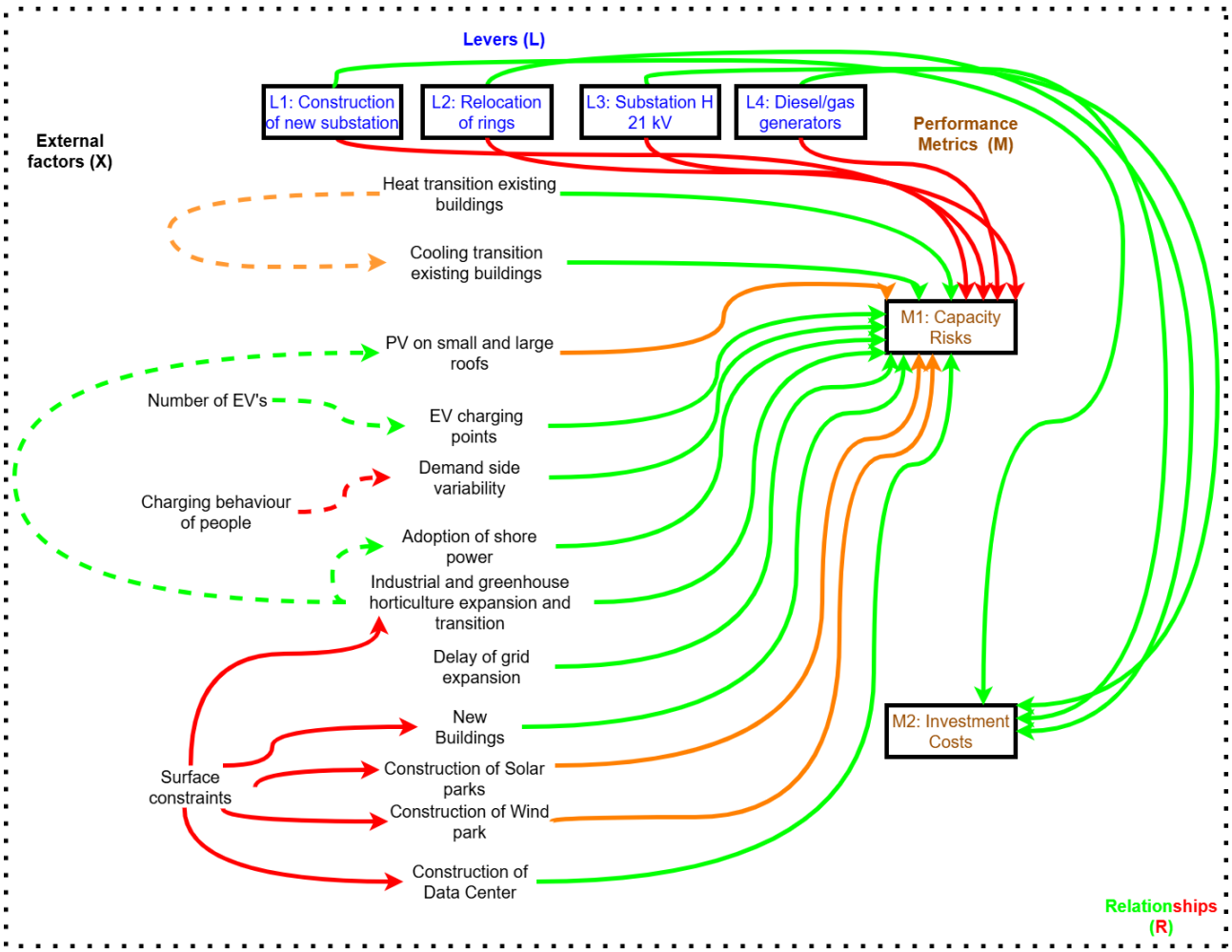

Figure 7: *XLRM Framework with additional uncertainties incorporated*

The answer to the first research question: *"What are the long-term uncertainties that influence the effectiveness of an investment strategy?"* can be answered using the knowledge from this Section. Both Figure 7 and Appendix *A* describe in detail which long-term uncertainties influence the effectiveness of an investment strategy. Sixteen categories of uncertainties influence electricity demand and generation profiles over time. In short, the following uncertainties are included: electric heating options, electric mobility, electrification of greenhouses and industry, solar and wind parks, datacenter demand and surface allocation for expansion. The latter has, as can be seen in the XLRM of Figure 7 an moderating effect on all model components with growth potential. Together, these long-term uncertainties form a vast uncertainty space that serves as input for the simulation model.

5 Data preparation

Prior to assessing the influence of long-term uncertainties on the simulation model outputs, it is essential to establish the input parameter settings and baseline hourly electricity demand. Both serve as the foundation for constructing the hourly demand and generation patterns for each substation.

5.1 Input Parameters and Assumptions

The class Ring of the simulation model takes fifteen input arguments during initialisation. Each instance of the Ring class represents a substation unit name and is characterised by attributes such as power demand, housing composition, solar adoption, vehicle count, heating technologies, cooling systems, industrial activity, greenhouse presence, shore power usage, and available surface area. The representation of the Ring class in Python is displayed here below.

Initialisation logic for Ring class

```
class Ring:
    def __init__(self, name, power_demand, num_houses, solar_houses,
                 vehicles, gas, HHP, eHP, heat_network, airco,
                 cooling, industry, greenhouses, shore_power,
                 available_surface):
                 .......
                 .......
```

The simulation model comprises six rings spread across two municipalities. Each ring therefore has a unique configuration of input data to ensure accurate model outputs for the masterplan scale. Every ring has an attribute name with a certain power_demand, this attribute will be described in Section 5.2. The input parameters for the remaining attributes of each ring are derived using a combination of municipal statistics, internal datasets and documented assumptions regarding housing, heating technologies, mobility, industrial activity, and available surface area. A detailed account of the underlying calculations, data sources and allocations of parameter values is provided in Appendix *B.1.* Table *5* summarises the input parameter values used in the simulation model.

Input Variables	Ring I	Ring II	Ring III	Ring IV	Ring V	Ring VI
num_houses[1,2] [#]	0	10416	1722	12844	0	10416
solar_houses [#]	0	3646	603	4495	0	3646
vehicles [#]	2370	9305	1838	15691	1258	11144
gas[3] [#]	0	8677	1435	11367	0	9218
HHP [#]	0	1255	207	1066	0	865
eHP [#]	0	446	74	378	0	307
heat_network [#]	0	38	6	33	0	26
airco [#]	0	75	10	206	0	206
cooling [#]	0	2406	398	2967	0	2406
industry[4] [#]	625	0	0	0	387	0
greenhouses[5] [m^2]	0	0	55700	0	0	0
shore_power [#]	1	0	0	0	1	0
available_surface [ha]	3.5	25	875	83	7.5	15

[1] Data from (AlleCijfers.nl, 2025c) for Ring III.
[2] Data from (CBS, 2024a) for the remaining rings.
[3] Data from (CBS, 2021) 83.3 % (municipality Z) to 88.5% (municipality H) of houses have gas fired boilers.
[4] Data from (AlleCijfers.nl, 2025a) & (AlleCijfers.nl, 2025b)
[5] Data from (CBS, 2024b)

Table 5: *Input values per ring for the simulation model*

5.2 Hourly Profile Construction

Apart from the input parameters, the simulation model utilises internal hourly electricity demand data from Stedin. The utilisation of this data serves two purposes. First, it establishes a clear baseline electricity load against which the simulated hourly load can be compared to. Second, it enhances the interpretability and traceability of the model outputs, which are important prerequisites for fostering stakeholder trust in the simulation model. The code behind the construction of the baseline profiles can be found in *Exploratory Data Analysis.ipynb*.

The hourly load of substations S and W, based on internal data, yielded the following hourly electricity demand and generation profiles for the period 2025-2052 of the KM scenario (see Figure *8*). The simulation model will replicate such hourly demand/generation values of 2025 to 2052 per substation for 10,000 scenarios. Each substation operates within upper and lower capacity limits. When the hourly electricity demand exceeds the upper or lower limit, the substation experiences capacity bottlenecks. For substation S and W, the upper limit is 45 MVA, while the lower limit corresponds to twice that value (90 MVA) due to the redundancy as represented by the red horizontal line. Figure *8* shows that both substations encounter capacity bottlenecks prior to 2032, underscoring the necessity for infrastructure expansion and improved uncertainty management by Stedin. Based on this forecast, a slice of the first 8760 values (representing all hours of 2025) were extracted to construct the initial hourly electricity demand patterns for substations S and W in the simulation model.

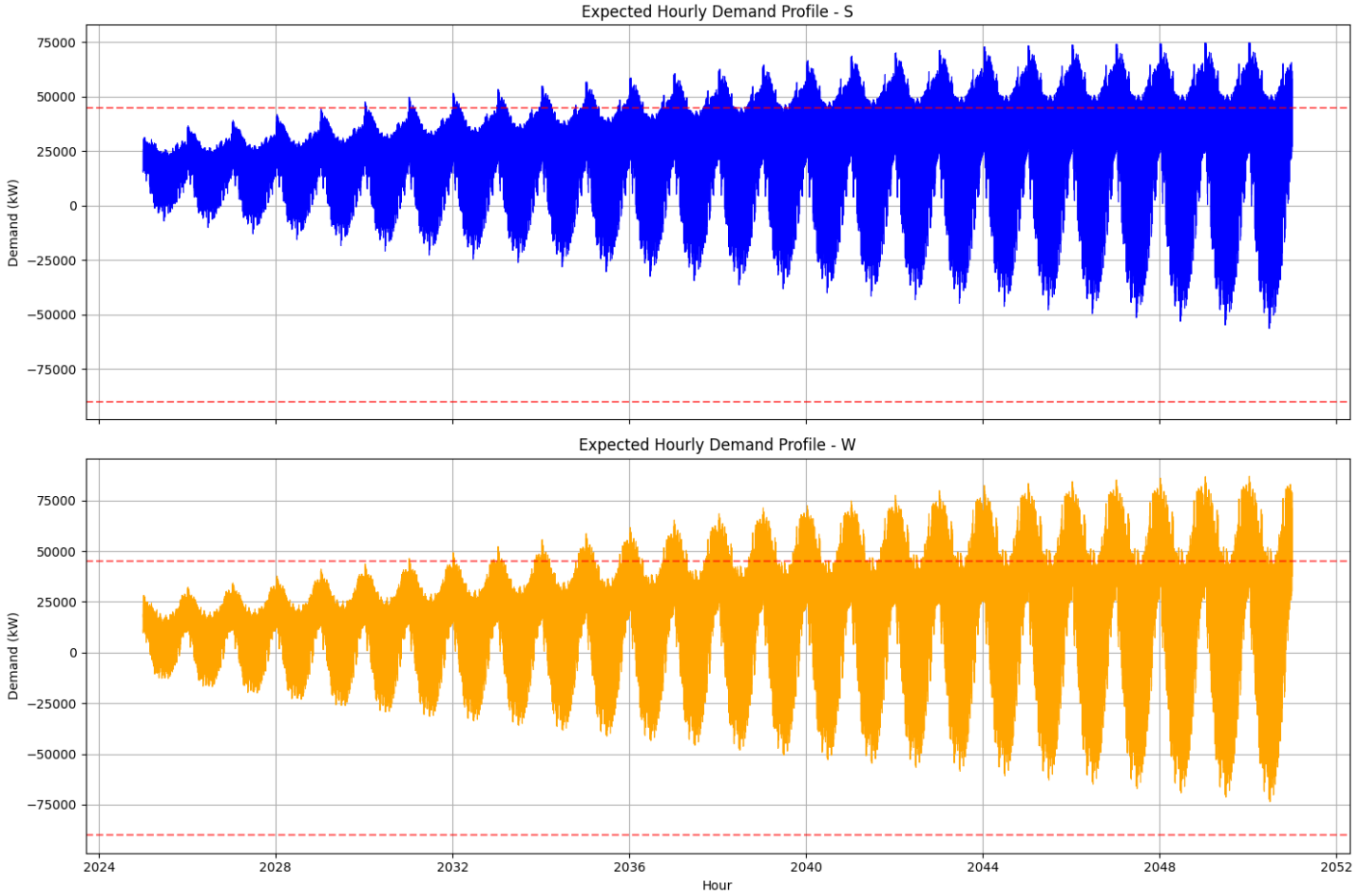

Figure 8: *Forecast of hourly electricity demand for substation S and W*

In addition, the hourly demand patterns of the six rings must be constructed. The catchment area of each individual ring was constructed using Vision, a grid visualisation tool. Each ring comprises multiple downstream distribution rooms, which collectively determine the hourly demand profile of the substations. In order to create the baseload of each ring, the hourly demand profile of each distribution room was grouped by catchment area. However, not all distribution rooms contained hourly demand data. Because of this, an approximation had to be made for each missing distribution room. A detailed description of this procedure is provided in Appendix *B.2*. The resulting hourly electricity demand patterns for all rings are presented in Figure *9*. These hourly electricity demand patterns form the power_demand attribute of the Ring class, as introduced in Section *5.1*.

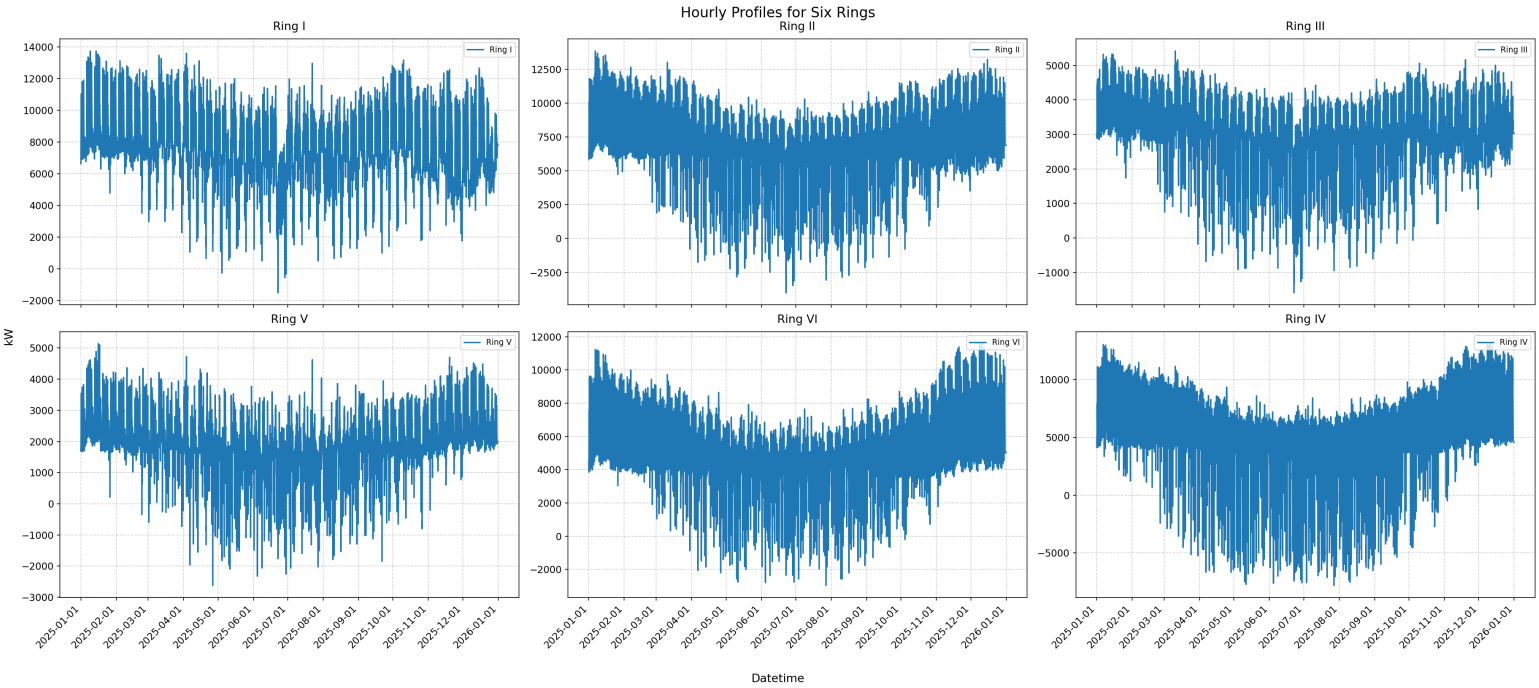

Figure 9: *Hourly electricity demand per ring*

5.3 Construction of KM Scenario for Simulation Integration

DSOs distinguish between four scenarios for long-term planning, one of which is the "Koersvaste Middenweg" (KM) scenario. Incorporating the KM scenario into the simulation model allows for a consistent basis for comparison between the simulated scenarios and a recognized scenario by all DSOs. Moreover, integration of the KM scenario reveals how varying scenario parameter values influence the model outcomes relative to the KM scenario, which enhances the interpretability of the results. Integration of the KM scenario results in one additional scenario which needs to be simulated, resulting in overall 10,001 simulation runs.

Table *6* presents the categorical alignment of the KM scenario with the uncertainty dimensions operationalised in the simulation model. The categorisation of the KM scenario was derived by translating the qualitative and quantitative scenario descriptions from Netbeheer Nederland (2025c) into categorical uncertainty bins (A, B or C). This translation was performed assessing each scenario driver against the model's defined uncertainty ranges and assigning the closest categorical representation. For example, according to the report the amount of new buildings in 2050 is 1.845 million houses for the KM scenario. This is a 22% increase compared to 2025. This percentage most closely resembles the growth parameter B for 2050 (125%) in the simulation model. For a detailed explanation of all uncertainty mappings see, Appendix *A.2*. Given that the KM scenario parameters used in this research are approximated from the official scenario values of Netbeheer Nederland (2025c), the KM scenario in this research will be denoted as KM' to reflect its derived nature.

Parameter Value	Name of Uncertainties in Simulation Model
A	airco_for_cooling, new_building_cooling, cooling_adoption, roof_growth, ev_growth, new_industry_mix, construction, data_center_growth, data_center_PUE, charging_behaviour
B	new_building_growth, lifespan_hybrid, mix_distribution, solar_adoption, solar_park_efficiency, solar_park_growth, ev_mix, charging_growth, new_building_mix, new_industry_growth, new_greenhouse_growth, shore_power_growth, extra_delay, roof_growth, wind_turbine_growth, wind_turbine_efficiency, total_use_ha
C	heat_transition, hybrid_adoption, vehicle_growth, charging_mix, new_greenhouse_mix, electric_ship_share, surface_mix

Table 6: *Summary of Uncertainty Mapping for KM' Scenario*

With all input variables now constructed and validated, this Section has established the foundational data required to run the simulation model. The subsequent Section introduces the formal structure of the model, describing how these inputs are operationalised within the simulation model.

6 Formalisation

This Section will discuss in detail how the simulation model is formalised. The simulation model is implemented in Python using an object-oriented approach and is designed to imitate the electricity demand in the catchment area of this study. To ensure computational efficiency and continuity beyond the scope of this thesis, the model was integrated into Stedin's internal simulation and data analysis environment. In doing so, the computational time was significantly reduced, from approximately three days to 24 hours. Furthermore, detailed load flow analyses using PandaPower are not taken into account in the simulation model. This study focuses on long-term strategic network planning under deep uncertainty, where simplified capacity based representations are sufficient for exploring capacity bottlenecks and investment needs. This Section elaborates on two of the concepts mentioned in Figure *4*: the application of Latin Hypercube Sampling, and the construction of the simulation model by addressing formulae for additional uncertainties and showing model adjustments.

6.1 Generation of Scenario Subset

All long-term uncertainties of the uncertainty space are categorically divided in this research. For more detail about this categorical division see *Appendix Uncertainties*. These long-term uncertainties influence the electricity demand and consumption within the study's catchment area. However, simulating the entire scenario space is computationally not feasible. The following numerical example will make this clear. The simulation model takes 32 long-term uncertainties, each with three possible states (A, B or C), the total number of scenarios then equals $3^{32} \approx 1853$ billion scenarios. Simulating such a large uncertainty space will take a long time. Therefore, sampling techniques that reduce computational time like Monte Carlo Sampling (MCS), Latin Hypercube Sampling or factorial methods can be used to create a representative scenario subset.

In this research, LHS is selected due to its ability to sample evenly from the entire sampling space and avoids clusters (Kobayashi et al., 2023). LHS achieves this by stratifying the Cumulative Distribution Function (CDF) of each parameter into intervals of equal probability mass, from which samples are drawn. This causes the entire scenario space to be sampled with uniform coverage of the input space. Although categorical data cannot be stratified the same manner as continuous data, the `LHSSampler()` of the `EMA Workbench` applies the same principle by stratifying the CDF of a `CategoricalParameter` into bins with equal length. In other words, the categorical LHS subset includes the extremes of all uncertainties. This approach ensures that the resulting sample set provides a solid representation of the underlying data distribution and preserves the extremes of the original dataset.

Next to this, LHS typically requires fewer samples than MCS to achieve the same level of precision (DataScienceGenie, 2025). Making it more computationally efficient. Moreover, LHS has better space filling properties than MCS as demonstrated by Rabitti and Tzougas (2025). This makes LHS more suitable than MCS for this research. Furthermore, LHS is preferred over full factorial methods because full factorial designs, are deterministic by nature (Kwakkel, 2024), meaning they always evaluate the same fixed combinations of parameter values. This limits coverage of the uncertainty space. Furthermore, since the uncertainty space consists of 32 categories with three levels, it is preferred to choose LHS over full factorial methods (Choi, Song, Yoon, & Koo, 2021). Consequently, LHS is adopted as sampling technique for scenario generation instead of MCS or full factorial designs. The Python code that generates the LHS sample set using the `EMA Workbench` can be found in *Latin Hybercube Sampling.ipynb*. This script produces a CSV file (`Latin_Hybercube_Sampling.csv`) containing 10,001 rows, each

representing a unique scenario, and 32 columns corresponding to the long-term uncertainties. The simulation model uses this CSV file as input for each scenario run.

Scenario	**Uncertainty 1**	**Uncertainty 2**	**...**	**Uncertainty 32**
1	B	C	...	C
2	A	A	...	B
		... (rows 3–10,000) ...		
10,001	C	B	...	A

Table 7: *Example of LHS subset used as input for the simulation model*

Note: A/B/C values here are illustrative and do not match the exact entries in `Latin_Hybercube_Sampling.csv`.

6.2 Capacity Risks and Investment Costs Metrics

This study focuses on two performance metrics: capacity risks and investment costs. Capacity bottlenecks are defined at scenario level, and represents the number of days on which substation demand exceeds the upper or lower capacity limits within a given year. Following the logic of Marang (2025), a day is classified as risky when demand exceeds 120% of substation capacity in any single hour, or 110% of capacity for at least six hours, see the pseudocode example of `calculate_risky_days()`. These thresholds are applied for all hours of all days in a scenario to determine the total number of risky days for that scenario. If a scenario has at least one risky day then the scenario experiences a capacity bottleneck.

For the PRIM analysis, a binary classification is needed. Therefore, scenarios with at least one risky day are classified as "risky", whereas scenarios with zero risky days are classified as "non-risky". The performance metrics of capacity risk is then calculated at an annual level as the percentage of scenarios in which at least one risky day occurs:

$$\text{Capacity Risk}_y = \frac{\text{Number of risky scenarios in year } y}{\text{Total number of scenarios}} \cdot 100\%$$

A lower capacity risk percentage indicates a higher level of robustness of the investment plan in that particular year.

The second performance metric are the investment costs. This study evaluates investment costs after the simulation runs are completed. The investment costs of the candidate investment plan consist of two new substations (H and K), a 150/50 kV transformer, new 150 and 50 kV cables and acquisition of land for the new substations. A detailed numerical summation of the investment costs is provided in Appendix *G.2*.

Pseudocode of `calculate_risky_days()`

```
risky_day_count = 0
lower_capacity = 2 * upper_capacity

for substation and year:
    if (demand > 1.10 * substations (lower/upper) capacity for 6 hours)
    elif (demand > 1.20 * substations (lower/upper) capacity for 1 hour):
        risky_day_count += 1
```

6.3 Mathematical Formulations of Added Model Components

To more accurately represent the electricity demand and generation in the simulation model three new model components require formalisation. This Section introduces three mathematical formulations that define these new model components. Each formula is designed to capture scenario dependent variability, with the scenario parameter values derived from the LHS subset. Each model component of the simulation model is verified in Appendix *C*.

6.3.1 Formalisation of Wind Park Component

One new model component, which was conceptually discussed in Section *4.3.1*, becomes operational in 2040 on substation K. The wind park starts at eight turbines and grows over time based on scenario dependent growth potentials. This new model component is formalised using the following equation. The equation formalises the relationship between the installed capacity, turbine efficiency and hourly demand profiles to estimate the total amount of power generated by the wind park in the catchment area.

$$P_{tot,windpark} = P_{turbine} \cdot g_y \cdot N_{turbines} \cdot \eta_{turbine} \cdot N_t$$

Where:

- $P_{tot,windpark}$ is the total power generation by the wind park
- $P_{turbine}$ is the average power generation by one turbine (3.6 MW) (Ministerie van Infrastructuur en Waterstaat, 2025)
- g_y is the scenario dependent growth factor of the wind park
- $N_{turbines}$ is the number of turbines inside the windpark
- $\eta_{turbine}$ is the efficiency of the turbine, capped at the Betz limit[1]
- N_t is the hourly generation profile of the wind park.

[1] The Betz limit is the fundamental physical limit on how much power a wind turbine can extract from the wind capping at 59.3% (Bouwmans, 2017).

6.3.2 Formalisation of Datacenter Component

Another new model component which adds extra uncertainty to the uncertainty space is datacenter construction. According to Aneli, Tina, and Gagliano (2025), the electricity consumption of a datacenter at each timestep i can be calculated as:

$$E_{tot,i} = E_{IT,i} + E_{cooling,i} + E_{devices,i}$$

Where:

- $E_{tot,i}$ is the total energy demand of datacenter
- $E_{IT,i}$ energy demand of IT equipment such as servers or storage systems
- $E_{cooling,i}$ energy demand by HVAC (Heating, Ventilation and Air Cooling) system
- $E_{devices,i}$ energy demand of other electrical devices (lighting systems, power systems and auxiliary)

In this study the electricity demand of devices is not taken into account, because such devices usually take up only 2% of energy demand (Shehabi et al., 2016). This simplification results in:

$$E_{tot,i} = E_{IT,i} + E_{cooling,i}$$

Since datacenters operate continuously ($E_{IT,i}$), the electricity demand used for cooling of the datacenter ($E_{cooling,i}$) is the primary factor causing fluctuations in electricity demand during summer and spring. Cooling demand increases on hotter days, which is represented through the Power Usage Effectiveness (PUE) metric. An ideal PUE is equal to 1.0 signifying that all electricity is used for IT operations, whereas a PUE of 1.5 signifies that 50% of electricity demand supports non-IT functions such as cooling. During summer and spring days, the PUE of a datacenter increases because of extra cooling needs for servers (PacketPower, n.d.). Meaning that the electricity demand for a datacenter increases during the summer and spring periods. Such seasonal fluctuations are handled within the simulation model, more on that will follow in Section *6.4*.

Wholesale datacenters typically consume between 10 and 40 MW of electricity (Patel, Ontiveros, & Nishball, 2024). In this study, a datacenter uses 10 MW of electricity initially, with electricity demand scaling proportionally with the growth of the datacenter. In other words, if the datacenter triples in size, the electricity demand will also increase threefold. The formula becomes:

$$E_{tot,i} = E_{IT,i} \cdot PUE_i \cdot g_y$$

Where:

- $E_{IT,i}$ is the amount of power that a wholesale datacenter typically consumes
- PUE_i is the Power Usage Effectiveness at timestep i, increasing on summer and spring days. A PUE of 1.2 is the regulatory norm in the Netherlands (Dutch Data Center Association, 2025).
- g_y is the scenario dependent growth potential of the datacenter in year y

6.3.3 Formalisation of Surface Constraints

Within the simulation model each ring has an attribute of available land. This available land is calculated using Google Maps, where grassland, agricultural land, parks or other types of land that uses little to no electricity, attribute to the available surface. Based on the estimated available surface, the growth potential of each model component within a ring is calculated, as formalised in the equation presented below.

- A_r is the available surface area (in hectares) of ring r.
- α_{tot} is the fraction of the total available surface allowed for growth (scenario-dependent).
- β_{c} is a fraction of α_{tot} allocated to model component c (scenario-dependent).
- $\bar{\mu}_{\text{c}}$ is the average surface area per unit of model component c (in hectares):
  - $\bar{\mu}_{\text{house}} = 0.0132$ hectares (CBS, 2025d).
  - $\bar{\mu}_{\text{industry}} = 0.85$ hectares (de Kort, Gradussen, & Groep, 2023).
  - $\bar{\mu}_{\text{greenhouse}} = 1.00$ hectares (see below).
  - $\bar{\mu}_{\text{datacenter}} = 1.20$ hectares (239 ha divided by 200 datacenters in total) (Grove, 2025).
  - $\bar{\mu}_{\text{wind turbine}} = 2.0$ hectares (see below).
  - $\bar{\mu}_{\text{solar park}} = 1.00$ hectares (standard 40 ha in 2040 due to solar park).

The average hectares of greenhouses and solar parks is set at one. Unlike other growth potentials, the expansion of greenhouses and solar parks does not require conversion from unit counts into surface areas, as the simulation model directly incorporates the total surface area of greenhouses within the catchment area. On the other hand, the average hectare needs for wind turbines is less straightforward. While the foundation on which it is built requires only 0.1 ha (NVDE, 2020), additional spacing between turbines is necessary. Therefore, this study takes on average 2 hectares per wind turbine to account for both the foundation and the needed space between turbines.

The maximum number of units of component c that can be added to the ring r is:

$$(1)\ \text{Max}_{r,c} = \left\lceil \frac{A_r \cdot \alpha_{tot} \cdot \beta_{\text{c}}}{\bar{\mu}_{\text{c}}} \right\rceil$$

The growth of each component c is modelled using a scenario-dependent growth factor g_y applied to the base count of their respective year. This respective base year can either be 2025 or 2040 depending on when the model component becomes active (y_b).

$$(2)\ \text{Unconstrained Growth}_{r,c,y} = Base_{r,c,y_b} \cdot g_y$$

The cumulative new units since year y_b is then capped by the spatial constraint:

$$(3)\ Cum_{r,c,y} = \min\left(\left\lfloor \text{Unconstrained Growth}_{r,c,y} - Base_{r,c,y_b} \right\rfloor, \text{Max}_{r,c}\right)$$

Thus, the total number of units in year y is:

$$(4)\ \text{Total}_{r,c,y} = Base_{r,c,y_b} + Cum_{r,c,y}$$

The ceiling function of Formula 1 ensures that any fractional result is rounded upward, thereby preventing the simulation model from constructing "half" houses or turbines. Conversely, the floor function in Formula 3 constraints cumulative growth to the largest integer that does not exceed the unconstrained growth. By calculating it this way, the simulation ensures never to exceed the maximum allowed surface for each individual model component.

6.4 Simulation Model Components

The simulation model developed in this thesis builds on the structural foundation introduced by Marang (2025), but was substantially adapted, extended and refactored to meet the requirements of EDEP on a masterplan scale. Furthermore, the simulation model was integrated into Stedin's internal modelling environment, which required transforming the original `.py` script into a modular `.ipynb` script. This process involved splitting and restructuring the code into cell based segments to ensure readability, maintainability and compatibility with Stedin's server infrastructure. Integrating the model internally therefore required considerable effort, rather than a straightforward transfer of the original script.

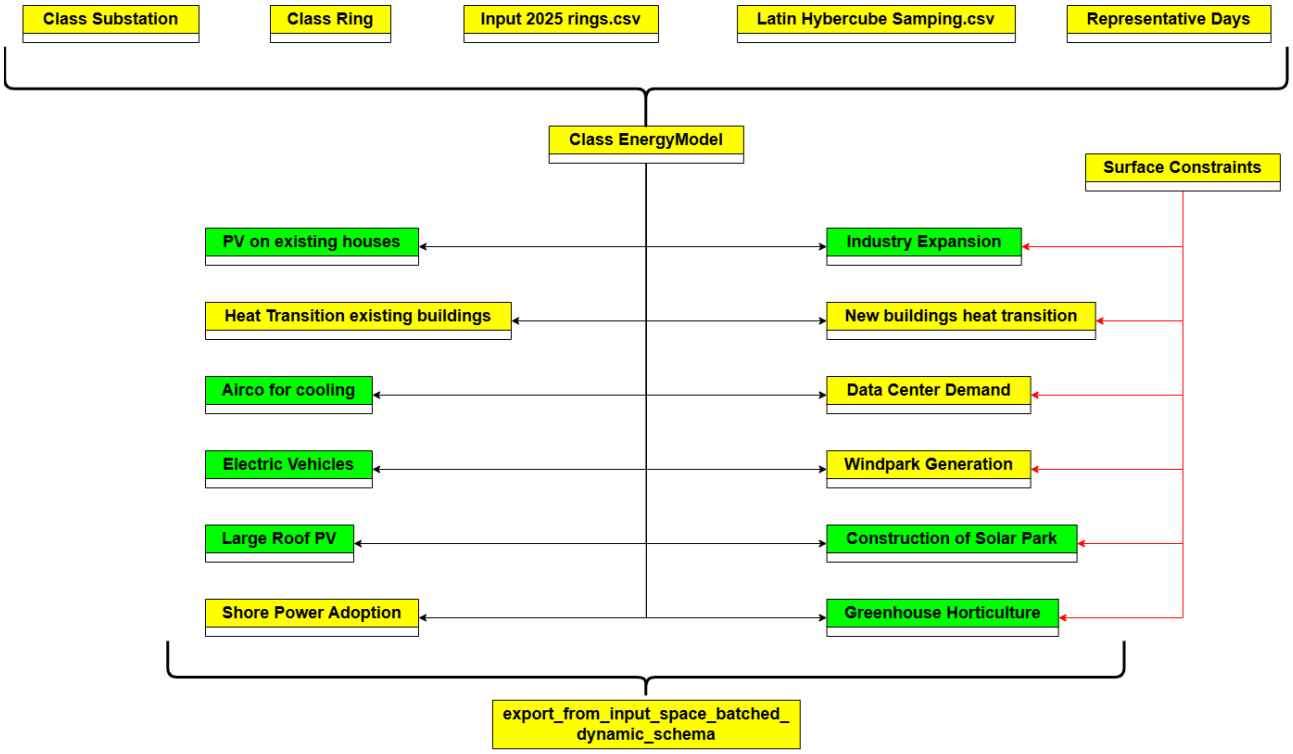

Figure 10: *Schematic simulation model layout, adjustments (yellow) no adjustments (green)*

Figure *10* shows the overall architecture of the simulation model. Components shown in yellow represent additions or revisions, such as the formalisation of wind park generation, datacenter electricity use, and surface constraints. Green components retain their original formalisation, but have, in some cases, underwent substantial code restructuring. For example, although the underlying electricity demand or generation formulae for industrial expansion, construction of solar park and greenhouse horticulture remain valid, additional code was introduced to ensure that all those components comply with spatial constraints at ring level. A comprehensive description of these structural and computational changes is provided in Appendix *D*.

Key adjustments for input of the simulation model include: simplifying and restructuring the Substation and Ring classes, replacing random discrete sampling with LHS, and adding windy days to the representative days of the simulation model. The inclusion of windy days enhances the simulation model's ability to capture seasonal fluctuations. Each representative day generates a 24 hour profile and is associated with year-specific weights. These year specific weights increase over time because of anticipated climate change potentially causing an increase in warm days. In doing so, the simulation model enables realistic future-oriented seasonal

fluctuations in electricity demand and generation. Moreover, several model components within the `EnergyModel` class were revised. The heat transition of existing and new buildings were corrected to use electric power demand instead of thermal power demand, the shore power formula was refined, the heating transition of new buildings was adjusted to account for energy consumption per heating source, and the lifespan of HHP parameter was recalibrated to ensure accurate scheduling of replacements. Moreover, surface constraints significantly reshaped the simulation model, requiring extensive code changes for six model components. Additionally, a function was added to export the simulation results using either PySpark tables or compressed CSV files.

In summary, while four components (PV on existing houses, airco for cooling, electric vehicles and large roof PV) remained structurally similar to their original form, the majority of the simulation model was conceptually extended and revised code-wise to support the research requirements.

7 Results

This section highlights the simulation results. This Section is structured as follows. First, the Exploratory Data Analysis (EDA) will discuss the amount of risky scenarios, the capacity analysis and feature scoring analysis. Subsequently, the PRIM analysis will uncover key drivers associated with risky days within the first simulation model results. Based on the identified key drivers, multiple mitigation measures are formulated and subsequently integrated into an adaptive investment plan that is stress-tested and analysed using a second simulation model. Finally, this Section will be concluded by comparing each investment plan based on short and long-term capacity risks and investment costs in order for Stedin to make an informed investment decision.

7.1 Exploratory Data Analysis (1st Iteration)

The analyses presented in this subsection are based on the first simulation model runs. The corresponding code scripts are available on the GitHub repository titled *Generic Analysis First Iteration.ipynb*. Before conducting this EDA, computational limitations were encountered due to the size of the simulation output. The raw output file comprised of approximately 109 million rows, which resulted in memory issues of the Python environment. In order to tackle this problem, two strategies were implemented. The first, involved saving per year and per scenario only the highest and the lowest value, which reduced the output to approximately 100,000 rows. The second, removed all duplications from the dataset, resulting in a reduced dataset of approximately one million rows. This reduced dataset of the second strategy was exclusively used for training four machine learning models and extracting their feature importances. This was done because, generally speaking, more data ensures more reliable machine learning models (Xu, Bi, Moeckel, Wiemer, & Ihlenfeldt, 2025). The first strategy was used for all other analyses of this Section and the PRIM analysis.

7.1.1 Robustness of Candidate Investment Plan

Substations	***2025***	***2028***	***2031***	***2034***	***2037***	***2040***	***2043***	***2046***	***2049***	***2052***
S	0	0	0	0	2	612	2538	4266	6610	8334
W	0	157	6615	0	0	17	452	1042	2039	3832
H	0	0	0	0	267	1292	2756	4602	6767	8262
K	0	0	0	0	0	0	0	0	1088	2177
Risky Scenarios S [%]	0%	0%	0%	0%	0%	6%	25%	43%	66%	83%
Risky Scenarios W [%]	0%	2%	66%	0%	0%	0%	5%	10%	20%	38%
Risky Scenarios H [%]	0%	0%	0%	0%	3%	13%	28%	46%	68%	83%
Risky Scenarios K [%]	0%	0%	0%	0%	0%	0%	0%	0%	11%	22%

Table 8: *Summary table of risky scenarios per substation per year* ($N = 10{,}001$)

The results presented in Table *8* indicate a clear increase of capacity risks over time. The higher proportions are in later years due to increasing electricity demand of future developments. For the year 2052, both substation S and H exhibit capacity risks in more than 80% of scenarios, while substation W and K experience a slightly lower capacity risk of 22% to 38%.

The results raise the question why substation H, which comprises only one residential ring, has a higher capacity risk than substation W despite the latter containing one residential and one industrial ring. An explanation for this difference lies in the input values of both substations.

Substation H serves approximately 2500 more households than substation W. In addition, substation H has roughly $\frac{83}{15} \approx 5.5$ times more available surface, allowing for greater expansion of residential housing, industry and renewable energy installations. For example, under scenarios that presume a residential housing focus, the number of houses can increase by more than 3000 households. Such expansions lead to higher electricity demand in the simulation model. This difference suggests that, given the modelling assumptions, substations that serve a larger residential housing stock substantially increase risky scenarios.

Returning to Table *8*, notably substation K does not experience capacity risks until later years of the simulation, with risky scenarios occurring only in 2049 and 2052. This indicates that there is unexploited capacity on substation K in the earlier simulated years. Specifically, the results indicate that potential reallocation of rings towards substation K is possible for earlier years which might results in an overall reduced capacity risk.

7.1.2 Substation Load and Capacity Analysis

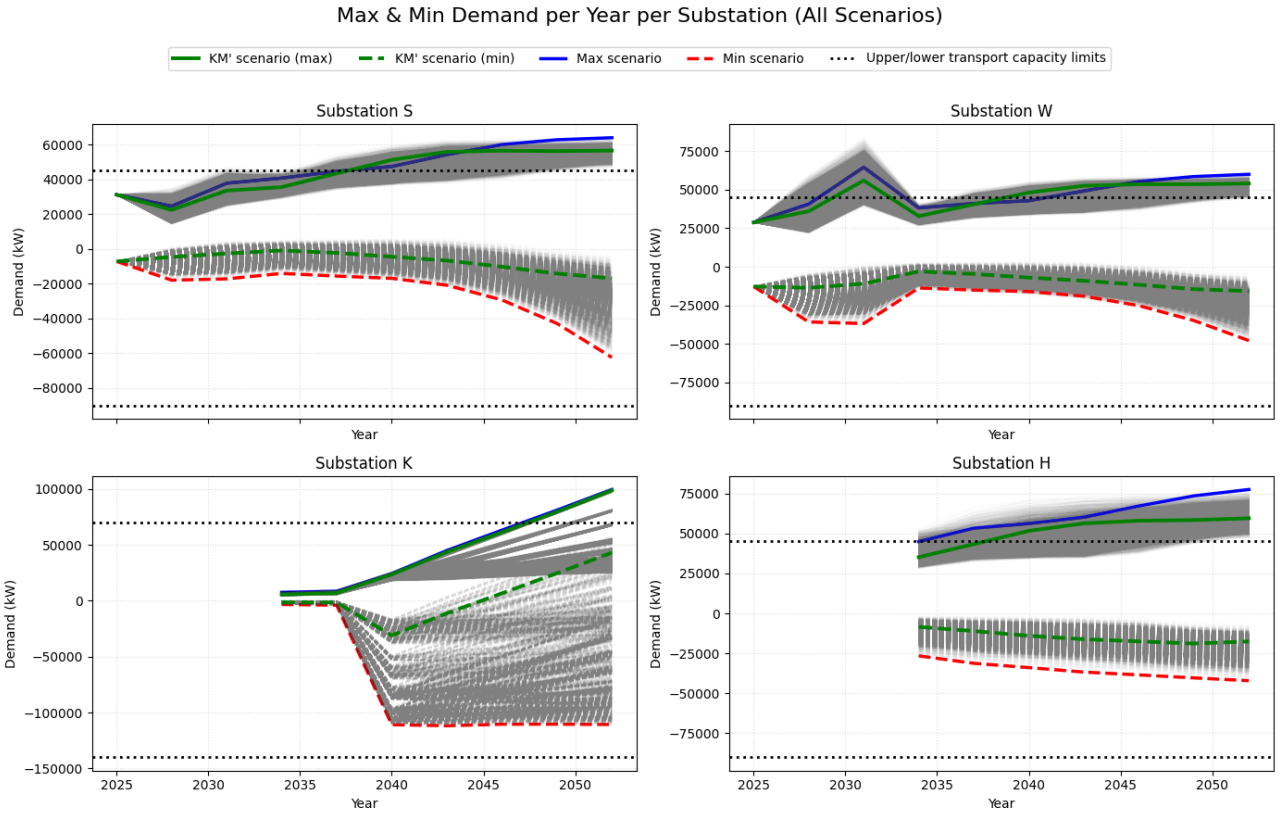

Figure 11: *Demand analysis for all substations*

In order to get a deeper insight into the insufficiency of the candidate investment plan, Figure *11* can be consulted. The figure presents the simulated maximum hourly electricity demand and generation feed-in, to the grid of the entire catchment area across all 10,001 scenario runs. For each substation, the figure highlights the scenario with the highest electricity demand capacity, represented by the blue curve, and the scenario with the highest generation feed-in capacity to the grid, as represented by the red curve. In addition, the KM' scenario included as the 10,001st scenario and widely adopted by Dutch DSOs as a reference scenario, is shown by the green

curve.

Overview of Substation Demand and Generation Profiles
Across all substations and scenarios, the simulated electricity generation remain below the lower capacity limits of the substations. Consequently, none of the scenarios lead to bottlenecks with regard to the lower capacity thresholds of each substation. This indicates that, given the long-term uncertainties, the candidate investment strategy is sufficient to accommodate future developments associated with electricity generation. In contrast, the results for the simulated electricity demand reveal frequent surpassing of the upper capacity limits of each substation. In the year 2052, the maximum demand scenarios of substations S, W, H and K exceed their respective capacity limits by approximately 19 MVA, 15 MVA, 33 MVA and 30 MVA. While Table *8* already quantified the proportion of scenarios that experience risky days, Figure *11* illustrates that, when solely considering demand without the risky days logic, nearly all scenarios exceed the installed capacity in the final year of assessment. Specifically, for substations S, W, and H, 100%, 100%, 99.81% of scenarios (represented by the grey lines) respectively exceed the upper capacity limits in 2052. The difference between these percentages and the percentages presented in Table *8* can be attributed to the application of the 110% and 120% risky days thresholds. Nevertheless, the results demonstrate that, from an electricity demand perspective, the capacity of substations S, W, and H is insufficient to accommodate long-term uncertainties without reinforcement of the upper capacity limits.

Implications of the KM' Scenario
The necessity for reinforcement of the substations is further underscored by the outcomes of the KM' scenario. This scenario is widely recognised by Dutch DSOs as a representative baseline reflecting "average" future development trends. Although the KM' scenario in this research is characterised by average growth assumptions for most uncertainty factors, with the exception of datacenter growth, the associated electricity demand exceeds the upper capacity limits of all substations in 2052. This finding suggests that even under the recognised KM' scenario the candidate investment plan is insufficient to accommodate future electricity demand.

Possible Short and Long-Term Reinforcement Options
In addition to the long-term capacity risks, the results further reveal a short-term capacity risk of 66% for substation W in 2031. A peak occurs in 2031, where electricity demand exceeds the upper capacity by approximately 32 MVA. This temporary capacity deficit must be mitigated by measures that are able to bridge the period until substation H becomes operational and takes over Ring IV. While temporary measures such as diesel or gas-fired generators can provide additional capacity for this period, such measures are associated with disadvantages such as noise-pollution and short circuit issues causing safety equipment of the electricity grid to become more overloaded, when such a generator is integrated in the grid (*Phase to Phase – Netten voor distributie van elektriciteit, hoofdstuk 10*, 2011). Although these disadvantages are relevant in practice, they are not included in this research because the simulation model evaluates only the capacity contribution of such temporary generation units. Operational and system protection considerations fall outside the scope of this study, and therefore this study focuses solely on whether such generators can provide sufficient short-term capacity relief on substation W.

Moreover, following the transfer of Ring IV to substation H, a small proportion of scenarios already exceed the upper capacity limit in 2034. While Table *8* shows that these scenarios do not cause risky days, they do suggest that the upper capacity of substation H is already

insufficient in some futures after becoming operational. Specifically, Stedin can opt for a 21 kV substation instead of the prospected 13 kV substation, thereby increasing capacity to 70 MVA. In doing so, substation H becomes more robust against future long-term uncertainties.

Substation K has unexploited capacity throughout most of the simulated scenarios. Although 22% of the scenarios in 2052 result in capacity risks, the results indicate that substation K retains sufficient room to accommodate additional electricity demand, especially before 2052. This opens up opportunities for reallocating the industrial rings of substation S and W, which exhibit capacity deficits of approximately 19 and 15 MVA respectively in 2052 for the maximum scenario. Since the electricity demand in 2052 of both industrial rings in the maximum scenario are roughly 19 and 15 MVA respectively, it could be possible that such reallocations mitigate capacity bottlenecks for both substations S and W across a subset of scenarios. However, one disadvantage of reallocating the industrial rings is that it may accelerate the onset of capacity risks at substation K.

Overview of Upstream Substation Demand and Generation Profiles

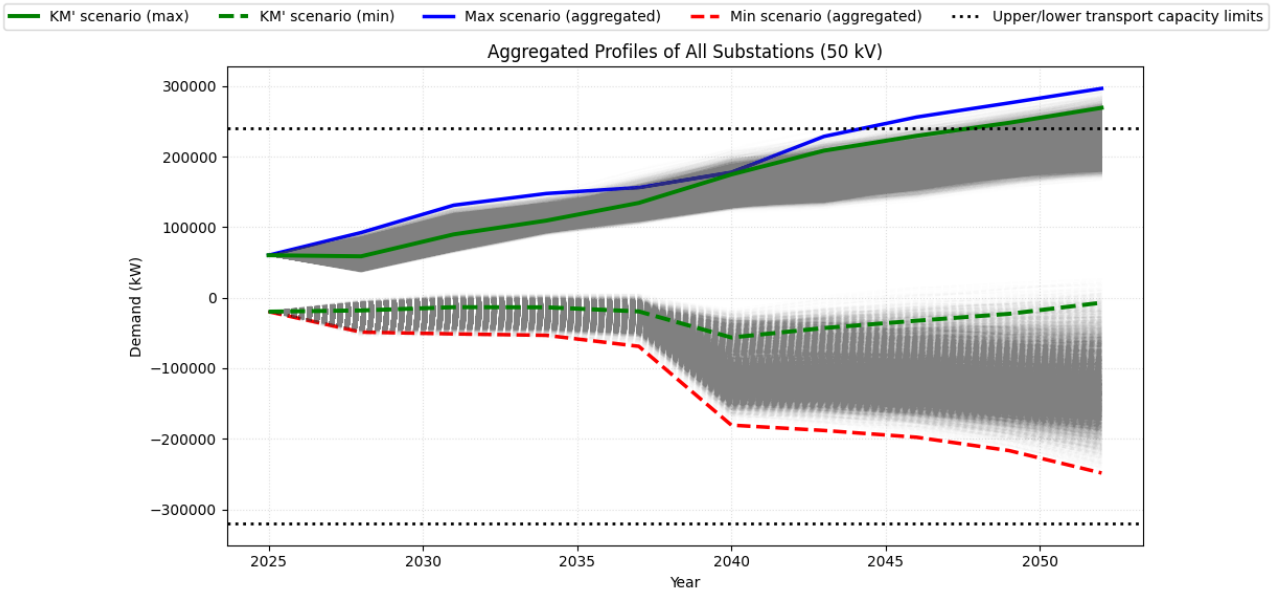

Figure 12: *Demand analysis for 50 kV network*

Finally, Figure *12* presents the aggregated electricity demand and generation profiles of the catchment area. In contrast to Figure *11*, upper limit capacity is not exceeded by any scenario in the years before 2043. This delayed onset indicates and further underscores that reallocation of rings can be a potentially adequate mitigation measures against capacity bottlenecks. Possible explanations of this late onset of capacity risks are the unexploited transport capacity of substation K and room reserved for direct connection to the 150 kV net for large consumers. Nevertheless, in 2052 the maximum aggregated demand scenario, which demands 296 MVA, exhibits a capacity deficit of 56 MVA. Furthermore, approximately 22% of all scenarios demand more than the upper capacity limit of the aggregated demand profiles allows. These results indicate that, despite there being unexploited capacity before 2043, long-term transport capacity reinforcements are still required for the aggregated profile.

All in all, the combined insights from Table *8* and Figure *11*, suggests that the current configu-

ration of the candidate investment plan is not adequate to face future long-term uncertainties. However, the results also indicate that within the current network configuration different choices can be made by reallocating industrial rings from substations S and W to substation K, or by constructing substation H as a 21 kV instead of 13 kV substation. Such measures could potentially improve the robustness of the electricity grid against future long-term uncertainties.

7.1.3 Substation Feature Scores

Figure *13* presents four substation specific feature importance scores. These feature importances are derived from four individual Random Forest (RF) classifier models. Each model is trained to classify whether a day within a scenario is deemed risky or not based on the long-term uncertainties. The distinction between individual simulation years is not made. Meaning that the features represent uncertainties influencing the models outcomes across all simulated years. This approach was adopted to avoid the need to construct forty separate year-specific RF models, which would have been a cumbersome approach with little added analytical value. Each RF Model has an accuracy of at least 0.75, indicating that the model correctly classifies 75% of cases as either risky or non-risky. On the other hand, the RF models show low recall (0.27 or lower) for risky days due to strong class imbalance. Despite this, the feature importance results remain analytically useful. Feature importances measure how strongly an uncertainty contributes to reducing impurity across decision splits, which provide a reliable sensitivity indication even when classification performance on the minority class is imperfect. The feature scores should be interpreted as model-based sensitivity-indicators of predictive influence rather than causal effects. More advanced Explainable AI tools such as SHAP or LIME plots have not been considered due to time constraints.

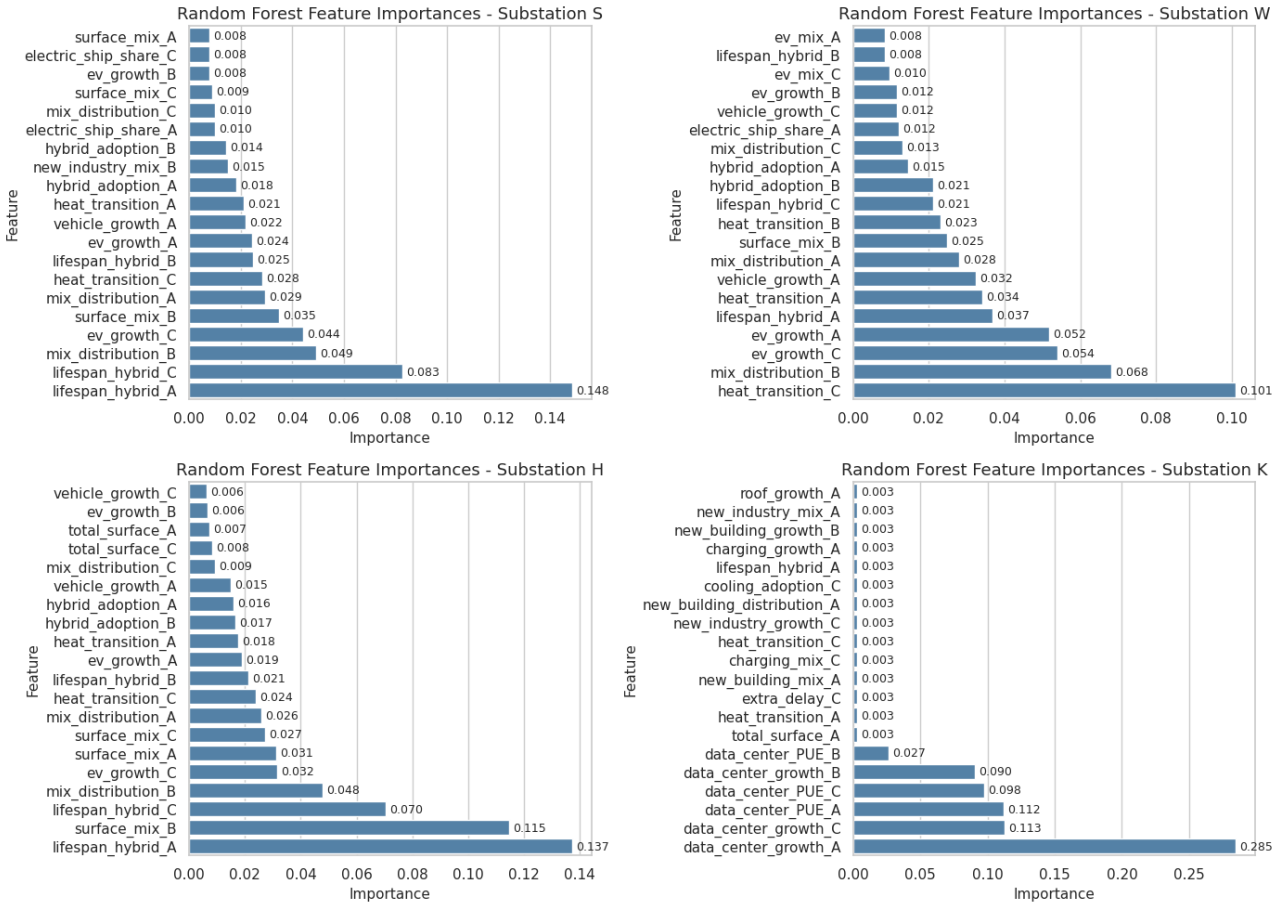

Figure 13: *Feature scores per substation across all simulated years*

Across all substations, the most prominent features include uncertainties related to the lifespan of HHPs, the mix distribution of heating units, the amount of EV growth and the surface mix. From a modelling perspective the predictive power of these features seems plausible. For instance, take the feature importance of lifespan of HHPs. In particular, uncertainty value A yields the highest feature importance for both substations S and H, as it assumes that after 10 years a HHP will be replaced by an eHP. This in contrast to uncertainty value B and C, which assume 15 and 20 years respectively. Given that an eHP requires 3 kW more electric power than an HHP, and the fact that around 35,000 houses will transition away from gas-based heating, the sooner an HHP will be replaced the sooner the electricity demand increases.

The mix distribution uncertainty reflects the share of eHPs in the simulation model. Uncertainty parameter value B represents the highest share of 40% compared to A and C which assume only 20% eHP share. Consistent with the reasoning applied to lifespan of HHPs, a higher share of eHPs increases overall residential electricity demand, making it plausible that scenarios with a higher eHP share exhibit an increased risk of capacity bottlenecks on residential substations. The surface mix uncertainty, specifically parameter value B, allocates a greater proportion of available land to residential development. Given that other uncertainties related to the residential housing transition also seem to increase capacity bottlenecks, such greater allocation of land will cause increased demand-side pressure on the substations. Consequently, scenarios that emphasise residential expansion seem to be more prone to capacity bottlenecks, as additional housing directly impacts electricity demand on residential rings.

In addition, for substation K the most prominent features are datacenter growth values. Indicating that large datacenters (data_center_growth_A) cause risky days on substation K across all simulated years. Interestingly, the feature importance results indicate that the uncertainty parameter value for datacenter growth C is considered more influential than uncertainty value B. This is odd, since datacenter growth value B is accompanied by higher electricity demand on substation K then datacenter growth value C. Such inconsistencies will be discussed in Appendix *E.2*.

All in all, the feature importance scores suggest that uncertainties regarding fast residential heating transition, fast transition towards electric mobility, residential housing expansion focus, and large datacenters can potentially increase capacity bottlenecks across all simulated years. While the feature importances do not identify specific combinations or threshold values of uncertainties leading to risky days, such as the PRIM analysis, they do offer complementary insights of the effect each uncertainty has on risky days across all simulated years. As such, the feature scoring results provide additional evidence for identifying which uncertainties are most influential in driving capacity bottlenecks. These insights are further examined in greater detail through the rule-induction analysis performed with PRIM, which will be discussed in the following Section.

7.2 Key Drivers of Capacity Risk (1st Iteration)

The feature scores provided an initial indication of which uncertainties contribute most strongly to the occurrence of risky days. A more accurate analysis that gives more precise vulnerabilities and numerical conditions under which the risky day appear is the PRIM analysis. Identifying these vulnerabilities and their corresponding threshold values is essential for enhancing the robustness and adaptiveness of the candidate investment plan. This Section discusses in detail which key drivers lead to risky days across the simulated years for each substation. The full PRIM analysis, including the selected boxes and the associated numerical uncertainty values linked to risky days is documented in *PRIM ANALYSIS I1.ipynb* and *PRIM I1.xlsx*.

7.2.1 General PRIM Choices and Explanations

Before discussing the PRIM results per substation, it is essential to establish thresholds for coverage and density. Coverage represents the fraction of all risky days that are captured by the PRIM box, meaning that high coverage explains a large share of risky model outcomes. On the other hand, density measures how pure that found box is, meaning that a high density box contains mostly outcomes that are risky (*PRIM-TMIP EMAT*, n.d.). A desirable PRIM box balances both coverage and density, capturing a large share of risky days while remaining sufficiently pure. As argued by Bryant and Lempert (2009), decision-makers should value coverage because it ensures that the identified conditions explain as many cases of interest as possible. In addition, decision-makers should value density because it ensures that these conditions are strong and reliable predictors of the outcome of interest. Although no universal thresholds exists, values around 0.8 for both coverage and density are used in the documentation of the EMA_workbench by Kwakkel (2023) and are subsequently adopted as thresholds for identifying high density boxes in this research. In practice, achieving both high coverage and high density is often challenging. For this reason, this research prioritises density over coverage. This choice ensures that the identified key drivers represent actual strong predictors for risky days. The disadvantage of this approach is that it may yield narrower boxes which captures only a limited region of the uncertainty space. This can potentially lead to the PRIM algorithm overlooking alterative combinations of uncertainties that also lead to risky days.

To potentially compensate for this limitation, an iterative PRIM procedure is employed by this research. Following the approach demonstrated by Guivarch, Rozenberg, and Schweizer (2016) and Marang (2025), the modified PRIM procedure operates as follows: once a high coverage and density box is identified, the cases of interest within that box are temporarily set to zero, thereby enabling the algorithm to uncover additional, less dominant but still relevant combinations of uncertainties causing risky days. This iterative process increases the diversity of the identified key drivers and mitigates the chance of overlooking meaningful uncertainty combinations. Throughout this thesis, these iterative PRIM procedures will be referred to as second or third PRIM iterations.

For illustrative purposes, Figure *14a* displays a typical PRIM trade-off curve for substation S in year 2043. The analysis begins with the full uncertainty space, covering all points of interest represented by value 1.0. As the PRIM algorithm peels away subsets of the input space the identified boxes become progressively smaller as represented by the curve moving to the left-side of the plot. The number of restricted dimensions represent the number of uncovered combinations of uncertainties that cause risky days. By selecting box 3, which has density > 0.8 and two restricted dimensions, Figure *14b* appears. The corresponding plot displays the exact numerical ranges for which risky days start to occur in the simulation model. In this case, this box reveals that for substation S in 2043 the medium-to-fast EV growth between 47% and 80% combined with a short lifespan of HHPs of 10 years results in capacity risks. The same procedure of trading off coverage and density and selecting appropriate boxes is repeated for each substation and for each simulation year, more on that can be found in *PRIM ANALYSIS I1.ipynb*.

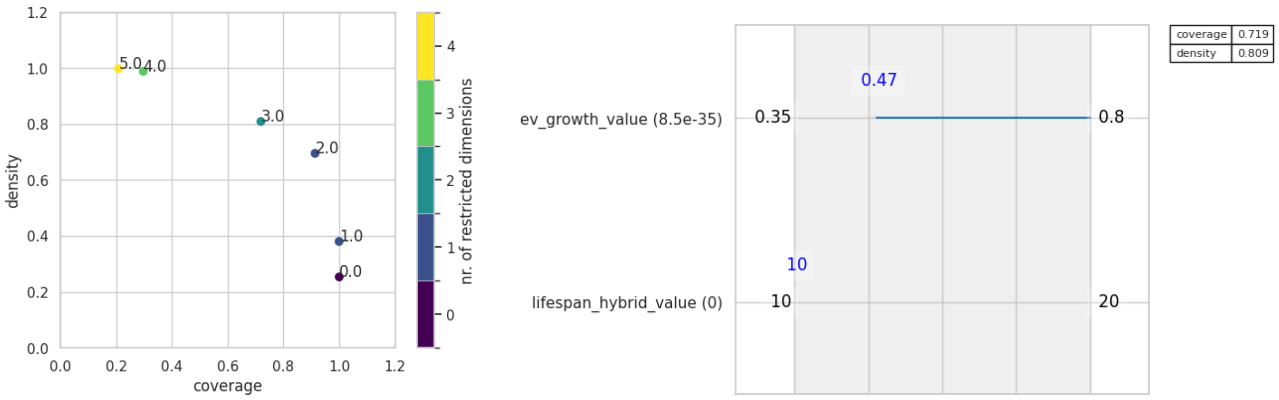

(a) PRIM trade-off coverage and density

(b) Selected PRIM box 3

Figure 14: *PRIM results: (a) trade-off between coverage and density; (b) selected box 3.*

7.2.2 Short-Term and Long-Term Drivers of Capacity Risks

The most important findings will be discussed in this Section. For a detailed substation and year-specific PRIM analysis see Appendix *F.1* and/or *PRIM I1.xlsx*. In summary, the PRIM analyses for substations S, W and H reveal a largely overlapping set of long-term uncertainties that drive capacity bottlenecks in three PRIM iterations. The first iteration identifies the most dominant drivers, most notably EV growth, the lifespan of HHPs and the eHP share, which appear repeatedly across substations and years. These drivers either individually or in combination cause capacity bottlenecks. These key drivers are primarily associated with the medium-to-fast residential heating transition away from gas-fired boilers to hybrid or full-electric heating options

and the medium-to-fast electric mobility growth. For example, EV_growth(47%–99%) shows that when the amount of EVs grows to 47% to 99% of the total fleet within the simulation model, then risky days occur on substation S on the long-term. Importantly, this pattern is consistent with the feature importance analysis, which also highlights high scoring features regarding fast residential heating electrification and EV growth as influential features of classifying as a risky days.

Next to this, the PRIM analysis also reveals several industry_mix_no_industry and surface_mix_solar_park uncertainties as drivers of capacity risks. These uncertainties serve as proxies for the "real" key drivers, which is explained in detail in Appendix *F.3*. In short, both uncertainties are strongly correlated with the underlying drivers of capacity risks. For example, the PRIM-identified key driver industry_mix_no_industry (10%-15%) emerges specifically in scenarios associated with parameter setting A, which also assumes 60% of electrification of industrial activities. Thus, although industry_mix_no_industry appears as a key driver in the PRIM box, it functions as a proxy for scenarios with high electrification of industrial activities. Likewise, the surface_mix_solar_park (6-6.8%) occurs under uncertainty parameter value B, which allocates 70% of available land to residential expansion. Because this allocation substantially increases electricity demand, also underscored by the feature importance scores, surface_mix_solar_park also acts as a proxy for scenarios characterised by a residential housing focus.

The appearance of these two uncertainties align with the feature importance scores of substation H, where surface_mix uncertainties also score highly. However, for substation W, the PRIM-identified uncertainty does not appear in the RF feature scores. A possible explanation for this is the low recall score of substation W (0.16) which indicates that some uncertainties that are important for decision splits were overlooked by the RF model. Since the industry_mix_no_industry uncertainty only pops up in the second PRIM iteration, it seems plausible that the feature score analysis overlooked this uncertainty as an important driver of capacity risks.

In contrast, the results for substation K indicate that large-scale datacenters, specifically those that demand more than 30 MVA, are the dominant driver of capacity risks on the catchment area of substation K. The range of three to five times the original datacenter size is associated with uncertainty parameter value A, indicating that capacity bottlenecks at substation K are primarily driven by large datacenters ($>$ 30 MVA). This also implies that medium to small scale datacenters fall within the operational limits of substation K in many scenarios and therefore do not constitute a dominant driver of capacity risks. This PRIM results aligns closely with the results of the feature importance analysis, thereby strengthening the evidence that a large scale datacenter is a dominant driver of capacity risks at substation K. A summary overview of all PRIM findings is provided in Table *9*. Note that the summarised results represent short-term and long-term ranges, therefore the named uncertainties are generalised to that range.

Short-Term Capacity Risks (2025–2040)	
Substation W	Medium-to-fast heat_transition_value (50%–80%): capacity risks occur during the transition away from gas-fired boilers when about 50%–80% are replaced by HHPs.
Long-Term Capacity Risks (2040–2052)	
Substation S	Short-to-medium HHP lifespan (10–15), which after replacement becomes fully-electric; combined with eHP share (20%–40%) replacing gas-fired boilers and medium-to-fast EV growth (47%–99%). Less dominant: share of "no industry" (10%–15%) serving as a proxy for high industrial electrification.
Substation W	Slight decrease (–10%) or increase (+10%) of total vehicles, together with medium-to-fast EV growth (57%–90%), eHP shares (20%–40%), and short-to-medium HHP lifespan (10–15). Less dominant: the share of "no industry" (10%–15%) acting as a proxy for high industrial electrification.
Substation H	High share of eHPs (20%–40%) replacing gas-fired boilers combined with short-to-medium HHP lifespan (10–15) and medium-to-high EV growth (53%–85%). To a lesser dominant extent: surface mix solar parks (6%–6.8%), serving as a proxy for residential housing focus.
Substation K	Fast datacenter growth (300%–500%) combined with low, medium, or high PUE (120%–170%).

Table 9: *Summary table of first simulation PRIM results*

7.2.3 Derivation of Storylines

Five storylines are distilled from the key drivers of capacity risk of Table *9*. The first storyline is "*medium-to-fast heating transition on residential rings*", in which gas-fired boilers are replaced by hybrid or full-electric heating options. The second storyline is "*medium-to-fast EV growth*", which involves increasing adoption of EVs. The first and second storylines often occur in combination and together act as key drivers of capacity risks. The third storyline, which is specifically focused on substation K is "*emergence of large datacenters in rural area*". The PRIM analysis showed that large datacenters (which demand more than 30 MVA) cause risky days to emerge. The fourth storyline is "*residential housing expansion combined with medium-to-fast residential heating transition*". While less dominant, the PRIM analysis indicated that substantial growth of the residential houses in the simulation model causes a significant extra burden on substations with residential rings. When such an housing expansion coincides with a medium-to-fast heating transition, the combined effect amplified electricity demand and generation by residential houses. This results hint to the fact that building a new city or village in already densely populated catchment areas causes capacity risks to occur on the substations. The last storyline is the "*high electrification of industrial activities combined with medium-to-fast EV growth*". Transitioning

away from methane-based energy sources to electric energy sources increases electricity demand of industrial activities. When this trend coincides with strong growth of EV, their combined impact elevates the risk of capacity bottlenecks on substations that have industrial rings.

Storylines as a Basis for Stakeholder Dialogue
By creating such storylines with the help of the PRIM results, this research enhances potential for stakeholder dialogue between grid operators and relevant societal actors. Each storyline can enable and enrich the discussions between grid operators and other actors, on questions how to mitigate capacity risks. In this sense, these storylines serve as a starting point of a discussion where both technical and non-technical stakeholders can discuss different objectives and interest in order to form strategic and relevant decisions regarding long-term expansion planning.

For instance, when the social dialogue centres on the storyline "emergence of large datacenters in rural area", the PRIM analysis reveals the exact ATPs under which substation K starts to experience capacity risks. Because substation K was originally intended to function as a buffer for future developments, the construction of such a large datacenter effectively nullifies this buffer function. In the social dialogue, this insight can be used to structure conversations about long-term planning under deep uncertainty. For example, if an investor such as a large technology firm proposes the construction of a new datacenter within the catchment area, Stedin can rely on the PRIM evidence indicating that large datacenters are key drivers of long-term capacity risks. This shifts the focus of the dialogue towards policy-relevant decisions, such as additional funding or the exploration of alternative siting options, rather than engaging in a debate about whether such developments would contribute to capacity risks. In doing so, the discussion can potentially reach earlier consensus and leaves all parties to make more informed decisions.

Collectively, the summary table and the five storylines answer the second research question: "*What are the vulnerabilities of the candidate investment plan, given the long-term uncertainties?*" Given the long-term uncertainties, the candidate investment plan suffers from vulnerabilities considering the medium-to-fast residential heating transition, the medium-to-fast growth of electric mobility and the coming of large datacenters in the catchment area. To a lesser dominant extend, the growth of residential houses combined with a medium-to-fast residential heating transition as well as electrification of the industry combined with medium-to-fast EV growth cause the candidate investment plan to showcase capacity bottlenecks in many different scenarios. Thus, this means that the candidate investment plan is vulnerable to these five long-term uncertainty drivers.

7.3 Construction of Robust and Adaptive Investment Plan

The PRIM results cannot only be used as a basis for stakeholder dialogue, it can also be used to formulate and integrate adaptive measures into the simulation model. This Section will first discuss a more robust network configuration which was provided by Stedin. Second, it will discuss under what conditions adaptive measures will be implemented. Third, this Section will highlight what changes were made to the simulation model.

7.3.1 Alternative Network Configuration

Before implementing adaptive measures, it is necessary to establish a more robust network configuration. Figure *15* shows a more robust version of the candidate investment plan, which is more robust but at higher investment costs. In this alternative network configuration, down-

stream capacity remains unchanged, while upstream capacity increases by 10 MVA. Note that this does not include the red transformer since that transformer is only active in some scenarios.

The aggregated electricity demand of Figure *12* shows that the highest demand scenario in 2052 reaches approximately 300 MVA. To accommodate such futures, an additional 150/50 kV transformer is required upstream in 22% of scenarios. In scenarios where demand remains below the 250 MVA, this additional investment is not necessary. This alternative network configuration therefore forms the basis for the adaptive investment plan, onto which scenario-dependent adaptive measures are subsequently integrated. Once the adaptive measures are implemented in the alternative network configuration, it is stress-tested against the same scenario subset of 10,001 scenarios in a second simulation model.

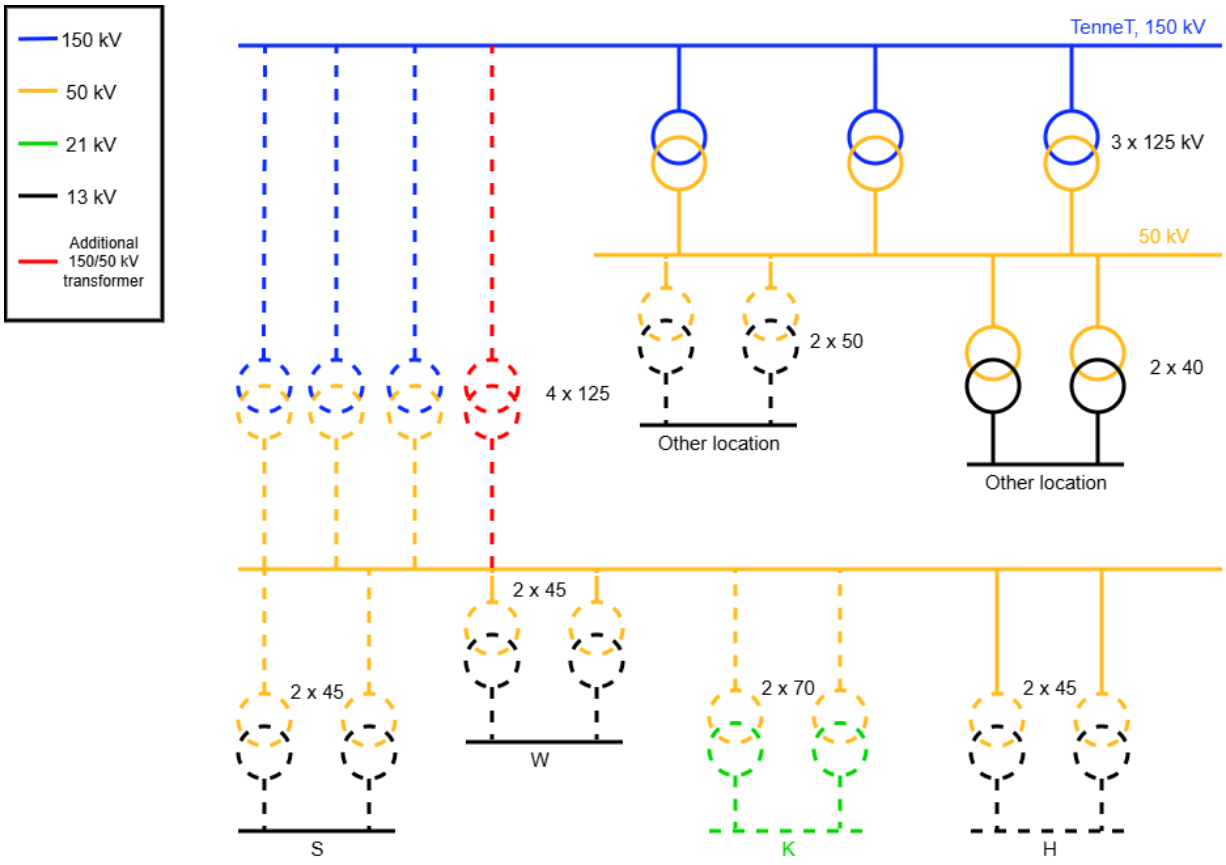

Figure 15: *Alternative Network Configuration*

7.3.2 Implementing Mitigation Measures

In order to mitigate capacity bottlenecks in a scenario four mitigation measures are available to Stedin. These measures stem directly from the XLRM framework of Section *4.3.4*. The costs differ per mitigation measure and are displayed between brackets. For a detailed breakdown of the costs of these measures, see Appendix *G*.

1. Reallocating industrial rings of S and W to substation K (€ 4.500.000 per ring reallocation)
2. Construction of an additional 21 kV substation downstream ("Substation X") (€ 128.980.000)
3. Construct substation H as a 21 kV station instead of a 13 kV substation (€ 55.000.000)

4. Diesel/gas generators for temporarily relieve of the demand peak on substation W (€ 5.750.000)

Both the reallocation of industrial rings and the construction of an additional 21 kV substation X are adaptive measures. That is, only when a scenario moves towards futures where capacity bottlenecks present itself, such a measure will be implemented. In the second simulation model, this implementation will be done instantaneously. This is deliberately done, as it enables a clear assessment of whether the adaptive measures are sufficient to reduce capacity risks across substations. The logic behind both adaptive measures is simple. Reallocating industrial rings to substation K relieves demand and generation peaks on S and W. In contrast, when the adaptive measure of substation X is implemented it takes over half the electricity demand and generation of substation K. Importantly, this does not involve the transfer of specific rings from K to X, rather it reflects a redistribution of half of overall electricity loads of K to X. Due to time constraints this simplification was made.

The mitigation measure of constructing substation H as a 21 kV substation is implemented in all scenarios. The results for substation H show that the maximum transport capacity scenario demands 77 MVA. If substation H is to be a 21 kV substation it is possible that across all scenarios substation H becomes fully robust. Moreover, making this choice timely is important because of path dependency. Lastly, diesel or gas generators can be implemented by Stedin to temporarily relieve the demand peak on substation W. This measure will not be explicitly modelled in the second simulation model because of time constraints.

Implementation Approach of Adaptive Measures
Not every mitigation measure needs to be implemented for each scenario. Only when a scenario moves towards a future where capacity bottlenecks reside, the adaptive measure must be taken. Due to time constraints, it was not feasible to develop elaborate monitoring systems that track the parameter value of long-term uncertainties that cause risky scenarios. Alternatively, a simplified but equally valid approach was incorporated into the second simulation model, which will be discussed below.

Example of Adaptive Rule: Building Substation X

```
# Rule for building Substation X (high datacenter growth pathway)

if data_center_growth == A and data_center_PUE in {A, B, C}:
    substation X is built and takes over half of the electricity loads of K
    substation_X = True
```

The simplified approach uses the numerical key drivers that the PRIM analysis provided. For instance, data_center_growth (3.8-5) and data_center_PUE_value (1.2-1.7) are the PRIM results for substation K in 2052 (see "Example of Adaptive Rule: Building Substation X"). This indicates that once the datacenter grows to 3.8 to 5 times his original size combined with either low, medium or high power usage effectiveness, substation K will experience capacity risks. However, the simulation model's input space is categorically defined (A, B, C). Only after running the simulation model, is this categorical uncertainty space translated into a numerical one for the purpose of scenario discovery, see *PRIM Analysis I1.ipynb*.

Consequently, the numerical PRIM results must be translated back into the original categorical uncertainty space that the simulation model knows. In the datacenter example, growth values

between 3.8 and 5 occur only in uncertainty parameter value A, while PUE values between 1.2 and 1.7 span all uncertainty parameter values (A, B and C). Thus, the resulting adaptive rule is triggered in one-third of all scenarios. However, Table *8* shows that for substation K only 22% of all scenarios experience risky days in 2052. This raises an important implication, the categorical uncertainty bins are coarse, so each adaptive rule may activate across a larger part of the uncertainty space. Consequently, some adaptive measures may be activated in scenarios that would not, in fact, evolve towards critical capacity conditions. Due to modelling choices made at the very start of this thesis, it became practically impossible to revise the input space into a continuous numerical form without altering the established modelling structure.

As a result, the categorical uncertainty space design reduces the level of refinement of the adaptive measures. Consequently, they become less sensitive to the uncertainty values that actually generate high electricity transport scenarios. Nevertheless, despite this simplification, the model results remain highly informative because they still provide clear evidence as to whether adaptive measures effectively reduce the occurrence of risky days across a wide range of plausible futures.

Mitigation Measures Table

Table *10* summarises the eight adaptive rules implemented in the second simulation model, each like the datacenter example. These adaptive rules are implemented based on the year-specific PRIM results (see Appendix *F.1*).

For the reallocation of the industrial ring S, several uncertainty combinations trigger the adaptive rules. First, reallocation occurs when EV growth ranges between 47%–99% (corresponding to uncertainty values A, B and C) combined with a short lifespan of HHPs of ten years (A). A second trigger arises when the share of eHPs lies between 30%–40% (B), together with a short-to-medium HHP lifespan (A or B). A third condition is met when EV growth ranges from 57%–90% (A or B), combined with a short-to-medium HHP lifespan and an eHP share of 20%–30% (A, C). Finally, reallocation is applied when the amount of total vehicles either decline by 10% (90%) or increase by 20% (120%), corresponding to uncertainty levels (A, B and C), combined with an eHP share of 20%–30% (A or C), a heat network share of 40%–50% (B) and high industrial electrification (A).

For substation W, the industrial rings of W need to be reallocated based on either the short team peak or long-term drivers of capacity bottlenecks. While diesel and gas generators temporarily relieve demand peaks on substation W, the key driver remains an important indicator for reallocating rings. Therefore, the first adaptive measure is based on the heat transition value of 50%–80% which corresponds to categorical uncertainty values (A and B). The second adaptive rule is triggered when the total amount of vehicles is between (90%–120%), in combination with EV growth of 57%–90% (A, B) and a short-to-medium HHP lifespan (A or B). A third rule applies in scenarios where total vehicle growth is again 90%–120% (A, B, C), accompanied by declining EV growth of 10% (A), high industrial electrification (A), an eHP share of 20%–30% (A or C), and a 50%–65% EV mix of cars (B or C).

The adaptive measure for datacenters is already extensively discussed. Note that two measures, constructing substation H as a 21 kV and diesel/gas generators, are implemented in all scenarios. The table below summarises the eight adaptive rules of the second simulation model. Pseudocode of these adaptive measures can be found in Appendix *H*.

Mitigation Measure		Adaptive Rules (Categorical)
Reallocation industrial ring S	**ATP1**	EV growth either A or B or C ∧ lifespan of HHP is A
	ATP2	Mix distribution is B ∧ lifespan of HHP either A or B
	ATP3	EV growth either A or B ∧ lifespan of HHP either A or B ∧ mix distribution is either A or C
	ATP4	Total vehicle growth is either A, B or C ∧ mix distribution is either A, B or C ∧ new industry mix is A
Reallocation industrial ring W	**ATP5**	Heat transition is either A or B
	ATP6	Total vehicle growth is either A, B or C ∧ EV growth is either A or B ∧ mix distribution is B ∧ lifespan HHP is either A or B
	ATP7	Total vehicle growth is either A, B or C ∧ EV growth is A ∧ new industry mix is A ∧ EV mix is either B or C ∧ mix distribution is either A or B
Construction of Substation X	**ATP8**	Datacenter growth is A ∧ datacenter PUE is either A, B or C

Table 10: *Categorical Adaptive Rules Implemented in Second Simulation Model*

Summary of Adaptive Investment Plan

The adaptive investment plan consists of the alternative network configuration combined with the decision to construct substation H as a 21 kV substation in 100% of scenarios. In addition, short-term demand peaks at substation W are temporarily mitigated through the use of diesel/gas generators for 100% of scenarios, although this measure is not specifically modelled in the second simulation model. Several adaptive rules are incorporated into the second simulation model: the reallocation of the industrial ring of S is activated in roughly 73% of scenarios, the reallocation of the industrial ring of substation W in 71% of scenarios, and the construction of substation X in 33% of scenarios. The additional 150/50 kV transformer will be implemented 22% of scenarios. The combined effect of the more robust alternative network configuration and the implemented adaptive measures is expected to substantially increase the overall robustness of the investment plan. The adaptive investment plan is subjected to a second round of stress-testing using the same scenario subset of 10,001 scenarios.

7.3.3 Comparison of First and Second Simulation Model

The simulation model keeps track of the adaptive measures by adding a boolean column to the model results. When an adaptive measure is implemented, the label stores True, otherwise False. Furthermore, adaptive measures are applied instantaneously once their trigger condition is met. The table below summarizes the specific adjustments made to the second simulation model.

	Simulation Model First Iteration.ipynb	**Simulation Model Second Iteration.ipynb**
Description	Stress-tests candidate investment plan. No adaptive measures are incorporated	Stress-test of the adaptive investment plan, while integrating eight adaptive rules derived from the PRIM results in the first iteration. Four mitigation measures are implemented, two of them based on adaptive trigger conditions per scenario.
(Added) Assumptions	Substation H and K become operational in 2032. A large solar and wind park, as well as a datacenter, will become operational in 2040. These future developments will be connected to substation K, since that station is designed to accommodate future electricity developments in the catchment area	All assumptions of the first simulation model continue in second simulation model. The short-term peak of substation W is always met by diesel or gas generators. When trigger conditions are met, adaptive measures are implemented in the second simulation model.
Computational Time (16 GB RAM, 4 cores)	24 hours	40 hours

Table 11: *Changes between First and Second Simulation Model*

7.4 Exploratory Data Analysis (2nd Iteration)

After adding the adaptive rules to the second simulation model, the same 10,001 scenarios were executed again. The same row-reduction strategy was used as discussed in *Exploratory Data Analysis (1st Iteration)*.

7.4.1 Robustness of Adaptive Investment plan

Substations	***2025***	***2028***	***2031***	***2034***	***2037***	***2040***	***2043***	***2046***	***2049***	***2052***
S	0	0	0	0	7	144	600	978	1447	1845
W	0	217	6763	0	0	0	28	217	279	598
H	0	0	0	0	0	0	0	0	0	0
K	0	0	0	0	0	0	0	569	25	415
Candidate Risky Scenarios S [%]	0%	0%	0%	0%	0%	6%	25%	43%	66%	83%
Candidate Risky Scenarios W [%]	0%	2%	66%	0%	0%	0%	5%	10%	20%	38%
Candidate Risky Scenarios H [%]	0%	0%	0%	0%	3%	13%	28%	46%	68%	83%
Candidate Risky Scenarios K [%]	0%	0%	0%	0%	0%	0%	0%	0%	11%	22%
Adaptive Risky Scenarios S [%]	0%	0%	0%	0%	0%	1%	6%	10%	14%	18%
Adaptive Risky Scenarios W [%]	0%	2%	68%	0%	0%	0%	0%	2%	3%	6%
Adaptive Risky Scenarios H [%]	0%	0%	0%	0%	0%	0%	0%	0%	0%	0%
Adaptive Risky Scenarios K [%]	0%	0%	0%	0%	0%	0%	0%	6%	0%	4%

Table 12: *Summary and Comparison table risky scenarios per substation per year* ($N = 10{,}001$) *second simulation model*

Table *12* shows a substantial reduction in the share of scenarios exhibiting capacity risks across all substations and simulated years when compared to the first iteration. The sole exception is the short-term peak at substation W. It is assumed that the mitigation measures (diesel and gas generators) fully resolve this peak and are therefore not explicitly modelled by the second simulation model. Nonetheless, these short-term peak numbers serve as validation that the calculation of risky days in the second simulation model are consistent with the first simulation model. The observed difference between the two simulation iterations can be attributed to representative days in the model. Overall, the reduction in risky scenarios indicates that the implementation of adaptive measures significantly decreases capacity risks.

For substation H, the results suggest that the substation is fully robust against all simulated scenarios. This outcome provides strong support for upgrading substation H from a 13 kV to a 21 kV substation. This decision should be taken ahead of the 13 kV implementation to prevent premature lock-in. However, note that such an upgrade requires reinforcement of the entire downstream electricity grid, as existing cables are designed for 13 kV and will need to be replaced.

Turning to substation K, the results show a clear reduction in the share of risky scenarios compared to the first simulation model. This may seem counter-intuitive, as substation K receives industrial rings in a large share of scenarios. For instance, in 71% of scenarios K receives industrial ring W, in 73% it receives industrial ring S and in 53% of scenarios it receives both industrial rings. Despite this, no substation increase in risky scenarios can be observed. Although risky days emerge slightly earlier (2046 instead of 2049), their overall share decreases in later years. This reduction is explained by the activation of substation X in one-third of the scenarios, specifically those characterised by high datacenter demand. By diverting half of this demand to substation X, the most load-intensive scenarios are no longer concentrated solely on substation K. As a result, substation K remains sufficiently robust even when it inherits the industrial rings of S and W. The findings indicate that, once high datacenter demand scenarios are mitigated, through construction of substation X or stakeholder decisions limiting datacenter development, substation K retains adequate unexploited capacity. It underscores the impact that large datacenters have on the robustness of the grid and highlights the importance of either additional substations or steadfast policy positions regarding large datacenters in the catchment area.

Lastly, both substations S and W experience a reduction in risky scenarios by reallocating their industrial rings to substation K. As stated before, this happens in 71% (W) to 73% (S) of all scenarios. The remaining risky scenarios for both substations are likely driven by the residential housing transition, since the remaining rings downstream of both substations are residential. Substation S remains more vulnerable than substation W because of the available surface on this ring. Assuming a residential housing focus scenario (B), substation S can have 1.67 times more houses equivalent to approximately 400 additional houses. Since the residential heating transition is a key driver of capacity risks, this difference plausibly explains higher share of remaining risky scenarios on substation S. The specific key drivers underlying these residential risks are further examined in the second PRIM iteration.

7.4.2 Substation Load and Capacity Analysis

The demand analysis shows the effect of the adaptive measures. Compared to Figure *16a*, a larger share of scenarios in Figure *16b* remain below the upper capacity limits of the substations. For substation K, Figure *16b* further shows that electricity generation exceeds the lower capacity limit for the first time. This indicates that the combined effect of solar and wind parks, together

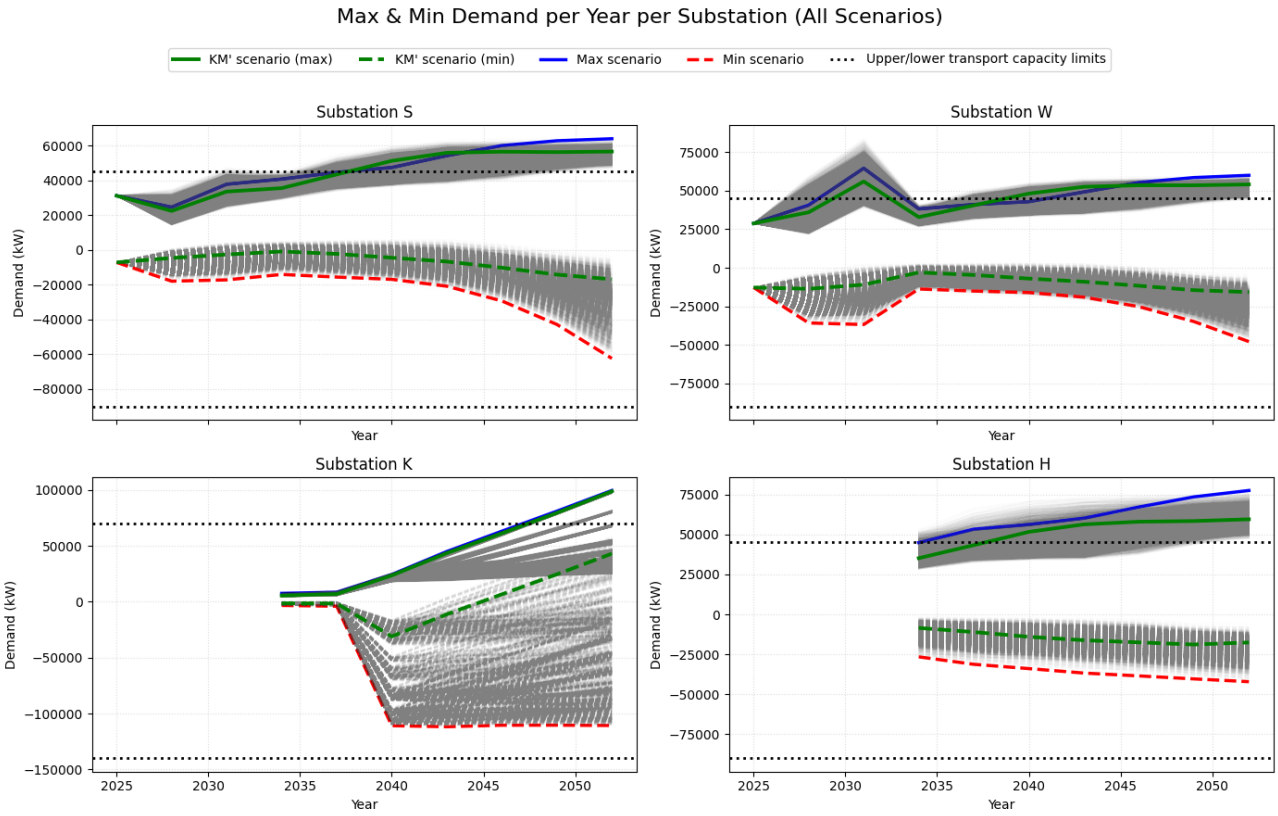

(a) *Demand analysis for all substations — first simulation model*

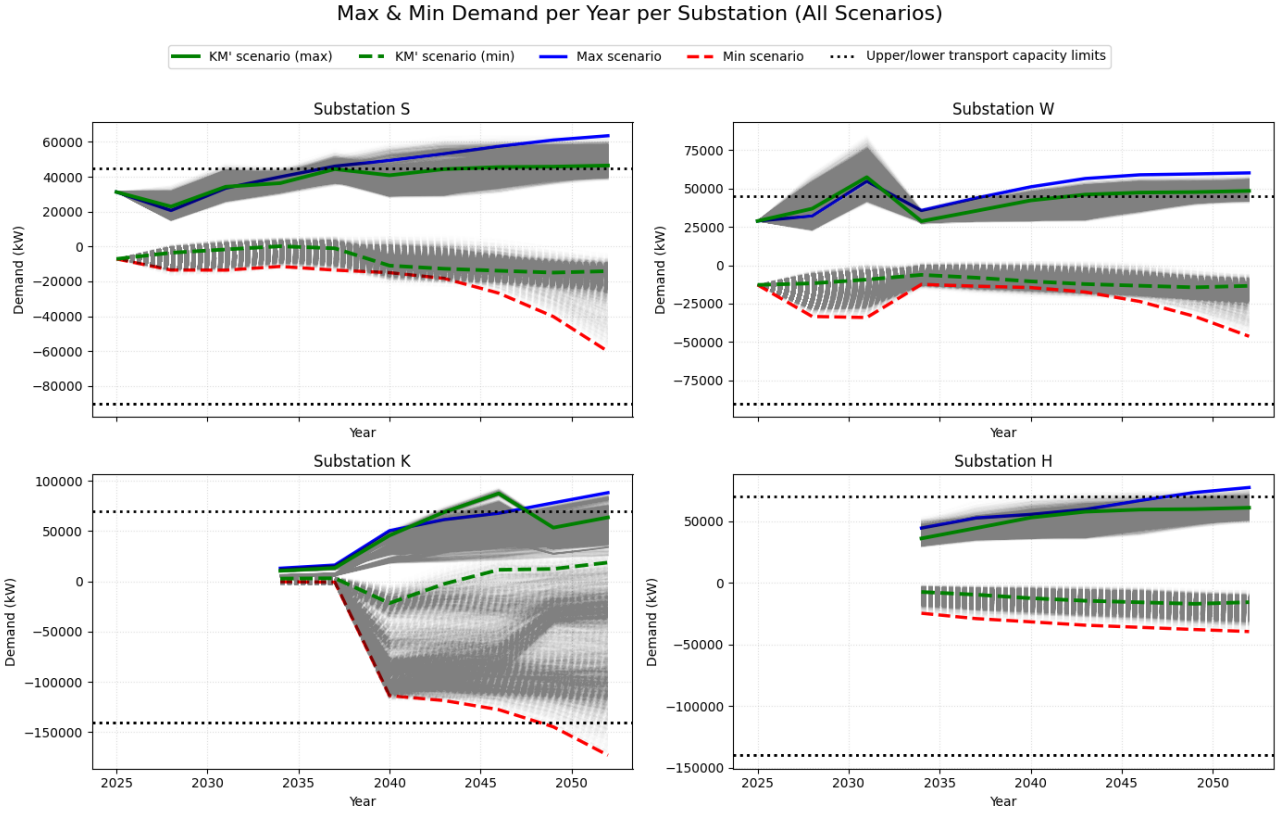

(b) *Demand analysis for all substations — second simulation model*

Figure 16: *Overview of demand analysis results: (a) first simulation model, (b) second simulation model.*

with PV installations on large industrial rooftops, leads to high-generation scenarios in which feed-in risks become apparent. As a result, reallocating industrial rings to substation K can, in some scenarios, introduce challenges related to reverse power flows. In other words, although ring reallocation reduces the risks for substations S and W, it may generate reverse power flow capacity bottlenecks on substation K. Next to this, the demand profiles of substation K also show that high-demand scenarios begin to exceed the upper capacity limit around 2046. In these scenarios substation X is subsequently activated as an adaptive measure and takes half the electricity load of substation K, as demonstrated by the decreasing KM' scenario line.

At first glance, Figure *16b* may appear to contradict the results of Table *12*, as several scenarios for substation S and W still seem to exceed upper capacity limits. Two clarifications are relevant. First, the definition of what constitutes a risky day, which is either exceeding 110% for six hours or 120% for one hour. This effect is not observable from the demand and generation profiles. Second, the figure does not visualise the erratic movement of the individual scenarios over time. For example, looking at the generation profiles of substation K, many scenarios exhibit a upwards trend around 2045. Following these upwards trends, the scenarios in 2052 cluster within the same dense region (between -50 MVA and -30 MVA). Such dense regions are not clearly visible in the demand figures of each substation because of the large amount of scenarios being displayed. This interpretation is supported by *Generic analysis Second Iteration.ipynb* which visualises the first 250 scenarios in more detail. The results reveal that such dense regions of scenarios are present in 2052. Although many scenarios approach the capacity limits, the scenario is not flagged as a risky scenario. Consequently, the figures are not contradictory to Table *12* but rather reflect challenges when visualising large amounts of scenarios.

Both Table *12* and Figure *16b* shows that the adaptive investment plan becomes overall more robust against many plausible futures. In other words, when the vulnerabilities of the candidate investment plan are translated into adaptive rules, these adaptive rules create a more robust and adaptive investment plan.

7.5 Key Drivers of Capacity Risk (2nd Iteration)

The remaining risky scenarios are analysed in *PRIM ANALYSIS I2.ipynb*. The same density threshold is used as in the first iteration, and the iterative PRIM procedure is again used to identify less dominant key drivers of capacity risks. However, none of the remaining risky scenarios yield PRIM boxes with high density (> 0.8) to allow for scenario discovery. This indicates that, after implementation of the adaptive measures, the remaining risky days are too diversely scattered across the uncertainty space to be explained by distinct combinations of uncertainties. For a more detailed description, see Appendix *Deeper Understanding of PRIM Results*. Consequently, this Section is rather short. In the following Section the sequence of investment paths is discussed.

7.6 Visualisation of Adaptive Investment Pathways

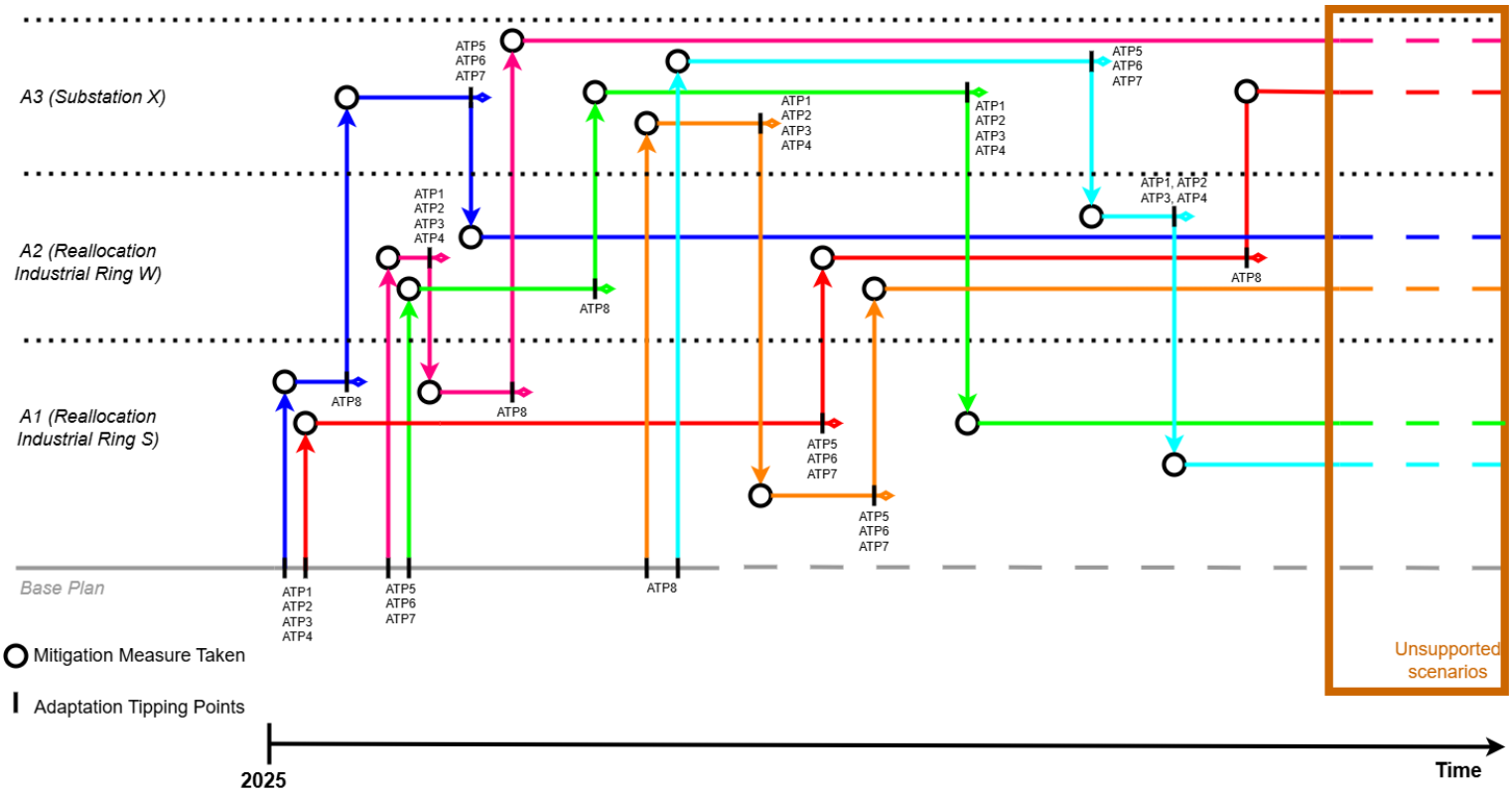

Figure 17: *Visualisation of the adaptive plan, using a DAPP MetroMap*

Figure *17* presents the adaptive policy pathways and their corresponding ATPs. Each ATP represents a set of scenario-dependent uncertainty combinations for which the candidate investment plan falls short. ATPs 1-4 correspond to conditions that trigger adaptive measure A1, ATPs 5-7 trigger A2, and ATP 8 triggers A3. The grey line represents the base plan, consisting of the alternative network configuration, the decision to construct substation H as a 21 kV substation in all scenarios and the temporary deployment of diesel and gas generators in all scenarios. This base plan forms the starting point from which all adaptive investment paths emerge.

7.6.1 ATP Interpretation

As the future evolves, the investment plan may encounter any of the ATPs, which require implementation of the corresponding adaptive measure. In line with the DAPP logic, these measures should ideally be taken before the ATP is reached, based on early-warning signals. The MetroMap should be read as follows: once an ATP is reached and a corresponding adaptive measure is taken, the system follows the line extending from the base plan. For example, when ATPs 1-4 occur, measure A1 is taken (red or blue line). Along these pathways, further ATPs may occur either ATP 8, which leads to A3 (construction of substation X), or ATPs 5-7 which leads to A2 (reallocation of industrial ring W). The adaptive pathways show path dependency. Once an adaptive measure is implemented, the investment plan follows the corresponding pathway and cannot revert to a previous state or switch to an alternative investment pathway. This reflects real-world irreversibility: once a ring is reallocated or a new substation is constructed the network configuration cannot readily return to its prior configuration.

7.6.2 Pathway Structure

The MetroMap displays six distinct investment paths that incorporate all adaptive measures. When ATPs 1-4 occur, measure A1 (reallocation of industrial ring S) must be implemented. Taking this action splits the base plan into two branches (blue and red), each characterised by a different order of subsequent adaptive actions. Investment paths where only one or two adaptive measures are implemented are indicated with the "$-\diamond$" symbol, reflecting futures in which the remaining uncertainty combinations do not satisfy the conditions for the remaining ATP/ATPs. Such investment paths can either be fully robust or experience remaining risky scenarios that are not captured by the adaptive rules implemented in the second simulation model.

7.6.3 Timing of Adaptive Measures

The MetroMap does not specify exact timings of when adaptive measures should be taken. On average, measures A1 and A2 require approximately one year to implement, whereas A3 requires seven years to implement. This difference in implementation times strengthens the case for the red or purple policy pathways as the preferred policy pathways. These two pathways invest gradually, allowing for lower cost and quick to implement measures to be deployed first while postponing the most expensive measure until it becomes strictly necessary. Table *12* shows that most substations begin to exhibit risky scenarios between 2040 and 2043. Since A1 and A2 can be implemented quickly, the decision to reallocate both the industrial rings of substation S and W should therefore be taken around 2039. The same table indicates that substation K begins to experience risky scenarios in 2049. Given that A3 (construction of substation X) requires roughly seven years, the decision to begin constructing this additional substation should be made around 2042. Note that this is only necessary if the future moves towards ATP8.

However, even with the implementation of all adaptive measures, a subset of the scenarios remains unsupported as shown by the brown box in the figure. No high-density PRIM boxes were identified for these remaining unsupported scenarios. In such cases, the feature importance results provide useful sensitivity indicators. For substation S, most-high scoring features (see *Substation Feature Scores*) are already incorporated as triggers in the adaptive rules. However, the feature scores also indicate uncertainty combinations that are not captured by the existing adaptive rules. For example, scenarios combining a high eHP share (mix_distribution_B) which is the third-highest feature for substation S with a long HHP lifespan (lifespan_hybrid_C) are not represented in any of the adaptive rules but can still produce risky scenarios. Such unmodelled combinations can explain the remaining unsupported scenarios.

7.7 Comparison of Investment Plans

In this Section the candidate, adaptive and worst case investment plan will be compared to each other. First the worst case investment plan configuration will be discussed. Thereafter, Table *13* will present a comparison table in which the investment plans are evaluated across three decision-criteria: short-term capacity risks (2025-2040), long-term capacity risks (2040-2052) and total investment costs. The underlying cost calculations can be found in Appendix *G*.

7.7.1 Worst Case Investment Plan Configuration

Before interpreting the scorecard, it is important to clarify the definition of the worst case investment plan. This investment plan represents a network configuration designed to withstand the most extreme demand and generation scenario with no regard of total investment costs.

Operationally, the worst case investment plan corresponds to the candidate investment network configuration combined with the assumption that all mitigation measures are implemented in 100% of scenarios, regardless of whether the underlying uncertainty conditions need them. In addition, the worst case investment plan includes the installation of an extra 150/50 kV transformer upstream. The complete network configuration associated with the worst-case investment plan is provided in Appendix *G.3.1*.

The worst-case investment plan eliminates capacity bottlenecks entirely by constructing all possible adaptive measures in every scenario. While this results in maximal robustness, it also is accompanied by the highest total costs, as every adaptive measure is implemented regardless of whether it is strictly necessary. In contrast, the candidate investment plan exhibits the lowest costs but performs poorly with respect to both short and long-term capacity risks.

7.7.2 Comparative Assessment of Investment Plans

The investment costs for the adaptive investment plan is the sum of the alternative network configuration plus in how many scenarios a mitigation measure is implemented. For instance, substation X is constructed in one-third of the scenarios, substation H is build as a 21 kV station in 100% of scenarios, and the reallocation of the industrial rings W and S occurs in roughly 70-73% of scenarios. The expected costs of the adaptive plan are therefore computed as:

$$\text{Total Costs [€]} = \frac{10001}{10001} \cdot € \text{ 55,000,000} + \frac{7320}{10001} \cdot € \text{ 4,500,000} + \frac{7090}{10001} \cdot € \text{ 4,500,000} + \frac{3334}{10001} \cdot € \text{ 128,980,000} = € \text{ 104,481,483}$$

When combined with the alternative network configuration costs (see Appendix *G.2*), this yields a total of expected investment costs of € 235.231.483 for the adaptive investment plan. Table *13* shows for each of the three investment plans, the short-term (ST) and long-term (LT) capacity risks, the total investment costs and the types of scenarios that cannot be supported. Since capacity risks and investment costs are expressed in different units and reflect different performance criteria, a Multi-Criteria Analysis (MCA) can be conducted in order to compare the investment plans. In this research, a MCA using min-max normalisation is included in Appendix *G.3.2*, purely as a demonstrative example. The responsibility for selecting and weighting the decision criteria ultimately rests with Stedin. Therefore, Table *13* shows a plain comparison between the three different investment plans and their total investment costs.

Decision Criteria \ Plans		Worst case	Candidate Investment Plan	Adaptive Investment Plan
Cap. Risks (ST)	**S**	0%	6%	1%
	W	0%	66%	0%
	H	0%	13%	0%
	K	0%	0%	0%
Cap. Risks (LT)	**S**	0%	83%	18%
	W	0%	38%	6%
	H	0%	83%	0%
	K	0%	22%	4%
Total Costs		€292.080.000	€83.700.000	€235.231.483
Unsupported scenarios		All scenarios can be supported	Scenarios with medium-to-fast heating transition in residential houses, medium-to-fast electric mobility, large datacenter scenarios, scenarios with a residential housing focus combined with medium-to-fast residential heating transition and scenarios with high electrification of the industry combined with medium-to-fast EV growth	Most scenarios can be supported. The remaining unsupported scenarios likely share the same key drivers of capacity risks as the candidate investment plan. However, these drivers are not fully captured by the current set of adaptive rules

Table 13: *Comparison table with multiple criteria per investment plan*

Overall, the comparison table demonstrates a clear trade-off between robustness and total investment costs. The worst-case plan maximises robustness at the expense of having invested too much. The candidate investment plan has the lowest costs but experiences the most capacity risks under long-term uncertainty. Especially scenarios that suffer from: medium-to-fast residential heating transition, medium-to-fast EV growth, residential expansion combined with the medium-to-fast residential heating transition and scenarios with high electrification of industrial activities combined with medium-to-fast EV growth, cannot be supported.

The adaptive investment plan provides a balanced outcome, maintaining a more robust and adaptive network configuration across a wide range of plausible futures while also limiting unnecessary investments. Furthermore, the remaining risky scenarios yield no dominant drivers of capacity risks, showcasing that the remaining capacity risks are diffuse across the uncertainty space. As a result, additional adaptive rules cannot be constructed based on the lack of dominant drivers in the second model iteration.

The adaptive investment plan aligns closely with Stedin's objective of managing deep uncertainty through a robust and adaptive investment plan. Taken together, the results of the first PRIM analysis and the second simulation iteration demonstrate how identified vulnerabilities can be translated into a more robust and adaptive investment strategy. In other words, it provides an answer for the third and final research question: "*How can these vulnerabilities be used to create a robust and adaptive investment strategy?*".

8 Discussion, Limitations & Recommendations

This Section will focus on the contribution of this thesis to the scientific debate, thereafter it will discuss the practical implications of this work, and limitations regarding this research will be discussed.

8.1 Scientific Debate

This research positions itself distinctly within existing literature. While the combined use of RDM and DAPP is well established, particularly in the context of flood risk management (Haasnoot et al., 2019; Ramm, Watson, & White, 2018), their application to electricity distribution expansion planning at a masterplan scale has never been done before. This research helps in creating an accessible narrative for robust and adaptive investment plans that reduce societal risks as described in the recommendations of (Wurth, 2022). Moreover, this research presents a noticeable step forward on the work of Marang (2025) by integrating adaptive measures to the electricity grid of the masterplan scale. Although coarse, the adaptive measures still prove effective in increasing robustness of the investment plan.

In addition, this research has been able to capture the complex nature of electricity demand and generation by simulating 10,001 plausible futures. Instead of complex model results, the PRIM analysis provided a limited number of key drivers for capacity risks. These drivers are subsequently translated into five interpretable storylines, thereby addressing one of the main concerns raised in the PRIM literature regarding the interpretability of scenario discovery results (Kwakkel & Cunningham, 2016). These storylines further enable stakeholder dialogue and participatory modelling. Academically, these storylines function as so-called boundary objects (Cuppen, Nikolic, Kwakkel, & Quist, 2020), bridging different social and professional domains. By translating complex PRIM results into policy-relevant narratives, the discussion shifts from technical system behaviour to strategic trade-offs such as the social acceptability of large scale datacenters in the area or increased urban expansion. Stakeholders may also introduce additional uncertainties, which can be readily integrated into the current modelling structure. In doing so, it increases transparency and trust in the simulation model and the broader RDM approach as tools for addressing deep uncertainty (Führer, 2025).

In contrast, Bloemen, Hammer, Van Der Vlist, Grinwis, and Van Alphen (2019) emphasize the critical role of monitoring systems for an successful implementation of adaptive strategies. Specifically, it is argued that the effectiveness of implementing adaptive strategies is dependent upon monitoring systems that can timely detect signals for plan adaptation. The development of such monitoring systems was beyond the scope of this thesis due to time constraints. Consequently, the design of a monitoring system that timely captures signals for plan adaptation is a recommendation for future research.

While recommending monitoring systems is a reasonable recommendation, it is important to note that developing such systems is not straightforward. In the simulation model, uncertainty parameters can be queried instantly, whereas in practice, many of these indicators are difficult to monitor, published infrequently or only available with substantial delay. Several key drivers identified in this research, such as residential heating transition, land use developments and EV growth illustrate this challenge. The CBS (2025b) publishes heat pump statistics, but the most recent data often lags by at least one year, meaning that real-time monitoring of heating transitions is not feasible. Furthermore, national land use statistics show even longer delays, with the latest figures dating back several years (CBS, 2017). In contrast, EV registrations

from the RVO (2026) are updated almost in real time, demonstrating that data availability and timelines vary significantly across uncertainties that need to be monitored. In summary, these differences imply that the practical value of a monitoring system depends strongly on whether timely, high-quality data streams exist for each identified long-term uncertainty that drives capacity risks.

8.2 Practical Debate

The results of this thesis demonstrate that the candidate investment strategy of Stedin is insufficiently robust against many plausible futures. In particular, capacity risks arise under scenarios combining the medium-to-fast residential heating transition with medium-to-fast EV growth, as well as under futures characterised by the emergence of large datacenters. By taking (adaptive) mitigation measures, the investment plan becomes significantly more robust against long-term capacity risks. Both the candidate and adaptive investment plans rely on the assumption that substation H an K will be realised in 2032, potentially with delays. The longer Stedin lingers to construct substation H and K, the less the electricity grid of the catchment area can cope with deep uncertainty. Therefore, Stedin must begin building substation H and K as soon as possible. When doing so, the results suggest that substation H should be constructed as a 21 kV substation instead of a 13 kV installation. Such a design choice provides full robustness for substation H against all simulated futures. In addition, reallocating the industrial rings of substations S and W to substation K significantly enhances robustness on substations S and W. Importantly, substation K avoids an substantial increase in capacity risks even though the industrial rings are reallocated to it. Finally, in scenarios characterised by the emergence of large datacenters, the results suggests that an additional substation may be required to prevent electricity overloads at substation K. In the absence of large-scale datacenter growth, substation K remains sufficiently robust.

From a practical perspective, the findings demonstrate that reliance on a small set of cornerstone scenarios is insufficient for managing deep uncertainty. Instead, the results show that adaptive planning approaches can be operationalised within a limited time frame and help increase robustness across a multiplicity of futures. While the simulation model and assumptions needs further refinement, the simulation model can already effectively assess two investment plans on robustness and adaptiveness. Importantly, as the simulation model has been internalised on Stedin's servers, it can be further generalised and applied to other electricity grids of Stedin. Furthermore, the interpretability of the PRIM results facilitate knowledge sharing across teams within Stedin. In doing so, it enriches the solution space and enables interdepartmental approaches to managing capacity risks under deep uncertainty.

Finally, a relevant policy discussion emerged during the final phase of this research. Dutch grid operators are currently debating whether to partially let go of the N-1 criterion (ACM, 2022). This criterion ensures availability of reserve capacity in the event of component failure. Relaxing this criterion would effectively increase the usable upper capacity of substations, thereby reducing the number of scenarios classified as risky. Ceteris paribus, under such "relaxing" conditions the candidate investment plan would become more robust. In the extreme, and highly unlikely, case where the N-1 criterion were fully abandoned, substation capacity would approximately double, rendering all simulated scenarios non-risky within the scope of this study. However, given regulatory constraints and practical considerations by grid operators, fully letting go of the N-1 criterion seems implausible. Should partially letting go of the N-1 criterion occur in practice, future research would need to explore if any key drivers of capacity risks are significantly effected by it.

8.3 Limitations

Certain limitations must be acknowledged. The categorical structure of the uncertainty space (bins A, B and C) resulted in coarse triggers, meaning that adaptive measures were sometimes activated in scenarios that did not strictly need them, thus increasing expected costs of the adaptive investment plan. Furthermore, even with the adaptive measures in place, some unsupported scenarios remain. These scenarios were not captured by the adaptive rules, meaning that there are still other combinations of uncertainties that lead to capacity risks. However, no high-density PRIM boxes could be found for the remaining risky scenarios. Therefore, future research should instead use continuous ranges to define the uncertainty space, as is done in many other scenario discovery papers (Bryant & Lempert, 2009; Wieles, Kwakkel, Auping, & Van Den End, 2024). In doing so, future research ensures that the adaptive measures are more accurate.

Next to this, other modelling limitations should also be acknowledged. A somewhat obvious limitation concerns the identification of long-term uncertainties. Different modellers or expert teams may identify additional uncertainties beyond those considered in this study. For instance, urban densification or the construction of entirely new cities have not been included. While urban densification has been an ongoing phenomenon in the Netherlands for several decades (RLI & BMC, 2023), the effect of densification is still debatable. While urban densification may lead to lower energy intensity per unit area (Trepci, Maghelal, & Azar, 2019), it can also result in higher peak electricity demand. Moreover, in response to the ongoing residential housing crisis, some political parties have proposed the construction of multiple new cities (AD, 2025a). The results of this research indicate that both residential heating transitions and residential expansion are key drivers of capacity risks. Although "black swans" like urban densification and construction of a city, have not been considered by this research, the findings suggest that including these long-term uncertainties would likely further increase capacity risks in the catchment area. More interesting, future research could extend the simulation model by introducing a "black swan" uncertainty. This uncertainty can be modelled to significantly increase or decrease demand or generation when activated. By allowing such an uncertainty to take extreme values in a subset of scenarios, the model can semi-account for disruptive future developments. Such an approach would strengthen the models ability to explore deep uncertainty and stress-test investment strategies.

In addition to long-term uncertainties, further adaptive measures could be explored. For example, the deployment of steerable HHPs has been advised to the Dutch House of Representatives by Netbeheer Nederland (2025b) as a means to improve congestion management. Due to time constraints, such measures were not implemented in this study. However, given that the lifespan of HHPs emerge across most substations as a key driver of capacity risks, future research into the effect of steerable HHPs represents a promising direction for further research. Moreover, while the adaptive measures prove effective in enhancing robustness, this research does not investigate the feasibility of each adaptive measure. For example, reallocating rings or constructing new substations involves regulatory, contractual and political challenges. While this is outside the scope of this thesis, such domains must be explored in order to effectively integrate the adaptive measures into the grid. Future research should focus on such aspects.

Another important modelling assumption concerns the electricity demand of heating technologies. The simulation model assumes a demand of 2 kW for HHPs and 5 kW for eHPs. These values typically occur only in extreme cold conditions and in houses with large loss areas. In other

words, under average conditions the actual electricity demand of such heating options is likely lower. With approximately 35,000 houses, a reduction of 2 kW would imply a 70 MVA demand reduction, which is comparable to the capacity of an entire 21 kV substation. As not all houses are assigned an eHP, this estimate serves more as thought experiment than a hard number. Nonetheless, it highlights that lowering the assumed eHP demand could significantly reduce substation electricity loads. Assuming that the categorical uncertainty space will become continuous as previously recommended, future research should take both heating options assumptions as an uncertainty with a continuos range. In doing so, sampling techniques like LHS can make a representative subset of this variable.

A similar consideration applies to the modelling of available surface of substation K. The ring downstream of substation K contains 875 ha of developable land, yet even in the most extreme scenario with the current uncertainty space the simulation model uses only 11% of this area. This indicates that, although spatial constraints were included as an uncertainty factor, the sampled scenario space was not broad enough to test the upper limits of land use in the catchment area of substation K. In other words, the scenario assumptions for growth potentials in the model (e.g. housing, industry, greenhouses, solar parks and wind turbines) may have been too conservative to meaningfully stress the land use constraint for substation K. Important to note is that for the other substations with less available land, the growth potentials do, in most scenarios, test the upper limits of land use for substations S, W and H. Nevertheless, future research should consider widening the scenario ranges for these growth potentials so that a larger share of the available surface is utilised on substation K. Doing so, would significantly increase electricity demand and generation in the catchment area, allowing the model to explore even more extreme futures.

During the implementation of the adaptive measures it became evident that the simulation model contained too few rings to allow meaningful reallocation across substations. For example, when adaptive measure "substation X" is implemented in a scenario, it takes over "half of the total electricity load" of substation K instead of taking over a ring, because there are not enough rings for reallocation. In practice, the area that is represented as a single ring in the simulation model often comprises multiple distinct rings in the real electricity network. If rings had been defined at a finer level, more nuanced and targeted adaptive reallocation measures could have been implemented. Note that this would not eliminate the capacity risks identified in this research, but it would allow for more optimal and/or realistic reallocation of electricity load across substations. Future research should therefore consider a finer level for ring aggregation.

A further limitation concerns the data reduction strategy applied prior to the PRIM analysis. To manage computational constraints of Python, two data reduction strategies were used. The first, retained per scenario ten datapoints each reflecting a specific simulated year (min-max reduction). The second, retained per scenario one hundred datapoints each reflecting ten representative days for each simulated year (no-duplicates reduction). Only the first strategy yielded PRIM boxes with sufficiently high density and was therefore used for scenario discovery. This introduces bias towards uncertainties that drive extreme peak demand, meaning that uncertainty combinations causing capacity risks through moderate demand/generation may be under-represented in the identified key drivers. The derived storylines remain valid, but the true vulnerability space may be somewhat broader than the results indicate.

Finally, computational performance represents a practical limitation. Simulating 10,001 different

scenarios already required roughly 24 hours of computation time. After introducing the eight adaptive measures, which were implemented as relatively simple conditional statements, total runtime increased to approximately 40 hours. For the model to be operationally useful to Stedin, future work should either increase available computational resources, such as additional cores and RAM, or encode the simulation model in a more computationally efficient programming language than Python, such as PySpark or C++ (Ahmed et al., 2026). Moreover, Stedin could hire a professional Python developer to optimise the code of the simulation model, thereby also improving computational efficiency and reducing overall runtime.

Despite the discussed limitations, the results provide valuable insights for assessing whether Stedin's investment plans are robust and adaptive across a wide range of plausible futures.

9 Conclusions

The main research question of this thesis is: "*How can an RDM based method be used to create a robust and adaptive investment strategy for electricity distribution networks on a masterplan scale?*"
In order to answer this main question, three sub-questions were constructed:

1. "*What are the long-term uncertainties that influence the effectiveness of an investment strategy?* "

2. "*What are the vulnerabilities of the candidate investment plan, given the long-term uncertainties?*"

3. "*How can these vulnerabilities be used to create a robust and adaptive investment strategy?*"

In addressing the first sub-question regarding long-term uncertainties, this study identified 32 long-term uncertainties across 16 categories. Such long-term uncertainties include: residential heating transition, residential/industrial PV installations, the growth of EVs, shore power adoption, construction of solar and wind parks, surface allocation constraints and datacenter construction. An important modelling choice was the moderating role of surface constraints. By capping the growth of different model components based on available land area, the simulation avoided unrealistic, unlimited growing electricity demand and generation profiles. The high number of uncertainties, which are all categorically divided, formed a vast uncertainty space with billions of scenarios. A subset of 10,000 scenarios was created by using LHS. In doing so, the sample set ensured uniform coverage over the input space.

Stress-testing the candidate investment plan revealed significant vulnerabilities, answering the second research question. The candidate investment plan proved insufficient under deep uncertainty, with substation S and H exhibiting capacity risks in approximately 83% of scenarios by 2052. While W and K exhibit lower proportions of risky scenarios (39% and 22% respectively), these levels remain insufficient for effectively managing deep uncertainty. Through the PRIM analysis, these found vulnerabilities were translated into five storylines: (1) medium-to-fast residential housing transition, (2) medium-to-fast electric mobility growth, (3) the emergence of large datacenters in rural area (>30 MVA), (4) residential housing expansion combined with medium-to-fast residential heating transition, (5) high-industrial electrification combined with medium-to-fast EV growth. These storylines cause significant capacity risks on the substations. Thus, showing the vulnerabilities of the candidate investment plan given the long-term uncertainties.

Knowing these five storylines, mitigation measures were formulated to answer the third and final research question. The adaptive investment plan combined the alternative network configuration with the decision to construct substation H as a 21 kV substation as well as temporary deployment of diesel/gas generators in all scenarios. Three distinct adaptive mitigation measures were available to Stedin: reallocation of industrial ring S, reallocation of industrial ring W, and the construction of one additional substation X. The implementation of adaptive measures significantly enhanced the robustness of the adaptive investment plan compared to the candidate investment plan. For example, reallocating rings reduced the share of risky scenarios on substation S from 83% to 18%, while the 21 kV substation choice rendered substation H fully robust against all simulated futures. Accordingly, the evidence supports a clear recommendation to construct substation H as a 21 kV substation. Thus, by converting the vulnerabilities of the

candidate investment plan into scenario dependent adaptive rules, Stedin now has a more robust and adaptive investment strategy that can adaptively deal with a wide range of plausible futures, answering the third research question. While this is technically not "**a** robust and adaptive investment strategy", it did show that incorporating adaptive rules significantly enhanced robustness of the investment strategy. Incorporating more adaptive rules may be able to provide fully robust investment strategies for Stedin.

By integrating the PRIM findings in a MetroMap visualisation, the timing of the adaptive measures can be further specified. The analysis indicates that industrial ring reallocation is a relatively quick measure that can be implemented. Given that capacity bottlenecks occur around 2040-2043 period for most substations, the choice to reallocate industrial rings must happen around 2039 in order to enhance the robustness on substations S and W. Finally, the construction of substation X becomes relevant in large datacenter growth scenarios, with the decision trigger occurring around 2042 given the seven years lead time of substation construction. Some scenarios remain unsupported in the adaptive investment plan. While the second PRIM analysis yielded no key drivers for these remaining risky scenarios, the feature importance scores of the first iteration indicate which uncertainties may still contribute to the remaining capacity risks. Some combinations of uncertainties (for example, a high eHP share occurring with a long HHP lifespan) did not appear in the PRIM analysis as high-density boxes and were therefore not incorporated into the adaptive rules logic. As a result, some scenarios will remain risky because their specific uncertainty combinations were not identified by the PRIM analysis of the first iteration. In order to fully mitigate all risky scenarios either more adaptive measures or monitoring systems must be built.

Beyond the technical functioning of the electricity grid, this research demonstrates that PRIM-derived storylines can improve stakeholder dialogue. It shifts the discussion from an expert-driven assessment of capacity risks towards a transparent evaluation of societal risk acceptance. In particular, it enables stakeholders to explicitly weigh pros and cons of the future developments such as new datacenter construction or residential housing projects against clearly defined limits (ATPs) at which the electricity grid becomes vulnerable to capacity risks. The comparison table of the three investment plans can also support stakeholder dialogue. In particular, it provides Stedin with a basis for deliberating the trade-off between increased robustness and the higher investment costs associated with the three investment plans.

Ultimately, the results yield a critical temporal recommendation: Stedin must proceed with the construction of substation H an K immediately (for without these two substations the electricity grid will succumb to deep uncertainty resulting in high capacity risks) and the decision to built substation H as a 21 kV substation must be finalised as soon as possible to accommodate the average lead time of building substations and to prevent early lock-in. Next to this, reallocating the industrial rings of S and W can significantly relieve long-term capacity bottlenecks especially when the future moves towards a medium-to-fast housing transition combined with medium-to-fast EV growth. Moreover, when the future moves towards the emergence of large datacenters, Stedin must construct an additional substation to relieve substation K of long-term capacity bottlenecks. This research concludes that an RDM based method provides the necessary analytical tool to create a more robust and adaptive investment strategy for electricity distribution networks on a masterplan scale, therefore answering the main research question.

References

ACM. (2022, 12). *Ontwerpcodebesluit enkelvoudige storingsreserve.* Retrieved from https://www.acm.nl/nl/publicaties/ontwerpcodebesluit-enkelvoudige-storingsreserve

Ahmed, I., Ahmed, N., Batool, K., Mahmood, J., Fatima, E., & Arshad, P. (2026). *Performance comparison of C++, Java, and Python: A comprehensive analysis of programming languages.* Retrieved from https://doi.org/10.1007/978-981-95-2212-5_24 doi: 10.1007/978-981-95-2212-5\{_}24

Aji, H., Goyal, N., Pfenninger, S., & Nikolic, I. (2025, 9). Considering adaptive power system planning for Indonesia in the face of climate uncertainties. *IEEE*, 143–148. Retrieved from https://doi.org/10.1109/ict-pep67281.2025.11232371 doi: 10.1109/ict-pep67281.2025.11232371

Algemeen Dagblad. (2025a). *D66-leider rob jetten: tien nieuwe steden bouwen.* Retrieved 2025-01-01, from https://www.ad.nl/politiek/d66-leider-rob-jetten-tien-nieuwe-steden-bouwen

Algemeen Dagblad. (2025b). *Datacenters niet welkom in Westland, zodat voldoende stroom overblijft voor inwoners en bedrijven.* Retrieved from https://www.ad.nl/westland/datacenters-niet-welkom-in-westland-zodat-voldoende-stroom-overblijft-voor-inwoners-en-bedrijven~ad583384/?referrer=https%3A%2F%2Fwww.google.com%2F

AlleCijfers.nl. (2025a, 10). *Gemeente XXXXXXXXX in cijfers en grafieken.* Retrieved from https://allecijfers.nl/gemeente/XXXXXXXXX/

AlleCijfers.nl. (2025b, 10). *Gemeente XXXXXXXXX in cijfers en grafieken.* Retrieved from https://allecijfers.nl/gemeente/XXXXXXXXX/

AlleCijfers.nl. (2025c, 10). *Woonplaats XXXXXXXXX (gemeente XXXXXXXXX) in cijfers en grafieken.* Retrieved from https://allecijfers.nl/woonplaats/XXXXXXXXX/

Aneli, S., Tina, G. M., & Gagliano, A. (2025, 8). Modelling and experimental surveys on the energy consumption of a small-scale data center. *Energy Efficiency*, *18*(6). Retrieved from https://doi.org/10.1007/s12053-025-10357-7 doi: 10.1007/s12053-025-10357-7

Arciniegas Rueda, I., Gill, D., & van Soest, H. (2025, 12). *The Cost of Misforecasting: How Ignoring Non-AI demand risks the grid.* Retrieved from https://www.rand.org/pubs/commentary/2025/12/the-cost-of-misforecasting-how-ignoring-non-ai-demand-risks-the-grid.html

Atwa, O. S. E. (2019). *Substations.* Elsevier eBooks. Retrieved from https://doi.org/10.1016/b978-0-12-816858-5.00002-2 doi: 10.1016/b978-0-12-816858-5.00002-2

Bartholomew, E., & Kwakkel, J. H. (2020). On considering robustness in the search phase of Robust Decision Making: A comparison of Many-Objective Robust Decision Making, multi-scenario Many-Objective Robust Decision Making, and Many Objective Robust Optimization. *Environmental Modelling & Software*, *127*, 104699. Retrieved from https://doi.org/10.1016/j.envsoft.2020.104699 doi: 10.1016/j.envsoft.2020.104699

Bloemen, P. J. T. M., Hammer, F., Van Der Vlist, M. J., Grinwis, P., & Van Alphen, J. (2019). *DMDU into Practice: Adaptive Delta Management in The Netherlands.* Retrieved from https://doi.org/10.1007/978-3-030-05252-2_14 doi: 10.1007/978-3-030-05252-2\{_}14

Borozan, S., Giannelos, S., & Strbac, G. (2021, 12). Strategic network expansion planning with electric vehicle smart charging concepts as investment options. *Advances in Applied Energy*, *5*, 100077. Retrieved from https://doi.org/10.1016/j.adapen.2021.100077 doi: 10.1016/j.adapen.2021.100077

Bouwmans, I. (2017). *TB241E - Fysische Transportverschijnselen.* Retrieved from https://

eduweb.eeni.tbm.tudelft.nl/TB241E/?energie_wind#:~:text=Bovendien%20is%20de%20toestand%20stationair,zien%20is%20in%20figuur%201.&text=Daarmee%20kunnen%20we%20het%20theoretisch,de%20inhoud%20van%20deze%20module.

Bryant, B. P., & Lempert, R. J. (2009, 10). Thinking inside the box: A participatory, computer-assisted approach to scenario discovery. *Technological Forecasting and Social Change*, *77*(1), 34–49. Retrieved from https://doi.org/10.1016/j.techfore.2009.08.002 doi: 10.1016/j.techfore.2009.08.002

Canon van Nederland. (n.d.). *Het plan van Lely.* Retrieved from https://www.canonvannederland.nl/nl/flevoland/flevoland/het-plan-van-lely

Caterpillar PM1360. (n.d.). Retrieved from https://www.agriaffaires.nl/tweedehands/generators/44527404/caterpillar-pm1360.html

Centraal Bureau voor de Statistiek. (2017). *CBS Statline.* Retrieved from https://opendata.cbs.nl/#/CBS/en/dataset/70262ENG/table

Centraal Bureau voor de Statistiek. (2021). *Woningen; hoofdverwarmingsinstallaties, regio 2017-2022.* Retrieved from https://opendata.cbs.nl/#/CBS/nl/dataset/84948NED/table

Centraal Bureau voor de Statistiek. (2024a). *CBS Statline.* Retrieved from https://opendata.cbs.nl/#/CBS/nl/dataset/81955NED/table?fromstatweb

Centraal Bureau voor de Statistiek. (2024b). *CBS Statline Landbouw.* Retrieved from https://opendata.cbs.nl/#/CBS/nl/dataset/80781NED/table?fromstatweb

Centraal Bureau voor de Statistiek. (2025a). *Elektriciteitsbalans.* Retrieved from https://opendata.cbs.nl/#/CBS/nl/dataset/84575NED/line?ts=1746558564792

Centraal Bureau voor de Statistiek. (2025b). *Groei aantal warmtepompen neemt af.* Retrieved from https://www.cbs.nl/nl-nl/nieuws/2025/19/groei-aantal-warmtepompen-neemt-af

Centraal Bureau voor de Statistiek. (2025c). *Prijzen nieuwbouwkavels stegen verder door in 2024.* Retrieved from https://www.cbs.nl/nl-nl/nieuws/2025/14/prijzen-nieuwbouwkavels-stegen-verder-door-in-2024

Centraal Bureau voor de Statistiek. (2025d). *Voorraad woningen; gemiddeld oppervlak; woningtype, bouwjaarklasse, regio.* Retrieved from https://opendata.cbs.nl/#/CBS/nl/dataset/82550NED/table?fromstatweb

Choi, Y., Song, D., Yoon, S., & Koo, J. (2021, 1). Comparison of factorial and Latin hypercube sampling designs for Meta-Models of building Heating and Cooling loads. *Energies*, *14*(2), 512. Retrieved from https://doi.org/10.3390/en14020512 doi: 10.3390/en14020512

Cuppen, E., Nikolic, I., Kwakkel, J., & Quist, J. (2020, 10). Participatory multi-modelling as the creation of a boundary object ecology: the case of future energy infrastructures in the Rotterdam Port Industrial Cluster. *Sustainability Science*, *16*(3), 901–918. Retrieved from https://doi.org/10.1007/s11625-020-00873-z doi: 10.1007/s11625-020-00873-z

DataScienceGenie. (2025). *Latin Hypercube Sampling vs. Monte Carlo Sampling – Data Science Genie.* Retrieved from https://datasciencegenie.com/latin-hypercube-sampling-vs-monte-carlo-sampling/#:~:text=One%20can%20say%20that%20a,to%20obtain%20some%20particular%20precision.

Dawes, G., Kirant-Mitić, T., Jiang, Z., Dréau, J. L., Cai, H., Cui, J., ... Dong, B. (2025a, 7). Energy flexibility at multi-building scales: A review of the dominant factors and their uncertainties. *Energy and Buildings*, 116157. Retrieved from https://doi.org/10.1016/j.enbuild.2025.116157 doi: 10.1016/j.enbuild.2025.116157

De Haan, A., & De Heer, P. (2015). *Solving complex problems.* Boom uitgevers Amsterdam.

de Kort, E.-J., Gradussen, M., & Groep, S. (2023, 4). *Feiten en cijfers bedrijventerreinen in Nederland* (Tech. Rep.). Retrieved from https://www.rli.nl/sites/default/files/

stec_groep_rapport_feiten_en_cijfers_def.pdf

De Lima, T. D., Lezama, F., Soares, J., Franco, J. F., & Vale, Z. (2024, 7). Modern distribution system expansion planning considering new market designs: Review and future directions. *Renewable and Sustainable Energy Reviews*, *202*, 114709. Retrieved from https://doi.org/10.1016/j.rser.2024.114709 doi: 10.1016/j.rser.2024.114709

Dialogic. (2025). *Verkenning regionale impact datacenters Zuid-Holland* (Tech. Rep.). Retrieved from https://www.zuid-holland.nl/publish/besluitenattachments/behandelvoorstel-motie-1718-provinciale-datacenterstrategie/verkenning-regionale-impact-datacenters-zuid-holland.pdf

Dutch Data Center Association. (2025, 1). *Factsheet - Dutch Data Center Association.* Retrieved from https://www.dutchdatacenters.nl/en/factsheet/#:~:text=Data%20centers%20have%20been%20actively,%3C1.2%20in%20the%20MRA).&text=With%2055%25%20of%20the%20working,CO2%20emissions%20from%20Greater%20London.

Ehsan, A., & Yang, Q. (2019, 1). State-of-the-art techniques for modelling of uncertainties in active distribution network planning: A review. *Applied Energy*, *239*, 1509–1523. Retrieved from https://doi.org/10.1016/j.apenergy.2019.01.211 doi: 10.1016/j.apenergy.2019.01.211

Engholm, A., & Kristoffersson, I. (2025, 7). Exploring "Many Objective Robust Decision Making" for managing uncertainty in climate policy analysis for the transport sector. *Transportation Research Interdisciplinary Perspectives*, *32*, 101524. Retrieved from https://doi.org/10.1016/j.trip.2025.101524 doi: 10.1016/j.trip.2025.101524

Führer, K. (2025, 10). *Participatory Decision-Making under Deep Uncertainty: Modeling mobility transitions.* Retrieved from https://doi.org/10.4233/uuid:dfde52d8-0f64-4f21-8759-76c0c2b7e84b doi: 10.4233/uuid:dfde52d8-0f64-4f21-8759-76c0c2b7e84b

Gemeente. (2023). *Gemeente XXXXXXXXX.* Retrieved from https://www.XXXXXXXXX.nl/Alle_onderwerpen/Bouwen_en_verbouwen/Ruimtelijke_plannen/Zonnepark_XXXXXXXXX/Ontwerp

Gemeente. (2024, 7). *Energietransitie.* Retrieved from https://www.XXXXXXXXX.nl/Alle_onderwerpen/Duurzaamheid/Energietransitie

Grove, S. (2025, 1). *Aantallen en oppervlaktes - Dutch Data Center Association.* Retrieved from https://www.dutchdatacenters.nl/aantallen-oppervlaktes/

Groves, D. G., Molina-Perez, E., Bloom, E., & Fischbach, J. R. (2019). *Robust Decision Making (RDM): application to water planning and climate policy.* Retrieved from https://doi.org/10.1007/978-3-030-05252-2_7 doi: 10.1007/978-3-030-05252-2\{_}7

Guivarch, C., Rozenberg, J., & Schweizer, V. (2016, 3). The diversity of socio-economic pathways and CO2 emissions scenarios: Insights from the investigation of a scenarios database. *Environmental Modelling & Software*, *80*, 336–353. Retrieved from https://doi.org/10.1016/j.envsoft.2016.03.006 doi: 10.1016/j.envsoft.2016.03.006

Haasnoot, M., Warren, A., & Kwakkel, J. H. (2019). *Dynamic Adaptive Policy Pathways (DAPP).* Retrieved from https://doi.org/10.1007/978-3-030-05252-2_4 doi: 10.1007/978-3-030-05252-2\{_}4

Hellema, J. P. D. (2012). *Hoe Nederland neutraal probeerde te blijven tussen 1914 en 1918.* Retrieved from https://studenttheses.uu.nl/handle/20.500.12932/10166

Hemmati, R., Hooshmand, R.-A., & Taheri, N. (2015, 6). Distribution network expansion planning and DG placement in the presence of uncertainties. *International Journal of Electrical Power & Energy Systems*, *73*, 665–673. Retrieved from https://doi.org/10.1016/j.ijepes.2015.05.024 doi: 10.1016/j.ijepes.2015.05.024

Hennig, R. J., De Vries, L. J., & Tindemans, S. H. (2023, 9). Congestion management in

electricity distribution networks: Smart tariffs, local markets and direct control. *Utilities Policy*, *85*, 101660. Retrieved from https://doi.org/10.1016/j.jup.2023.101660 doi: 10.1016/j.jup.2023.101660

Hennig, R. J., De Vries, L. J., & Tindemans, S. H. (2024, 1). Risk vs. restriction—An investigation of capacity-limitation based congestion management in electric distribution grids. *Energy Policy*, *186*, 1-2. Retrieved from https://doi.org/10.1016/j.enpol.2023.113976 doi: 10.1016/j.enpol.2023.113976

Hommelberg, M., Biemans, A., Janssen, G., & Poiesz, T. (2025, 1). *Netimpact woningen met warmtepomp* (Tech. Rep.). Retrieved from https://www.rvo.nl/sites/default/files/2025-02/Rapport-Netimpact-woningen-met-warmtepomp.pdf

Jiang, H., Vogt-Schilb, A., Spyrou, E., & Hobbs, B. F. (2025). Using robust decision analysis to develop adaptive strategies for power system expansion in Bangladesh. *Energy Systems*. Retrieved from https://doi.org/10.1007/s12667-025-00725-8 doi: 10.1007/s12667-025-00725-8

Keen, J., Giraldez, J., Cook, E., Eiden, A., Placide, S., Hirayama, A., ... Eldali, F. (2022). *Distribution Capacity expansion: current practice, opportunities, and decision support* (Tech. Rep. No. NREL/TP-6A40-83892). Retrieved from https://www.nrel.gov/docs/fy23osti/83892.pdf

Kieviet, E., & Dietvorst. (2025, 2). *Rotterdamse haven krimpt, gemeente en provincie slaan alarm bij kabinet.* Retrieved from https://nos.nl/artikel/2555301-rotterdamse-haven-krimpt-gemeente-en-provincie-slaan-alarm-bij-kabinet

Klimaatmonitor. (n.d.). Retrieved from https://klimaatmonitor.databank.nl/Jive?workspace_guid=46540e4a-c3a8-40ad-89a4-48fd4b53a58e

Kobayashi, H., Kaihara, T., Kokuryo, D., Tanaka, R., Hara, M., Miyachi, Y., & Sariddichainunta, P. (2023). *A Proposal of Resilient Supply Chain Network Planning Method with Supplier Selection and Inventory Levels Determination Using Two-Stage Stochastic Programming.* Retrieved from https://doi.org/10.1007/978-3-031-43688-8_49 doi: 10.1007/978-3-031-43688-8\{_}49

Koelman, M., Hartmann, T., & Spit, T. J. (2025, 7). Stepping up regionally: Governing local land use conflicts through regional energy approaches. *Energy Research & Social Science*, *127*, 104228. Retrieved from https://doi.org/10.1016/j.erss.2025.104228 doi: 10.1016/j.erss.2025.104228

Kremers, E. (2013). *Modelling and simulation of electrical energy systems through a complex systems approach using Agent-Based models.* Retrieved from https://books.google.nl/books?hl=nl&lr=&id=7l3SXJ_FJEEC&oi=fnd&pg=PP2&dq=(%22complex+systems%22)+and+(%22electricity%22)&ots=aWO2F8nllt&sig=0z2Ak6FJighhj5tnIOhD86U7D0w#v=onepage&q=(%22complex%20systems%22)%20and%20(%22electricity%22)&f=false

Kruglov, L., & Brodsky, Y. (2021). MODEL-ORIENTED PROGRAMMING. *Proceedings of CBU in Natural Sciences and ICT*, *2*, 63–67. Retrieved from https://doi.org/10.12955/pns.v2.154 doi: 10.12955/pns.v2.154

Kwakkel. (2017). The Exploratory Modeling Workbench: An open source toolkit for exploratory modeling, scenario discovery, and (multi-objective) robust decision making. *Environmental Modelling & Software*, *96*, 239–250. Retrieved from https://doi.org/10.1016/j.envsoft.2017.06.054 doi: 10.1016/j.envsoft.2017.06.054

Kwakkel. (2018). *A generalized many-objective optimization approach for scenario discovery.* Retrieved from https://www.deepuncertainty.org/wp-content/uploads/2018/12/dmdu2018_a_generalized_many-objective_optimization_approach_for_scenario

_discovery.pdf
Kwakkel. (2023). *Open exploration — Exploratory Modeling Workbench.* Retrieved from https://emaworkbench.readthedocs.io/en/latest/indepth_tutorial/open-exploration.html
Kwakkel. (2024). *Open exploration & vulnerability analysis lecture 3.* Retrieved from https://brightspace.tudelft.nl/d2l/le/content/681279/viewContent/4124179/View
Kwakkel, & Cunningham, S. (2016, 7). Improving scenario discovery by bagging random boxes. *Technological Forecasting and Social Change*, *111*, 124–134. Retrieved from https://doi.org/10.1016/j.techfore.2016.06.014 doi: 10.1016/j.techfore.2016.06.014
Kwakkel, & Haasnoot, M. (2019). *Supporting DMDU: A Taxonomy of Approaches and tools.* Retrieved from https://doi.org/10.1007/978-3-030-05252-2_15 doi: 10.1007/978-3-030-05252-2\{_}15
Kwakkel, Haasnoot, M., & Walker, W. E. (2016). Comparing Robust Decision-Making and Dynamic Adaptive Policy Pathways for model-based decision support under deep uncertainty. *Environmental Modelling & Software*, *86*, 168–183. Retrieved from https://doi.org/10.1016/j.envsoft.2016.09.017 doi: 10.1016/j.envsoft.2016.09.017
Kwakkel, & Jaxa-Rozen. (2015, 12). Improving scenario discovery for handling heterogeneous uncertainties and multinomial classified outcomes. *Environmental Modelling & Software*, *79*, 311–321. Retrieved from https://doi.org/10.1016/j.envsoft.2015.11.020 doi: 10.1016/j.envsoft.2015.11.020
Lawrence, J., Haasnoot, M., McKim, L., Atapattu, D., Campbell, G., & Stroombergen, A. (2019). *Correction to: Dynamic Adaptive Policy Pathways (DAPP): from theory to practice.* Retrieved from https://doi.org/10.1007/978-3-030-05252-2_18 doi: 10.1007/978-3-030-05252-2\{_}18
Lempert, R. J. (2019). *Robust Decision Making (RDM).* Retrieved from https://doi.org/10.1007/978-3-030-05252-2_2 doi: 10.1007/978-3-030-05252-2\{_}2
Liander. (2024). *Ontwerp Investeringsplan 2024 Elektriciteit en gas* (Tech. Rep.). Retrieved from https://www.liander.nl/-/media/files/financiele-communicatie/investeringsplannen/investeringsplannen-2024/investeringsplan-liander-elektriciteit-en-gas-2024-consultatieversie.pdf
Löffler, C., Geertsma, R., Polinder, H., & Coraddu, A. (2025, 7). Energy management for hybrid and fully electric vessels via a multi-objective Equivalent Consumption Minimization Strategy. *Energy Conversion and Management*, *343*, 120150. Retrieved from https://doi.org/10.1016/j.enconman.2025.120150 doi: 10.1016/j.enconman.2025.120150
Maier, H., Guillaume, J., Van Delden, H., Riddell, G., Haasnoot, M., & Kwakkel, J. (2016). An uncertain future, deep uncertainty, scenarios, robustness and adaptation: How do they fit together? *Environmental Modelling & Software*, *81*, 154–164. Retrieved from https://doi.org/10.1016/j.envsoft.2016.03.014 doi: 10.1016/j.envsoft.2016.03.014
Marang, M. (2025). *Robust investment strategies for electricity distribution network expansion* (Tech. Rep.). Retrieved from https://github.com/mmarang/Thesis/tree/main/Report
Marchau, V. A. W. J., Walker, W. E., Bloemen, P. J. T. M., & Popper, S. W. (2019a). *Decision Making under Deep Uncertainty.* Retrieved from https://doi.org/10.1007/978-3-030-05252-2 doi: 10.1007/978-3-030-05252-2
Marchau, V. A. W. J., Walker, W. E., Bloemen, P. J. T. M., & Popper, S. W. (2019b). *Introduction.* Retrieved from https://doi.org/10.1007/978-3-030-05252-2_1 doi: 10.1007/978-3-030-05252-2\{_}1
Ministerie van Algemene Zaken. (2025, 6). *Europese en wereldwijde samenwerk-*

ing tegen klimaatverandering. Retrieved from https://www.rijksoverheid.nl/onderwerpen/klimaatverandering/europese-en-wereldwijde-samenwerking-tegen-klimaatverandering

Ministerie van Economische Zaken en Klimaat. (2023). *Nationaal plan energiesysteem (NPE).* Retrieved from https://www.rvo.nl/onderwerpen/energiesysteem/nationaal-plan-energiesysteem

Ministerie van Infrastructuur en Waterstaat. (2025). *Kaarten — Atlas Leefomgeving.* Retrieved from https://www.atlasleefomgeving.nl/kaarten?config=3ef897de-127f-471a-959b-93b7597de188&use=piwiksectorcode&layerFilter=Standaard%20gebruiker&gm-x=150000&gm-y=460000&gm-z=3&gm-b=1544180834512,true,1;1673944133227,true,1

Ministerie van Klimaat en Groene Groei. (2024). *Reactie over onderinvesteringen op investeringsplannen netbeheerders.* Retrieved from https://www.rijksoverheid.nl/documenten/rapporten/2024/05/21/bijlage-2-brief-reactie-aan-acm-melding-acm-van-onderinvesteringen-op-de-investeringsplannen-van-de-netbeheerders-en-brief-n-a-v-toetsing-gelakt

Ministerie van Klimaat en Groene Groei. (2025). *Schakelen naar de toekomst* (Tech. Rep.). Retrieved from https://www.rijksoverheid.nl/documenten/rapporten/2025/03/07/schakelen-naar-de-toekomst-over-bekostiging-elektriciteitsinfrastructuur

Netbeheer Nederland. (2025a, 2). *Groei aantal huishoudens met zonnepanelen flink afgenomen.* Retrieved from https://www.netbeheernederland.nl/artikelen/nieuws/groei-aantal-huishoudens-met-zonnepanelen-flink-afgenomen

Netbeheer Nederland. (2025b). *Inbreng voor het eerste debat Netcongestie van de nieuwe Kamer.* Retrieved from https://www.netbeheernederland.nl/artikelen/nieuws/inbreng-voor-het-eerste-debat-netcongestie-van-de-nieuwe-kamer

Netbeheer Nederland. (2025c). *Netbeheer Nederland Scenario's editie 2025.* Retrieved from https://www.netbeheernederland.nl/publicatie/netbeheer-nederland-scenarios-editie-2025

Netbeheer Nederland, Stedin, Enexis, Gasunie, Liander, TenneT, ... Elaadnl (2019). *Basisdocument over energie-infrastructuur (oktober 2019).* Retrieved from https://www.netbeheernederland.nl/publication/basisdocument-over-energie-infrastructuur-oktober-2019

Nikolic, I., Warnier, M., Kwakkel, J., Chappin, E., Lukszo, Z., Brazier, F., ... Palensky, P. (2019). Principles, challenges and guidelines for a multi-model ecology. *Google Scholar*. Retrieved from https://repository.tudelft.nl/islandora/object/uuid%3A1aa3d16c-2acd-40ce-b6b8-0712fd947840 doi: 10.4233/uuid:1aa3d16c-2acd-40ce-b6b8-0712fd947840

NOS. (2025, 12). *Datacenters gebruiken enorm veel stroom: wat kost het en wat levert het op?* Retrieved from https://nos.nl/artikel/2594731-datacenters-gebruiken-enorm-veel-stroom-wat-kost-het-en-wat-levert-het-op

NVDE, N. V. D. E. (2020, 1). *Hernieuwbare energiebronnen op land in de Regionale Energiestrategie (RES)* (Tech. Rep.). Retrieved from https://www.nvde.nl/wp-content/uploads/2020/02/NVDE-Hernieuwbare-energiebronnen-op-land-in-de-Regionale-Energiestrategie-feb2020.pdf

Ovaere, M., & Proost, S. (2016, 1). Electricity transmission reliability: The impact of reliability Criteria. *SSRN Electronic Journal*. Retrieved from https://doi.org/10.2139/ssrn.2874192 doi: 10.2139/ssrn.2874192

PacketPower. (n.d.). *How warmer weather impacts data center cooling and power consumption.* Retrieved from https://www.packetpower.com/warmer-weather-impacts-data

-center-cooling-and-power-consumption
Painuly, J. P., & Wohlgemuth, N. (2020). *Renewable energy technologies: barriers and policy implications.* Retrieved from https://doi.org/10.1016/b978-0-12-820539-6.00018-2 doi: 10.1016/b978-0-12-820539-6.00018-2
Parmar, N. M. D., & Parmar, N. S. (2024, 4). Survey on Concept of Object-Oriented Programming. *International Journal of Scientific Research in Computer Science Engineering and Information Technology*, *10*(2), 427–431. Retrieved from https://doi.org/10.32628/cseit243647 doi: 10.32628/cseit243647
Patel, D., Ontiveros, J. E., & Nishball, D. (2024, 10). *Datacenter Anatomy Part 1: Electrical systems.* Retrieved from https://newsletter.semianalysis.com/p/datacenter-anatomy-part-1-electrical
Petřík, T. (2024). *Distribution Strategy Planning: A Comprehensive Probabilistic Approach for Unpredictable Environment* (Tech. Rep. No. IES Working Papers 19/2024). Retrieved from https://www.econstor.eu/handle/10419/300176
Phase to Phase – Netten voor distributie van elektriciteit, hoofdstuk 10. (2011). Retrieved from https://www.phasetophase.nl/boek/boek_2_10.html
PRIM-TMIP EMAT. (n.d.). Retrieved from https://tmip-emat.github.io/source/emat.analysis/prim.html
PWC, P. A. N. (2025). *Financiële Impact Energietransitie voor Netbeheerders ("FIEN+")* (Tech. Rep.). Retrieved from https://bijlagen.nos.nl/artikel-22251257/download.pdf
R News. (2021, 12). *Onderzoek: Windmolens XXXXXXXXX naar XXXXXXXXX.* Retrieved from https://www.XXXXXXXXX.nl/nieuws/141562/onderzoek-windmolens-XXXXXXXXX-naar-XXXXXXXXX
Raad voor Leefomgeving en Infrastructuur and BMC Yacht Group. (2023). *Stedelijke verdichting* (Tech. Rep.). Retrieved from https://www.rli.nl/sites/default/files/casusrapport_stedelijke_verdichting_0.pdf
Rabitti, G., & Tzougas, G. (2025, 2). Accelerating the computation of Shapley effects for datasets with many observations. *European Actuarial Journal*, *15*(3), 885–898. Retrieved from https://doi.org/10.1007/s13385-025-00412-z doi: 10.1007/s13385-025-00412-z
Rahim, S., & Siano, P. (2022, 5). A survey and comparison of leading-edge uncertainty handling methods for power grid modernization. *Expert Systems with Applications*, *204*, 117590. Retrieved from https://doi.org/10.1016/j.eswa.2022.117590 doi: 10.1016/j.eswa.2022.117590
Ramm, T. D., Watson, C. S., & White, C. J. (2018, 6). Strategic adaptation pathway planning to manage sea-level rise and changing coastal flood risk. *Environmental Science & Policy*, *87*, 92–101. Retrieved from https://doi.org/10.1016/j.envsci.2018.06.001 doi: 10.1016/j.envsci.2018.06.001
Rijksdienst voor Ondernemend Nederland. (2025, 8). *Wat is netcongestie?* Retrieved from https://www.rvo.nl/onderwerpen/netcongestie/wat-is-netcongestie
Rijksdienst voor Ondernemend Nederland. (2026). *Elektrisch vervoer - Personenauto's - Nederland.* Retrieved from https://duurzamevoertuigen.databank.nl/mosaic/nl-nl/elektrisch-vervoer/personenauto-s
Roerdink, Y. (2025, 8). *Overvol stroomnet bedreigt techsector: 'Bedrijven overwegen te vertrekken'.* Retrieved from https://nos.nl/nieuwsuur/artikel/2578544-overvol-stroomnet-bedreigt-techsector-bedrijven-overwegen-te-vertrekken
RVO, Netbeheerder Nederland, Techniek Nederland, Biemans, A., Hommelberg, M., Janssen, G., & Poiesz, T. (2025, 1). *Netimpact woningen met warmtepomp* (Tech. Rep.). Retrieved from https://www.rvo.nl/sites/default/files/2025-02/Rapport-Netimpact-woningen

-met-warmtepomp.pdf
Shehabi, A., Smith, S., Horner, N., Azevedo, I., Brown, R., Koomey, J., ... Lintner, W. (2016). *United States Data Center energy usage report* (Tech. Rep.). Retrieved from https://eta-publications.lbl.gov/sites/default/files/lbnl-1005775_v2.pdf
Silvestro, F., Pilo, F., Araneda, J. C., Braun, M., Taylor, J., Alvarez-Herault, M.-C., & Heymann, F. (2019, 6). Review of transmission and distribution investment decision making processes under increasing energy scenario uncertainty. *Academia.edu*, 4. Retrieved from https://www.cired-repository.org/handle/20.500.12455/511 doi: 10.34890/735
Spyrou, E., Hobbs, B., Chattopadhyay, D., & Mukhi, N. (2024). How to assess Uncertainty-Aware frameworks for power system Planning? *IEEE Transactions on Energy Markets Policy and Regulation*, 1–13. Retrieved from https://doi.org/10.1109/tempr.2024.3365977 doi: 10.1109/tempr.2024.3365977
Stedin. (2024). *Investeringsplan Stedin 2024-2026* (Tech. Rep.). Retrieved from https://www.stedin.net/-/media/project/online/files/jaarverslagen-en-publicaties/investeringsplan-stedin-2024-2026.pdf
Stratix. (2020). *Management samenvatting* (Tech. Rep.). Retrieved from https://www.zuid-holland.nl/publish/pages/25983/rapportage_datacenters_zuid-holland_management_samenvatting.pdf
Stratix. (2022, 11). *Rapportage Datacenters Impact en Feiten* (Tech. Rep.). Retrieved from https://www.stratix.nl/wp-content/uploads/2023/02/Stratix-Rapport-objectivering-datacenters-2022.pdf
TenneT. (2025). *Netcapaciteitskaart.* Retrieved from https://www.tennet.eu/nl/de-elektriciteitsmarkt/congestiemanagement/netcapaciteitskaart
Trepci, E., Maghelal, P., & Azar, E. (2019, 12). Effect of densification and compactness on urban building energy consumption: Case of a Transit-Oriented Development in Dallas, TX. *Sustainable Cities and Society*, *56*, 101987. Retrieved from https://doi.org/10.1016/j.scs.2019.101987 doi: 10.1016/j.scs.2019.101987
Universiteit Leiden. (2025). *Verkiezingen: dit zeggen onze experts over de belangrijkste verkiezingsthema's.* Retrieved from https://www.universiteitleiden.nl/nieuws/2025/10/verkiezingen-dit-zeggen-onze-experts-over-de-belangrijkste-verkiezingsthemas
Vaghefi, S. A., Muccione, V., Van Ginkel, K. C., & Haasnoot, M. (2021, 10). Using Decision Making under Deep Uncertainty (DMDU) approaches to support climate change adaptation of Swiss Ski Resorts. *Environmental Science & Policy*, *126*, 67. Retrieved from https://doi.org/10.1016/j.envsci.2021.09.005 doi: 10.1016/j.envsci.2021.09.005
Vahidinasab, V., Tabarzadi, M., Arasteh, H., Alizadeh, M. I., Beigi, M. M., Sheikhzadeh, H. R., ... Sepasian, M. S. (2020a, 1). Overview of Electric Energy distribution networks expansion planning. *IEEE Access*, *8*, 34750–34769. Retrieved from https://doi.org/10.1109/access.2020.2973455 doi: 10.1109/access.2020.2973455
Venema, T., van Swieten, T., van den Boogaard, S., Bieze, R., & Group, B. C. (2024, 9). *Haal de kink uit de kabel: Zes interventies om de congestie op het Nederlandse elektriciteitsnet versneld te verlichten* (Tech. Rep.). Boston Consulting Group. Retrieved from https://www.bcg.com/publications/2024/netherlands-haal-de-kink-uit-de-kabel
Wang, Z., Liao, P., Long, F., Wang, Z., Ji, Y., & Han, F. (2025, 9). Maritime Electrification Pathways for Sustainable shipping: Technological advances, environmental drivers, challenges, and prospects. *eTransportation*, *26*, 100462. Retrieved from https://doi.org/10.1016/j.etran.2025.100462 doi: 10.1016/j.etran.2025.100462
Weultjes, J. (2025, 9). *Cv-ketel vermogen.* Retrieved from https://www.cvtotaal.nl/blog/

post/het-vermogen-van-je-cv-ketel-bepalen
Wieles, C., Kwakkel, J. H., Auping, W. L., & Van Den End, J. W. (2024, 1). Scenario discovery to address deep uncertainty in monetary policy. *SSRN Electronic Journal*. Retrieved from http://dx.doi.org/10.2139/ssrn.5014209 doi: 10.2139/ssrn.5014209
Wu, Z., Sun, Q., Gu, W., Chen, Y., Xu, H., & Zhang, J. (2020, 1). AC/DC hybrid distribution system expansion planning under Long-Term uncertainty Considering flexible investment. *IEEE Access*, *8*, 94958–94959. Retrieved from https://doi.org/10.1109/access.2020.2990697 doi: 10.1109/access.2020.2990697
Wurth, T. (2022). *Gridmaster HIC* (Tech. Rep.). Retrieved from https://gridmaster.nl/wp-content/uploads/2022/11/20221124-report-GridmasterHICRdam_public_final.pdf
Xu, X., Bi, J., Moeckel, M., Wiemer, H., & Ihlenfeldt, S. (2025). Quantitative assessment of data volume requirements for reliable machine learning analysis. *IEEE Access*, *13*, 101545-101557. doi: 10.1109/ACCESS.2025.3578528
Zhang, X., Liu, Y., Li, Y., Lv, X., Xiao, F., & Gao, W. (2024, 10). Analyzing variability and coordinated demand management for various flexible integrations of residential distributed energy resources. *Renewable Energy*, *237*, 121619. Retrieved from https://doi.org/10.1016/j.renene.2024.121619 doi: 10.1016/j.renene.2024.121619

A Appendix Uncertainties

The long-term uncertainties categories 1 until 13 presented in Table *14* stem from earlier work of (Marang, 2025). These uncertainties are used to evaluate the robustness of the candidate investment plan. The corresponding parameter values are provided in *Uncertainty_space_for_scenario_creation.csv* which contain two sheets: one detailing the parameter values for this research, including validation of the parameter values, the other presenting the values used in the study of (Marang, 2025). Adjustments to the values were made based on expert input from multiple employees within Stedin. Discussions with these stakeholders revealed that current practice of quantifying uncertainty values are based on national trend lines. Consequently, the uncertainty parameter values were adjusted to reflect these trends, while also maintaining the more extreme scenario values. Moreover, the dialogue with the experts in the field identified implausible uncertainty parameter values, which were subsequently corrected.

Category	Uncertainty	A	B	C
1	a. Adoption new heating systems	Fast	Medium	Slow
	b. Adoption hybrid heat pumps	High adoption	Medium adoption	Low adoption
	c. Mix eHP, heat network, airco (heat)	20/40/40	40/40/20	20/60/20
	d. Life span of hybrid heat pump	10 years	15 years	20 years
2	a. Airco (cooling)	Fast adoption	Medium adoption	Slow adoption
3	a. Adoption system (PV)	Fast adoption	Medium adoption	Slow adoption
4	a. Growth of total vehicles	Fast	Medium	Low
	b. Growth of E-vehicles	Fast adoption	Medium adoption	Slow adoption
	c. Mix cars/vans/buses/trucks	70/20/5/5	60/25/10/5	50/30/15/5
5	a. Growth of charging points	Fast adoption	Medium adoption	Slow adoption
	b. Mix home/company/public	60/30/10	50/30/20	40/30/30
6	Grid aware/average/grid unaware (% of e-vehicles)	Fast	Medium	Slow
7	a. Growth of new buildings	High	Medium	Low
	b. Mix eHP, heat network	60/40	50/50	40/60
	c. Airco (cooling)	High	Medium	Low
8	a. Growth of new industry	Increase	Stay the same	Decrease
	b. Mix electrification, biogas/hydrogen, no industry	60/30/10	40/40/20	30/60/10
9	a. Growth of new greenhouse horticulture	Increase	Stay the same	Decrease
	b. Mix electrification, biogas/hydrogen/geothermal, no greenhouses	50/40/10	30/40/30	30/60/10
10	a. Growth of solar park capacity	High	Medium	Low
	b. Production (% of max)	High efficiency	Average efficiency	Low efficiency
11	a. Delay new substation	High	Medium	Low
12	a. Growth of shore power connections	Fast adoption	Medium adoption	Slow adoption
	b. Electric ships	Fast adoption	Medium adoption	Slow adoption
13	a. Growth of suitable roofs (industry only)	Fast	Medium	Slow
	b. Construction	High	Medium	Low
14	a. Wind turbine growth	Fast	Medium	Slow
	b. Wind turbine efficiency factor	High	Medium	Low
15	a. Power Usage Effectiveness (PUE)	High effectiveness	Medium effectiveness	Low effectiveness
	b. Data center growth	Fast	Medium	Slow
16	a. Total use of surface	High	Medium	Low
	b. Surface mix	Focus on Renewable Energy	Focus on Housing	Focus on Greenhouses

Table 14: *Overview of uncertainties and scenario value meaning*

A.1 Structuring the Decision-Making Problem

Figure *A.18* presents the XLRM framework structure used to organise the long-term uncertainties that influence the two performance metrics of capacity risks and investment costs. The framework summarises the external factors incorporated into this study and clarifies how they relate to the system as a whole.

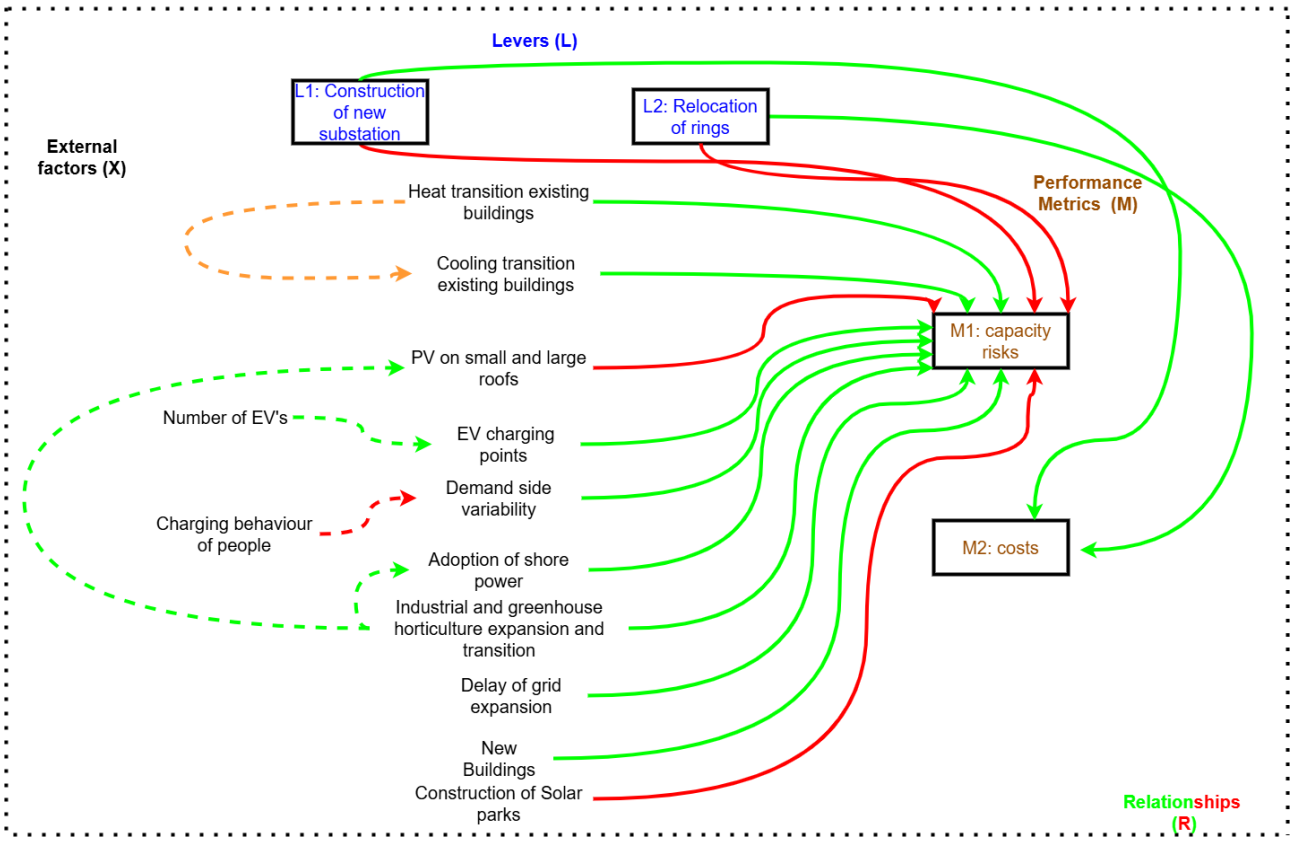

Figure A.18: *XLRM Framework adapted from (Marang, 2025)*

The green lines in the diagram represent relationships that increase hourly demand patterns, thereby contributing to potential capacity risks. In contrast, the red lines indicate uncertainties that reduce hourly demand patterns by feeding electricity back into the grid. Dotted lines signify relationships that depend on each other. For instance, the number of EV influences the required amount of EV charging points. Similarly, industrial expansion is associated with an increase in PV on large roofs. Furthermore, the charging behaviour of end-users affects the variability of electricity demand, greater grid awareness among those end-users tends to reduce overall peak demand (Zhang et al., 2024). A unique orange dotted line illustrates the complex interplay between the heating transition and the cooling transition. Some electric heat pumps can also provide cooling, depending on the installation type. From the XLRM of Figure *A.18* one can deduce that most uncertainties have a amplifying effect on the hourly demand patterns of a substation, thereby increasing capacity risks. Next to this, construction of a new substation or the relocation of rings tend to mitigate such capacity risks. However, these measures are associated with higher costs, underscoring the trade-off that Stedin has to deal with between system reliability and preventing unnecessary grid infrastructure investment.

A.2 KM' Scenario Mapping

In order to determine appropriate uncertainty parameter values for the KM' scenario, the report by Netbeheer Nederland (2025c) served as the primary reference. All parameters that get their value here are based on assumptions within that report. Among the scenarios presented, the KM scenario represents the most balanced or "average" outlook. Consequently, when specific data were unavailable, parameter value B was selected, as it generally reflects the most typical conditions across uncertainties. For simplicity it is assumed that the catchment area of this study follows the same trends as the whole of the Netherlands.

The amount of **new buildings** are assumed to increase to 1.845 million in 2050, which is

compared to today a 22% increase which most closely aligns to parameter value **B**. The report further indicates that 8% of homes will remain heated without electric heat pumps (eHPs), hybrid heat pumps (HHPs), or heat networks by 2050. This share was interpreted as the residual presence of gas-fired boilers (**heat_transition**), aligning with parameter value **C**, which extends gas boiler use until 2040. Similarly, the adoption of HHPs (22%) and eHPs (55%) in 2050 suggest that the **hybrid_adoption** parameter aligns with parameter value **C**, as this scenario assumes 20% of gas boilers will be replaced by HHPs. The report notes that hybrid heat pumps will dominate early adoption, while all-electric heat pumps will become prevalent by 2050 following insulation improvements. Because of this scenario **B** seems plausible for **lifespan_hybrid**, reflecting the transition period between the two alternative heating options around the year 2040. The overall heating mix also aligns with parameter value **B**, since that most closely aligns with the eHP and heat network prediction of the report.

The KM scenario supports the idea that 40% of all houses will have an **airco for cooling** in 2050, uncertainty parameter value **A** aligns best with this. For solar adoption, the KM scenario expects average growth in residential solar panels but does not specify figures, thus **solar_adoption** will get parameter value **B** since that is the most average uncertainty parameter value. Next to this, the KM scenario takes 60% of the large roof potential for PV installations on large roofs, this aligns best with parameter value **A** for **roof_growth.** The **solar_park_efficiency**, which accounts for transmission and technical losses, was assigned value **B** due to insufficient data. Solar park capacity is projected at 40 GW in the KM scenario, which is approximately 1.4 times the current installed capacity, this corresponds best to parameter value **B** for **solar_park_growth**.

All scenarios in the Netbeheer Nederland report assume full electrification of transport by 2050, aligning with parameter value **A**. The mix of electric vehicles corresponds to value **B**, reflecting the most uniform distribution of electric vehicles. Both passenger transport and cargo ton kilometres steadily rise when going to 2050, both rising to 120% in comparison to 2025. Scenario **C** for **vehicle_growth** aligns best with this growth. Charging infrastructure and the mix in which this happens (homes, company, public etc.) are assigned values **B** and **C**, respectively. **Charging behaviour** was assumed to be intensive, corresponding to parameter value **A**. For **new buildings**, the KM scenario anticipates 50% eHP adoption and 20% heat network coverage, aligning with parameter value **B**. **Industrial and greenhouse growth** is assumed to remain stable, corresponding to parameter value **B**.

Electricity demand for industry is projected, in the KM scenario, to rise from 60 TWh in 2025 to 120 TWh in 2050, while hydrogen demand increases from 25 TWh to 90 TWh. Calculating the ratio of electrification to hydrogen in 2050 gives 57% to 43%, thus **new_industry_mix** most closely aligns with parameter value **A**. For greenhouses the ratio between electrification and other forms of electricity use is 30% electrification to 58% other forms. Therefore, **new_greenhouse_mix** most closely aligns with parameter value **C**. The growth of **shore power connections** is assumed to align with scenario parameter value **B**. In contrast, the **share of ships** that use electricity for their ships is around 20% by 2050, corresponding to parameter value **C**. Large roof PV installations are expected to utilize 60% of potential, with **roof growth** assumed to follow parameter value **B**. The **construction** of PV installations on those suitable roofs is equal to parameter value **A**, reflecting the 2050 KM scenario expectations. **Wind energy demand** is expected to increase by 63% between 2025 and 2052, corresponding to parameter value **B**. **Data center** electricity use is projected to grow from 8 GW in 2025 to

52 GW in 2052 (550% increase) aligning with parameter value **A**. Next to this, the KM scenario accounts for a 15% decrease in demand due to **data center efficiency** improvements. Which corresponds to a PUE closer to 1, which is closest to parameter value **B**. For **total_use_ha**, parameter value **B** was selected to maintain a balanced allocation of land for housing, industry, and recreation. Since only half the available land can be used for industry, housing or greenhouse growth, the other half can go to recreation or other urban developments. Finally, the KM scenario's description of global economic growth and industrial policy aligns with parameter value **C** for **surface_mix**, reflecting its industry-oriented focus.

B Appendix Data Preparation

In this appendix the way the input parameters are calculated are discussed and the construction of hourly electricity demand per ring will be discussed.

B.1 Calculation of Input Parameters

The calculation of the parameter values are done as follows. For instance, the municipality containing the Rings II and VI is assumed to have its housing stock evenly divided between these two rings. Additionally, it is assumed that 35% of houses in all rings are equipped with solar panels, reflecting the Dutch national average of 2025 (Netbeheer Nederland, 2025a). Vehicle data is based on totals per municipality. Municipality Z (comprising of Ring I, II, III, V and VI) has a total of 24,648 vehicles (including 2370 company cars) and municipality H has 16,949 total vehicles (including 1258 company cars) (*Klimaatmonitor*, n.d.). Company cars are allocated to the industrial rings (Ring I and Ring V), while the remaining vehicles are distributed across residential rings. In municipality Z, the vehicle count is split between Ring II and Ring VI, with a further adjustment made for Ring III, which is also in municipality Z, based on its share of housing ($\frac{1722}{10416} \cdot 100\% = 16,5\%$).

Heat network coverage of both municipalities is minimal, with only 0.5% in municipality Z and 2.2% in municipality H (CBS, 2021). The number of houses using hybrid heat pumps (HHP) and electric heat pumps (eHP) is calculated as the residual of total housing minus gas and heat network connections $num\_houses - (gas + heat\_network) = HHP + eHP$. The ratio between HHP and eHP is derived from a study of the RVO Hommelberg, Biemans, Janssen, and Poiesz (2025), which reports 4197 hybrid and 1486 full electric heat pumps in their study which corresponds to the ratios 73.8% HHP and 26.2% eHP. This breakdown is validated for Ring II, where the sum of gas (8677), HHP (1255), eHP (446) and heat network (38) equals the total number of houses (10,416). Since each house is assumed to rely on a single heating system, the aggregate number of heating technologies cannot exceed the total number of houses of a ring.

However, there are air conditioning systems used for heating that are assumed to be complement to existing heating systems (gas, HHP, eHP or heat networks). Internal data identifies 413 airco units used for heating, evenly split between Rings IV and VI (both get 206 initial airco's for heating). Additionally, substation S has 85 airco's that are used for heating. Next to heating, airco's can be used for cooling. Dutch national statistics indicate 1.9 million installed airco's, divided by the total number of houses in the Netherlands this comes to 23.1% (CBS, 2025b). Which is a figure that is applied for all rings.

Only Ring III is assumed to contain greenhouses due to the agricultural character of this ring. While substations S and W currently lack shore power connections, industrial rings (Ring I and V) do have the facilities to host such power connections due to their proximity to a river and

existing harbours. Given the growing electrification of inland shipping, which in turn increases the demand for shore power (Wang et al., 2025), it seems plausible that in the future this might lay a potential burden on the grid. Because of this, the model assumes only one shore power connection for both rings with the potential to grow more connection in the future.

Finally, the available_surface attribute represents the maximum area available for new developments. These values are estimated using the "measure distance" tool of Google Maps, with irregular shaped areas being approximated as geometric figures such as rectangles or triangles. Areas which were currently not in use for electricity purposes, like sand beds, agricultural land and parks, were added to the available surface of a ring.

B.2 Construction of Hourly Electricity Profiles per Ring

This appendix provides a detailed explanation of how the hourly electricity demand profiles were constructed. The underlying code implementation can be found in *Exploratory Data Analysis.ipynb*. Each ring distinguished in this research consists of multiple distribution rooms, which collectively determine the hourly electricity demand and generation profile of that ring. However, for some distribution rooms, hourly electricity demand and generation data was missing due to incomplete datasets. In total, 98 distribution stations lacked hourly demand data, while 224 stations contained complete data. Furthermore, the hourly demand and generation profiles of the substations were known. Because of this, the missing hourly demand and generation values could be imputed as follows:

Step 1: Calculate the total amount of missing electricity per substation:

Start by determining the difference between the total electricity demand of 2025 at substation level and the sum of electricity demand across all non-missing distribution rooms. This difference is the total amount of missing electricity:

$$E_{\text{missing}}^{\text{substation}} = E_{\text{total}}^{\text{substation}} - \sum_{i=1}^{n} E_i^{\text{known}}$$

Where:

- $E_{\text{total}}^{\text{substation}}$= total electricity demand for 2025 of substations S or W
- E_i^{known} = electricity demand of distribution room i with available data
- n = number of distribution rooms with known data

Step 2: Allocate missing electricity across rings:

Rings that have a larger proportion of missing stations get more missing electricity share:

$$\omega_r = \frac{N_{\text{missing}}^{r}}{N_{\text{missing}}^{\text{total}}}$$

Where:

- ω_r = relative weight for ring r
- N_{missing}^{r} = Number of missing distribution rooms for ring r

- $N_{\text{missing}}^{\text{total}}$ = total number of missing distribution rooms across all rings

Step 3: Compute missing electricity per distribution room:

Finally, the missing electricity for each distribution room r is equal to:

$$E_{\text{missing}}^{\text{room}} = \omega_r \cdot E_{\text{missing}}^{\text{substation}}$$

The formula ensures that rings with more missing distribution rooms receive a larger share of the missing electricity.

C Appendix Model Calculations and Verification

This appendix provides a systemic verification of the internal calculations of the simulation model. The objective is to confirm that the implemented algorithms accurately reproduce the expected behaviour based on the formulas of (Marang, 2025). All formulas, with the exception of *C.9*, presented up to *C.10* stem from her work. The verification process focusses on a single scenario where all uncertainty parameters are equal to "B". Since the simulation model uses different names for the rings, Table *15* can be used to find the corresponding names to the ring names used in this paper.

Simulation Ring names	Research Paper Ring names
industry_S	Ring I
residential_S	Ring II
rural_S	Ring III
residential_W_H	Ring IV
industry_W	Ring V
residential_W_Z	Ring VI

Table 15: *Correspondence between simulation ring names and ring names referenced in this study*

C.1 Solar Profile

The simulation model calculates the amount of PV electricity generation for residential buildings equipped with solar panels. Each ring contains a number of solar houses, which evolves over time according to the solar_adoption_factor. The hourly PV generation is calculated as:

$$\text{Hourly generation} = N_{\text{solar houses}} \cdot N_{\text{panels per house}} \cdot P_{\text{panel}} \cdot \eta_{\text{eff}} \cdot \text{Profile}_{hour}$$

Where:

- $N_{\text{solar houses}}$ = Number of houses with solar panels in reference year
- $N_{\text{panels per house}} = 10$
- $P_{\text{panel}} = 0.4$ kW
- η_{eff} = A year specific efficiency factor from solar_park_efficiency
- Profile_{hour} = Normalized hourly generation profile

The normalized profile ensures zero production during nighttime and a peak around midday (approximately 13:00), while incorporating representative day patterns to capture seasonal fluctuations.

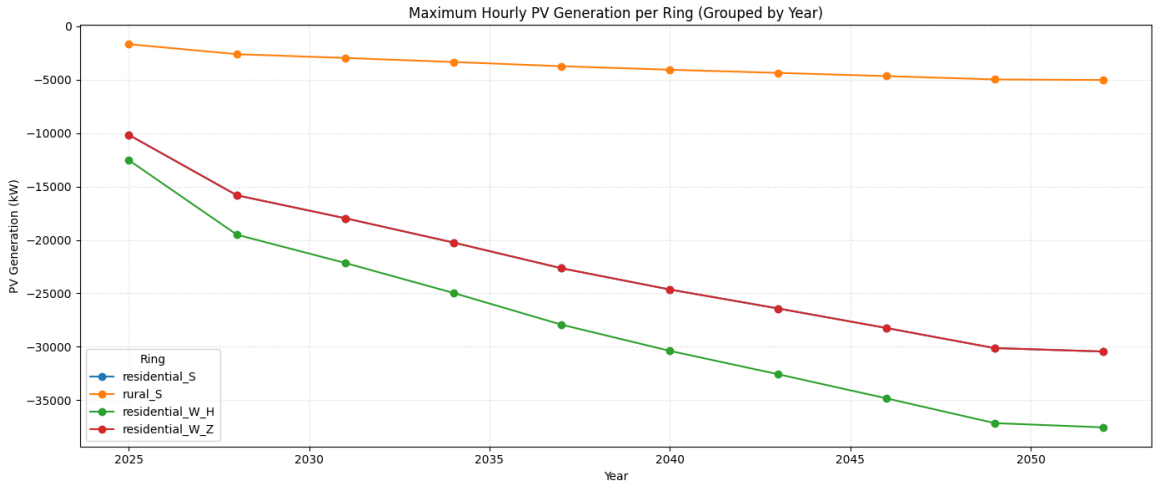

Figure C.19: *Maximum (abs) peaks per reference year of PV*

The figure shows the absolute maximum hourly peaks per reference year for PV installations at substation S. To verify these findings, the base year (2025) and the end year (2052) will be manually calculated and compared to the Figure. In the year 2025, the number of solar houses in substation S equals 4249, with an efficiency factor of 0.7 this results in 11.897 kW. For the year 2052, the solar adoption factor increases to 65% which means a total of 7890 solar houses with an efficiency factor of 0.95 this results in 35628 kW. The blue line of Ring II is exactly the same as Ring VI, which proves that the choices considering input are properly managed by the model. Both yearly estimates align with the order of magnitude observed in the simulation outputs (Ring III + Ring II), albeit with minor deviations attributable to the normalized hourly profile and seasonal adjustments. The sharp increase of PV generation in the first year can be contributed to the fact that suddenly 30% of extra houses adopt PV installations. Hereafter, the decline follows a linear decrease for all rings with the exception of the last year, where the increase in PV installations is less pronounced than the previous years.

C.2 Heating Transition in Existing houses

The heating transition in existing buildings shows the transition away from gas-fired boilers. Instead, the use of hybrid heat pumps and full electric heat pumps will increase over time. The more hybrid and electric heat pumps there are the greater the pressure on the electricity grid. The hourly energy use profiles are calculated as:

$$\text{Hourly Heating} = \sum_i N_i \cdot E_i \cdot \text{Profile}_{hour}$$

Where:

- N_i = Number of houses using technology i
- E_i = Hourly energy consumption of technology i
- Profile_{hour} = Normalized hourly demand

- With [Gas boiler[1], eHP[2], HHP[3], Heat network, Airco] resp. corresponding to [12, 5, 2, 3, 2] kW.

[1] (Weultjes, 2025)
[2,3] (RVO et al., 2025)
Note that the technical report for eHP's and HHP's states that the electricity demand on a cold day for an eHP is estimated at 4.5 kW and 1.6 for an HHP. This study rounds these numbers up to 5 resp. 2 kW to account for the potential impact of climate change. More extreme weather conditions can lead an increase in electricity demand of both types of heat pumps.

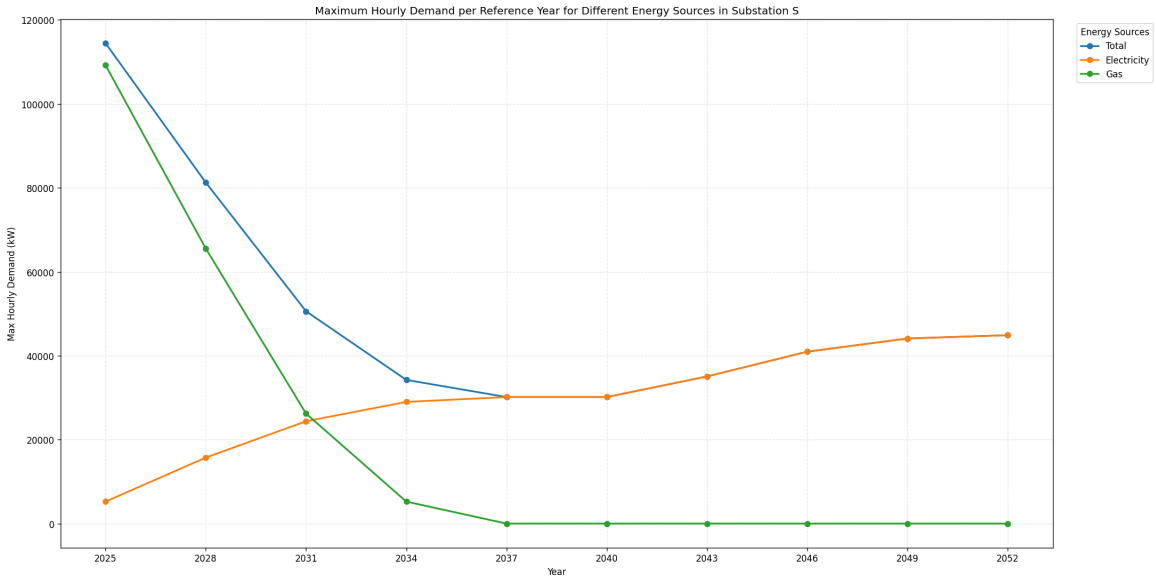

Figure C.20: *Consumption peaks per Energy Source*

The simulation model assumes that approximately 83% of all houses use gas as primary heating source in 2025. However, emergent technologies of HHPs and eHPs change this landscape which in turn causes the electricity demand of households to increase. This is reflected by the Figure C.20, with 10112 houses in substation S connected to gas which corresponds to 120.000 kW in 2025. The figure has a slightly lower value due to the normalized time profile. Additionally, in 2025, 1,462 houses use HHPs, 520 houses use eHPs, 44 houses are connected to a heating network, and 85 houses have an additional airco unit. Multiplying these numbers with their energy consumption value results in an electricity demand of 5826 kW, which aligns with the figure. Over time, gas usage is being phased-out while electricity use for heating purposes increases. After 2040, the gas fired boilers that were replaced in 2028 are replaced by eHP which has a higher average energy consumption than an HHP $\Delta E_i = 3$ kW which explains the upwards going trend after the year 2040.

C.3 Cooling transition existing buildings

Houses have airco's for cooling, they can be either big or small. The energy use of such airco's is calculated as:

$$E_{cooling} = N_{small} \cdot \frac{1}{2} E_{airco} + N_{big} \cdot E_{airco}$$

Where:

- N_{small} = The amount of small airco's

- N_{big} = The amount of big aircos

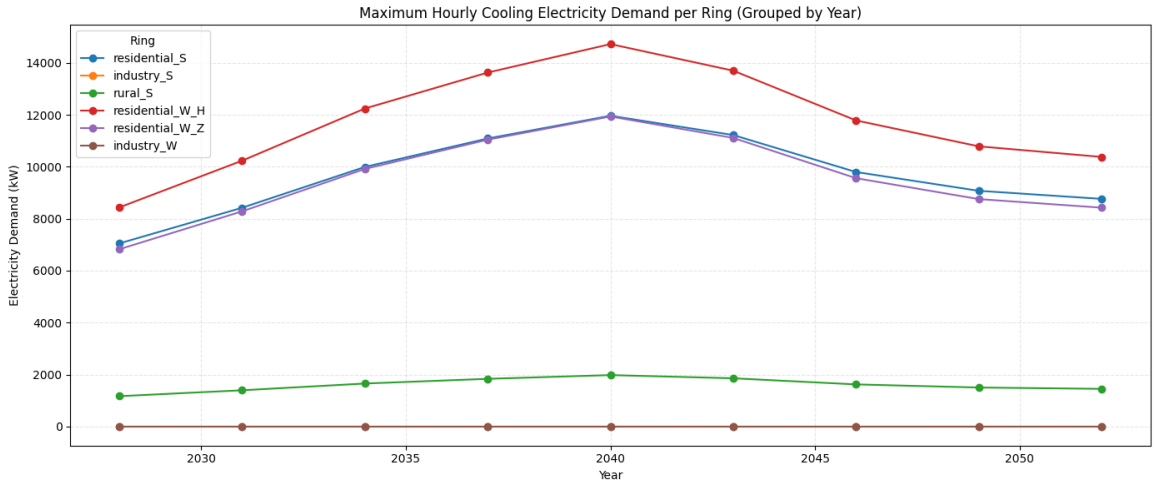

Figure C.21: *Consumption peaks of Air-conditioner units (both big and small)*

At the start of the simulation, a steady increase of electricity demand exhibits itself for air-conditioning units. The amount of eligible houses are based on their heating systems. Houses that have a connection to the heat network or have hybrid heat pumps are considered eligible. For the year 2028, the amount of eligible houses is equal to $4075 \cdot 0.3 = 1222$ units, of which 456 are small air conditioners and 756 are large units. In addition, 2406 air conditioning units are pre-installed. The corresponding electricity demand is computed as: $456 \cdot \frac{1}{2} \cdot 2 + (765 + 2406) \cdot 2 = 6798$ kW, which is in line with the amount displayed in the figure for Ring II. Over time, the observed electricity demand declines after the year 2040. This can be explained by the before mentioned interaction between model components. In the simulation model, the cooling adaption is proportional to the number of buildings eligible for air conditioning, which includes HHPs. After 2040, the share of HHPs decreases due to the lifespan of these systems and subsequent replacement by eHPs. This reduces the 'total eligible' cooling adoption population, leading to less electricity demand.

C.4 Electric Vehicles Charging Stations

The number of EV comprises different sub-calculations, for a more detailed explanation see the work of (Marang, 2025). In order to calculate the hourly demand of EVs several things must be known: the growth of EVs in future years (which is captured by the uncertainty factor EV_adoption), the amount of average driven kilometres and the behaviour of the end-users in terms of Grid Awareness. The average driven kilometres can be calculated as:

$$D_{r,y}^{(c)} = EV_{r,y}^{(c)} \cdot \text{km\_per\_vehicle}(c)$$

Where:

- $D_{r,y}^{(c)}$ is the total amount of driven kilometres per ring r per vehicle category c
- $EV_{r,y}^{(c)}$ the number of EV of category c per ring r in year y
- km_per_vehicle(c) is an average annual driving distance per vehicle category c (constant over time).

This distance is then converted to an energy demand by multiplying the average driven distance per vehicle category to an energy consumption rate per kilometre (kWh/km) which differs for each vehicle category. There are four vehicle categories with each their own consumption rate namely: cars, vans, buses and trucks corresponding to 0.15, 0.18, 0,25 and 0.30 kWh/km. To convert this into annual charging hours the resulting number is divided by a power charging level. This yields the annual charging hours required per vehicle category. However, the timing of when an EV is being charged depends on the grid awareness of the user. That is why the simulation model distinguishes three categories: grid-aware, average and grid-unaware people. To calculate the daily charging needs based on grid awareness the following formula is used:

$$H^{(c)}_{r,y,beh} = H^{c}_{r,y} \cdot \alpha^{beh}_{y},$$
$$\text{with:} \sum_{beh} \alpha^{beh}_{y} = 1$$
$$h^{(c)}_{r,y,beh} = \frac{H^{(c)}_{r,y,beh}}{days_{3y}}$$

Where:

- $H^{(c)}_{r,y,beh}$ is the annual charging hours between different groups.
- α^{beh}_{y} is the behavioural share (net aware, average and net-unaware) which sums up to 1
- $h^{(c)}_{r,y,beh}$ is the daily charging hours, which is the annual charging hours divided by the number of days in three years

The daily charging hours are distributed among 24 hours, depending on the behaviour of the person they charge:

- Between 17:00-19:00 this are typically grid-unaware people
- Grid-Aware and average users charge during all other hours of the day

Their hourly charging for hour h being equal to:

$$\text{Load}^{(c)}_{r,y,h} = \frac{\text{DailyHours}^{(c)}_{r,y,group}}{\text{Hours}_{group}} \cdot P^{(c)}$$

Where:

- $\text{DailyHours}^{(c)}_{r,y,group}$ is the number of daily charging hours per behavioral *group*
- Hours_{group} is the number of hours allocated for charging
- $P^{(c)}$ is the charging power (in kW) for vehicle group c

The loads per vehicle group and behavioural group eventually sum up to get the following results displayed in the figure below:

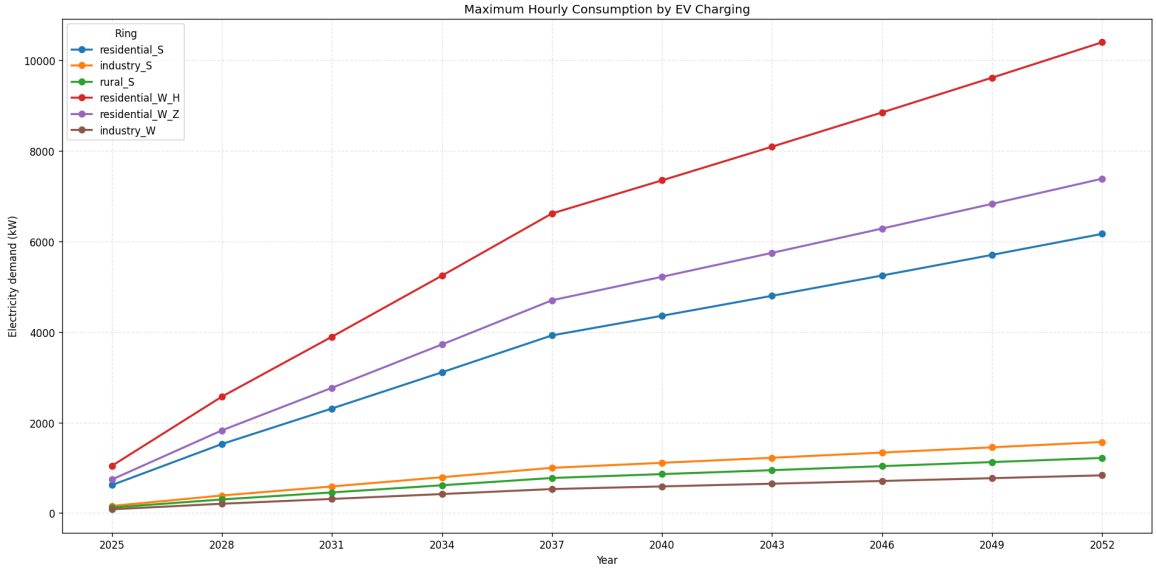

Figure C.22: *EV Charging Demand per Ring*

For Ring II (represented by the blue curve), the initial amount of EVs is equal to 8.27% (776 EVs) of the total amount of vehicles on a particular Ring. This number is allowed to grow to 7677 EV in 2052. The vehicle mix is 60% cars, 25% vans, 10% buses and 5% trucks. Furthermore, the energy intensity per driven kilometre is 0.15 kWh for cars, 0.18 kWh for vans, 0.25 kWh for buses and 0.30 kWh for trucks, with charging power of 11 kW for cars, 13 kW for vans, 15 kW for buses and 18 kW for trucks. Lastly, the charging behaviour evolves from 30% net unaware in 2025 to 5% net unaware in 2052. Like the formula, the charging hours were converted to daily averages over 1095 days and allocated across peak (17:00-19:00) and non-peak hours (all other hours in a day).
Using the formulae as described above, the peak hourly load in 2025 is 618 kW for the unaware behavioural group and 308 kW for the aware/average behavioural group. Both values together align with the value displayed in the figure for 2025. In the year 2052, the amount of EVs has increased almost tenfold while the behavioural unaware group has shrunk to 5%. The net unaware behavioural group have a demand of 1542 kW in 2052, while the net aware/average group has 4168 kW demand. The sum of these values align with the electricity demand depicted for Ring II in 2052. While one might expect the electricity demand to increase proportionally with the amount of EVs, the effect of charging once EV during off-peak hours shows the mitigating effect of being grid-aware.

C.5 New buildings Energy Mix

For each simulation year and ring, the model estimates electricity demand and solar generation for newly constructed buildings. New building counts are derived by comparing projected totals to the 2025 baseline. These buildings adopt heating technologies based on predefined shares: electric heat pumps (eHP) or district heating networks, like in Section C.2. A fraction of network-connected buildings also installs air conditioning (airco) for cooling. Hourly electricity consumption is calculated as:

$$E_{eHP,y,r,h} = N_{eHP,y,r} \cdot P_{eHP,h}$$

$$E_{\text{heat network},y,r,h} = N_{\text{heat network},y,r} \cdot P_{heat,h}$$

$$E_{airco,y,r,h} = N_{airco,y,r} \cdot P_{cool,h}$$

With the total hourly demand being equal to:

$$E_{demand,y,r,h} = E_{eHP,y,r,h} + E_{\text{heat network},y,r,h} + E_{airco,y,r,h}$$

Note that the production of new buildings is the same formula as C.1

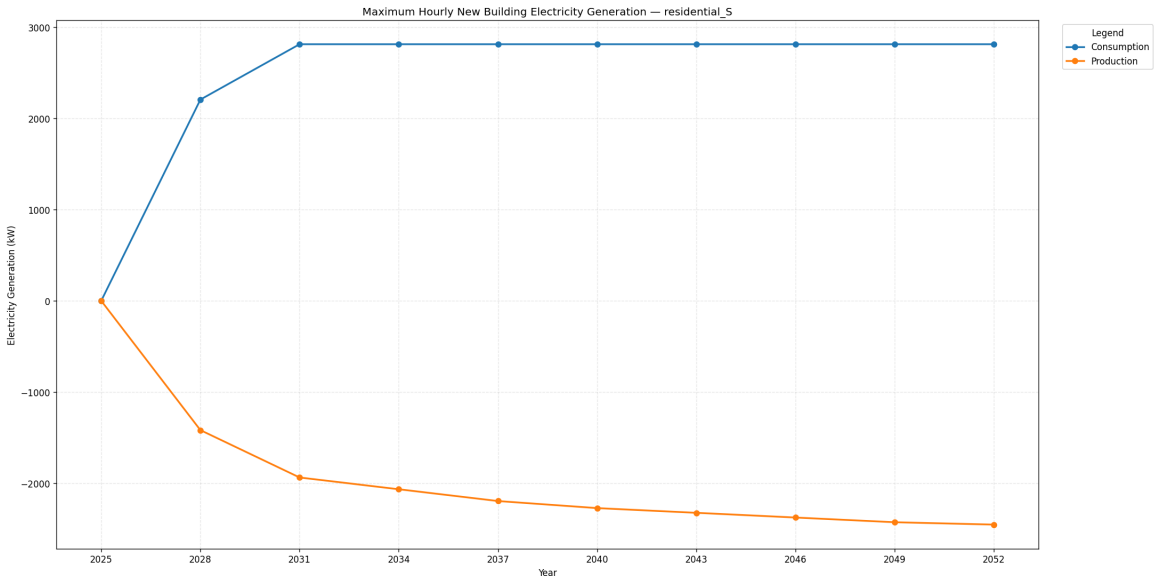

Figure C.23: *New Building Energy mix*

For the year 2025, all values are equal to zero since no buildings have been built yet on substation S. Over time, electricity consumption of new buildings increases while after 2031 this increase stops reflecting the exhaustion of available surface area within Ring II. In other words, that means that no new buildings are added to the simulation model. Conversely, solar panel production exhibits a steady upward going trend and approaches, but does not reach, a horizontal asymptote. This is attributable due to the production of solar panels steadily increasing from 70% in 2028 to 95% in 2052. The total number of new buildings for Ring II in this scenario is equal to 663 in year 2034. Due to the uncertainty factor new_building_mix 50% of new houses get an eHP while 50% are being connected to the heat network. In addition, for the year 2031 the amount of air conditioning units is 25% of new buildings. This gives $\frac{663}{2} \cdot 5$ kW $+ \frac{663}{2} \cdot 3$ kW $+ \frac{663}{2} \cdot 0.25 = 2815$ kW. This is in line with the consumption of new buildings in 2031. Moreover, the amount of production by new houses in the same year of assessment is $663 \cdot 10 \cdot 0.4 \cdot 0.75 = 1989$ kW. Which is also in line with the value displayed in the figure.

C.6 Industrial Expansion and Energy Mix

Industry has a base stock on Ring I, this stock can increase or decrease based on the scenario uncertainty value. Initially, 75% of the industry uses methane for energy use. The use of methane will be completely phased out in 2052. This is done using the following equation:

$$S_{electrification,y} = \frac{s_{electrification,y}}{s_{electrification,y} + s_{biogas/hydrogen,y}} \cdot S_{remaining,y}$$

$$S_{biogas/hydrogen,y} = \frac{s_{biogas/hydrogen,y}}{s_{electrification,y} + s_{biogas/hydrogen,y}} \cdot S_{remaining,y}$$

Where:

- $s_{electrification,y}$ and $s_{biogas/hydrogen,y}$ are the projected shares of energy sources which increase each year with 5 percent point per year for electrification and three percent point per year for biogas (capped at 100%).
- Annual energy consumption electrification: 900.000 kWh/year
- Annual energy consumption methane: 850.000 kWh/year
- Annual energy consumption biogas/hydrogen: 750.000 kWh/year
- Annual energy consumption no industry: 0 kWh/year

Converting such annual values to hourly values they are divided by 26.280 hours, which are all the hours in a three year period.

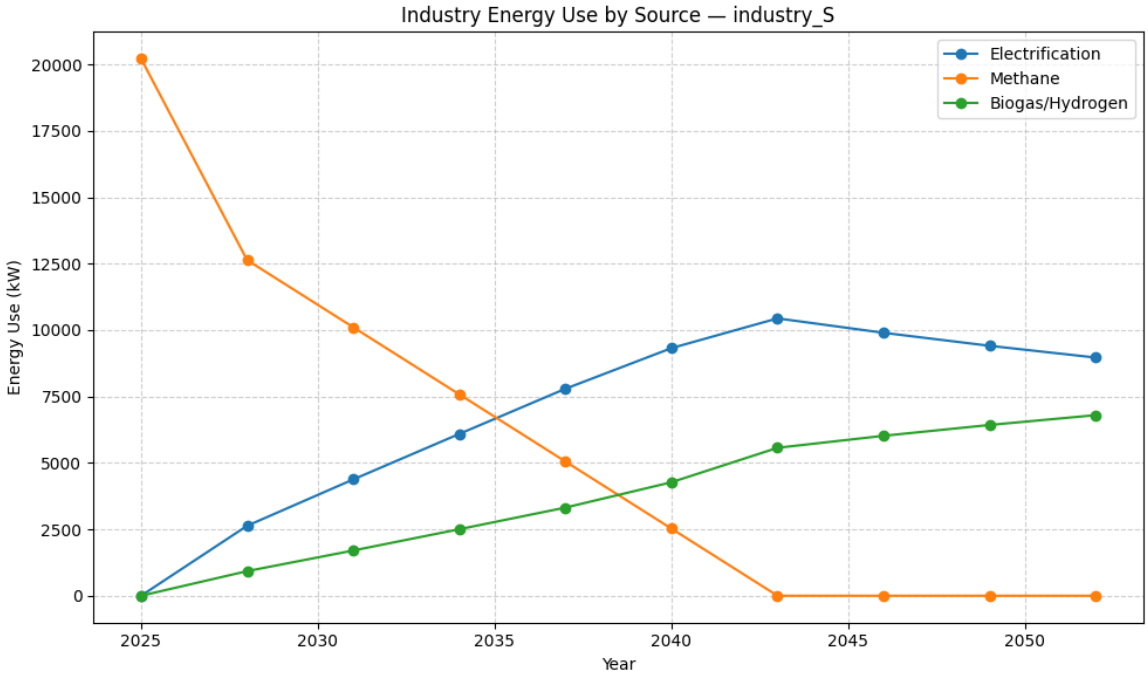

Figure C.24: *New Industry Energy mix*

In the year 2025, an initial amount of industry buildings belong to Ring I. In total 625 industrial buildings are multiplied by the annual energy consumption value of methane and divided by the three year time period. This gives $625 \cdot \frac{850000}{3 \cdot 365 \cdot 24} = 20214$ kW, which is aligned with the value for methane in 2025. In the first year a sharp decline can be seen due to the assumption that 75% of industry uses methane for energy use. This causes the model to start electrification and biogas use in 2028. Because of this modelling choice methane is already completely phased out in 2043. After 2043 one can see that electrification is slowly being replaced with biogas and hydrogen options resulting in an overall less energy consumption for greenhouses due to lower annual energy consumption.

C.7 Greenhouse Expansion and Energy Mix

The calculation of greenhouses follows the same approach as industrial expansion and energy use only with different values (since greenhouses are measured in m^2. Note that for greenhouses, it is assumed that 100% of methane is used for consumption.

- Electrification: 1200 kWh/m^2/year
- Methane: 1350 kWh/m^2/year
- Biogas/hydrogen: 1000 kWh/m^2/year
- No greenhouses: 0 kWh/m^2/year

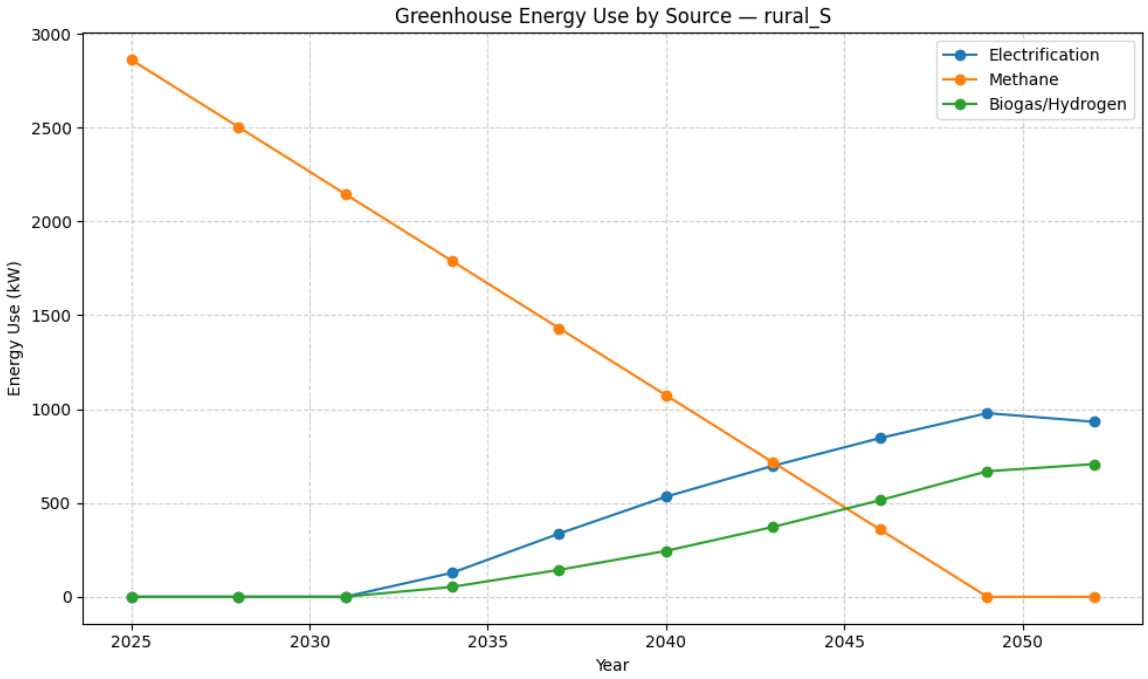

Figure C.25: *Greenhouse Energy Mix*

For the year 2025, 55700 m^2 of greenhouses using only methane, which means corresponds to 2861 kW which aligns with the value displayed in the figure. We see that the values in 2052, since the amount of greenhouses does not change the sum of electrification and biogas is approximately 1500 kW which is attributable to the lower energy intensity of electrification and biogas/hydrogen compared to methane.

C.8 Solar Park Construction

The simulation model takes into account solar park production in the year 2025 of one m^2 this solar park grows with a certain factor per year (g_y). The energy yield of a square metre of solar park is fixed at 360 kWh/m^2 and adjusted based on an efficiency factor of the solar park. This means production losses, transportation losses etc. In formula language:

$$A_y = A_{y-3} + (A_{y-3} \cdot g_y)$$
$$E_y = 360 \cdot \eta_y \cdot A_y$$

Where:

- A_{y-3} = surface area in previous year of assessment
- η_y = represents the efficiency of solar panels in terms of how many percent of the total production of a solar panel remains for consumption (think of transportation losses).

The model converts E_y to hourly production values by multiplying it by a normalized hourly demand pattern based on representative days.

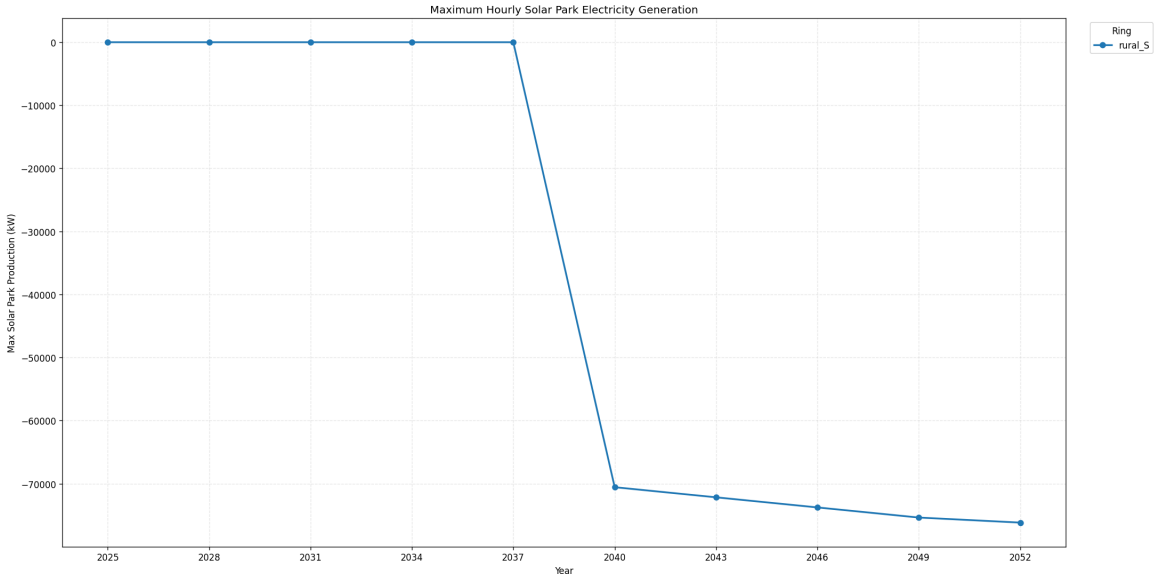

Figure C.26: *Solar Park Construction*

While the growth of solar parks is near zero in the first thirteen years of the simulation, after completion of the solar park on Ring III in 2040, the effect of solar parks does become apparent. It is assumed that a 400.000 m^2 solar park will be built on Ring III, which corresponds to 111780 kWh per day, when applying the normalized hourly profile and assuming that at midday 13:00 the normalized value equals 0.6 the electricity production is 67068 kW, which is in line with the value in the figure.

C.9 Shore Power Adoption

The adoption of shore power has in 2025 six connections which grows each year with an number of connections with a maximum of 8 new connections per Ring in 2052. The growth of shore power connections can be calculated like:

$$C_{r,y} = C_{r,y-3} + \Delta C_y$$

where ΔC_y denotes the increase of shore power connections based on the scenario. The annual electricity demand of shore power is defined by the hotel load and the charging load. The hotel load is the electricity consumption while docked and the charging load is the amount of electricity needed for charging the ship. Not every ship is electric, which is represented by the share of ships that is electric s_y. Then:

$$P_{r,y} = s_y \cdot (C_{r,y} \cdot P_{hotel} + C_{r,y} \cdot P_{charge})$$

where, P_{hotel} and P_{charge} are 300 kW and 1500 kW based on the outcomes of (Löffler, Geertsma, Polinder, & Coraddu, 2025). The hotel power is all electricity used for non-propulsion, while the charging power is for the charging of the engine. To convert this power demand to an hourly profile the $P_{r,y}$ is multiplied by a normalized time profile N_t. At its' peak half of all ships charge at the same time in the night, until the 6 am, whereafter no ships are being charged, it starts again in the evening around 18 pm.

$$E_{r,y} = P_{r,y} \cdot N_t$$

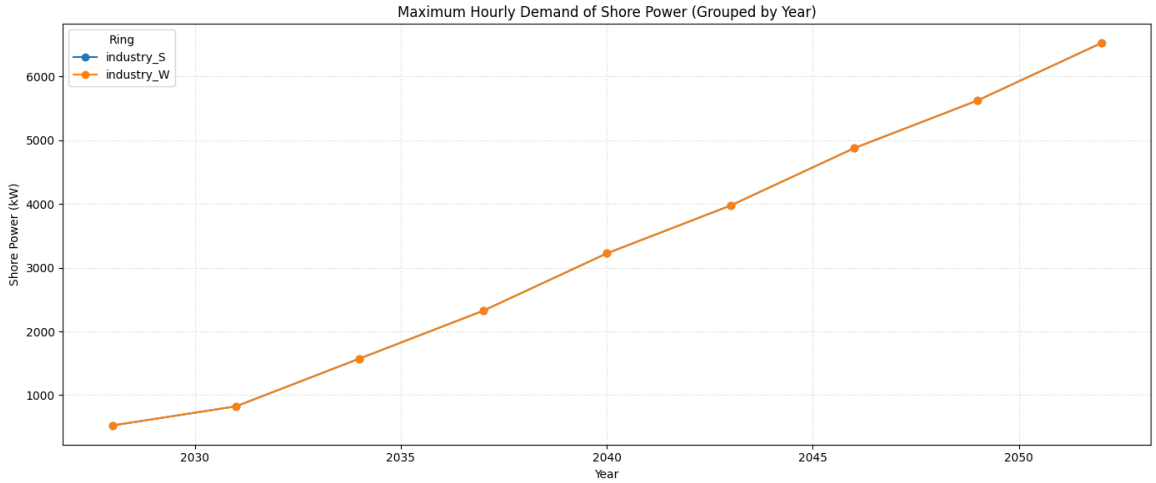

Figure C.27: *Shore Power connections*

Both rings illustrated in the figure have the same starting conditions and future conditions and therefore are identical in the figure. The growth of shore power demand can be explained by the growing number of connections, together with an increase in the number of electric ships in 2052 75%.

C.10 Large Roof PV

The way that large roof PV is being calculated is identical to the way a normal solar panel is being calculated. The key difference is that such large roof PV can only be constructed on industrial rings. Furthermore, it is assumed that large roof PV consists of 20 panels and a wattage of 0.5 kW per panel instead of 0.4 kW.

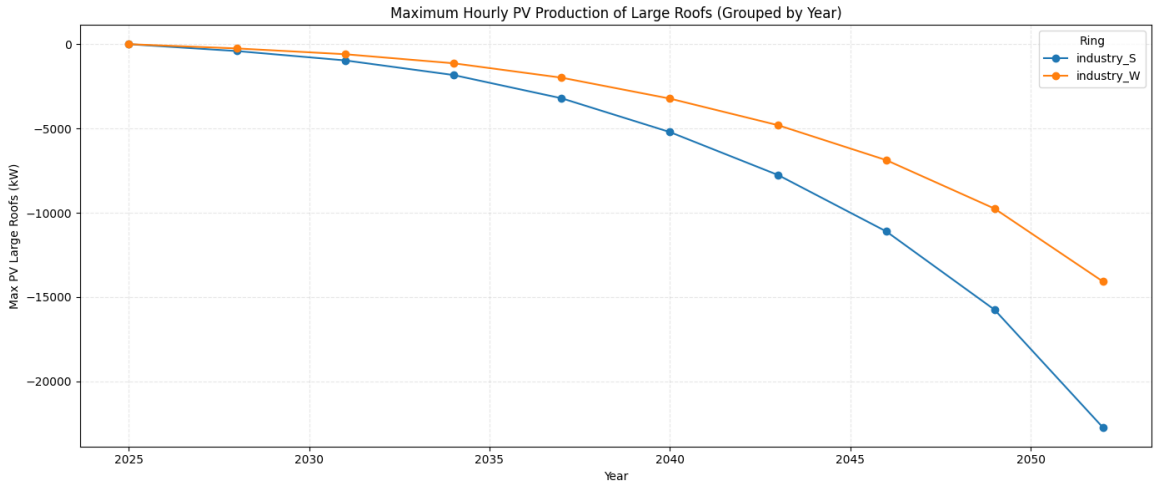

Figure C.28: *Solar panels on large roofs (exclusively on Industrial Rings)*

For the year 2025 the amount of large roof PV is equal to 0 kW since no panels are installed yet on industrial buildings. Over time the panels do become installed, with the amount of suitable roofs growing over time. Eventually, in 2052 this results in 2173 suitable roofs which corresponds to $2173 \cdot 20 \cdot 0.5 \cdot 0.95 = 20643$ kW which is aligned with the value of Ring I for 2052.

C.11 Wind Park Construction

The formulae are presented in *6.3.1* cause the behaviour of the simulation model to look like this:

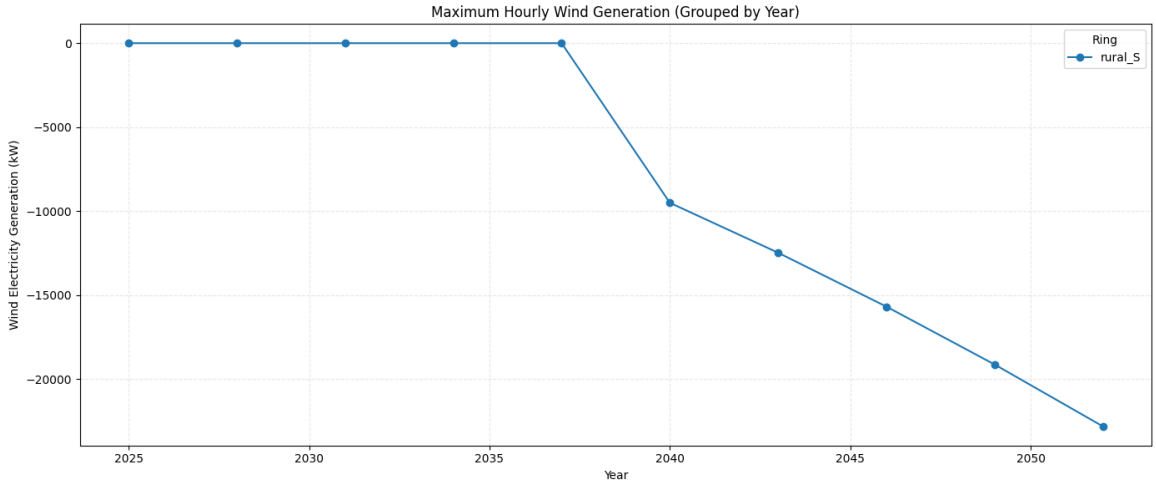

Figure C.29: *Wind Park Generation*

As displayed in the figure wind park electricity production are all zero values until 2040. After that year the construction of a wind park begins. The number of wind turbines is equal to 8 with an efficiency of 40% and a capacity per turbine of 3600 kW this results in 11.520 kW. This is in line with the value displayed in the graph, with minor deviations attributed to the representative days. On windy days the output of wind parks will be more than on non windy days. In 2052, the wind park has increased in size, being 2 times larger than the year 2040 which means that there are 16 turbines with an efficiency factor of 48% resulting in $3600 \cdot 16 \cdot 0.48 = 27648$ kW which is in line with the year 2052.

C.12 Data Center Construction

The formulae presented in *6.3.2* show how the datacenter caculation has been done.

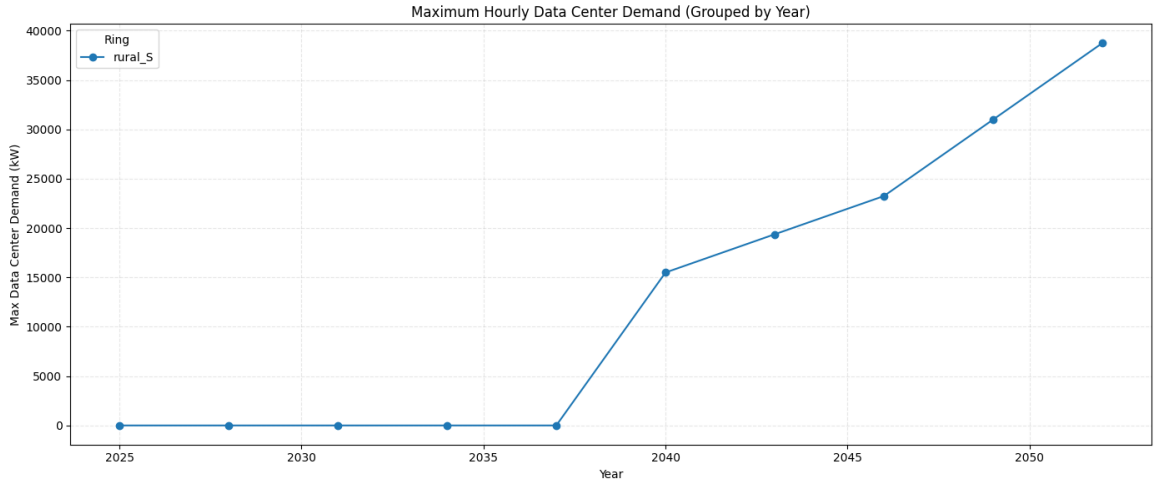

Figure C.30: *Data Center Demand*

Wholesale datacenters typically consume between 10 and 40 MW of electricity (Patel et al., 2024). In this study, a datacenter uses 10 MW of electricity initially, with electricity demand scaling proportionally with to the growth of the datacenter. In other words, if the datacenter triples in size, the electricity demand will also increase threefold. For the year 2040, applying the PUE of 1.35 to the initial electricity demand results in a total electricity demand of 13.5 MW, which is in line with the order of magnitude seen in the figure. The deviations can be

attributed to the representative day weights. The datacenter grows after 2040, reaching 250% in 2052. This means that the datacenter demands $25 \cdot 1.35 = 33.75$ MW. Again, the remaining 4 MW can be contributed to the representative day in the model.

C.13 Surface Constraints

As explained in Section *6.3.3*, the simulation model incorporates surface availability constraints in a Ring. The model components which are subject to such constraints include the amount of new buildings, amount of new industry, the amount of new greenhouses, solar park growth, wind park growth and datacenter growth. In contrast to the other verification sections, this section focuses solely on uncertainty parameters with value A, as these represent scenarios where the maximum amount of land can be allocated and growth potential is highest, leading to the fastest use of available surface area. The sole exception is the surface_mix uncertainty factor, which is assigned value B to reflect residential housing focus.

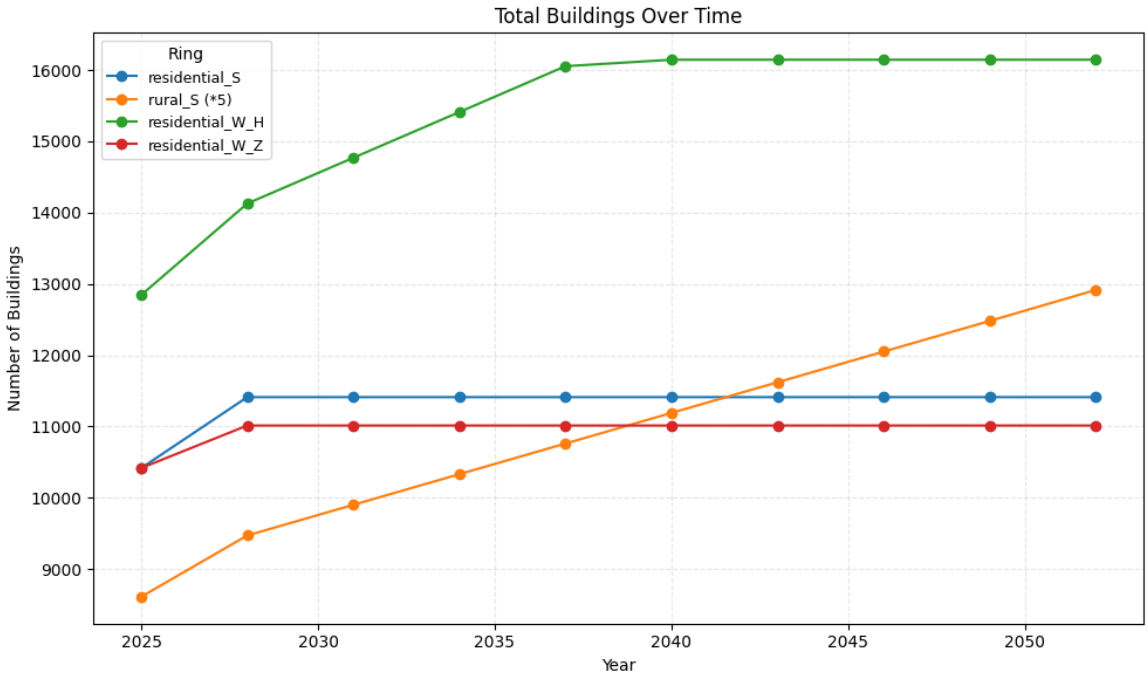

Figure C.31: *Growth of total buildings with spatial constraints*

The figure shows the effect that spatial constraints have on the simulation model. Ring III (orange line) has the highest available surface for new buildings, which is represented by its approximate linear growth over time. In contrast, Ring VI (red line) and Ring II (blue line) experience initial growth, after which no further expansion occurs due to the exhaustion of available surface area. In order to demonstrate the implementation of spatial constraints, the following table was constructed for this specific scenario. On average, a single house occupies 0.0132 hectares of land. By multiplying the values in the second, third and fourth columns and dividing by the average land requirement of houses, the fifth column is obtained.

Simulation Ring names	Available surface	Total use ha	Surface Mix Housing Factor	Maximum allowed growth
residential_S	25	0.75	0.70	995
rural_S	875	0.75	0.70	34802
residential_W_H	83	0.75	0.70	3302
residential_W_Z	15	0.75	0.70	597

Table 16: *Total number of allowed growth of houses for one scenario*

Comparing the results from the table with the outcomes of the figure confirms that the implemented algorithm works. The blue curve increases with almost a thousand houses, while the red curve reflects an increase roughly half that magnitude. Similarly, the growth of Ring IV shows an increase of more than 3000 residential houses which is in line with the number in the table.

D Appendix Simulation Formalisation and Adjustments

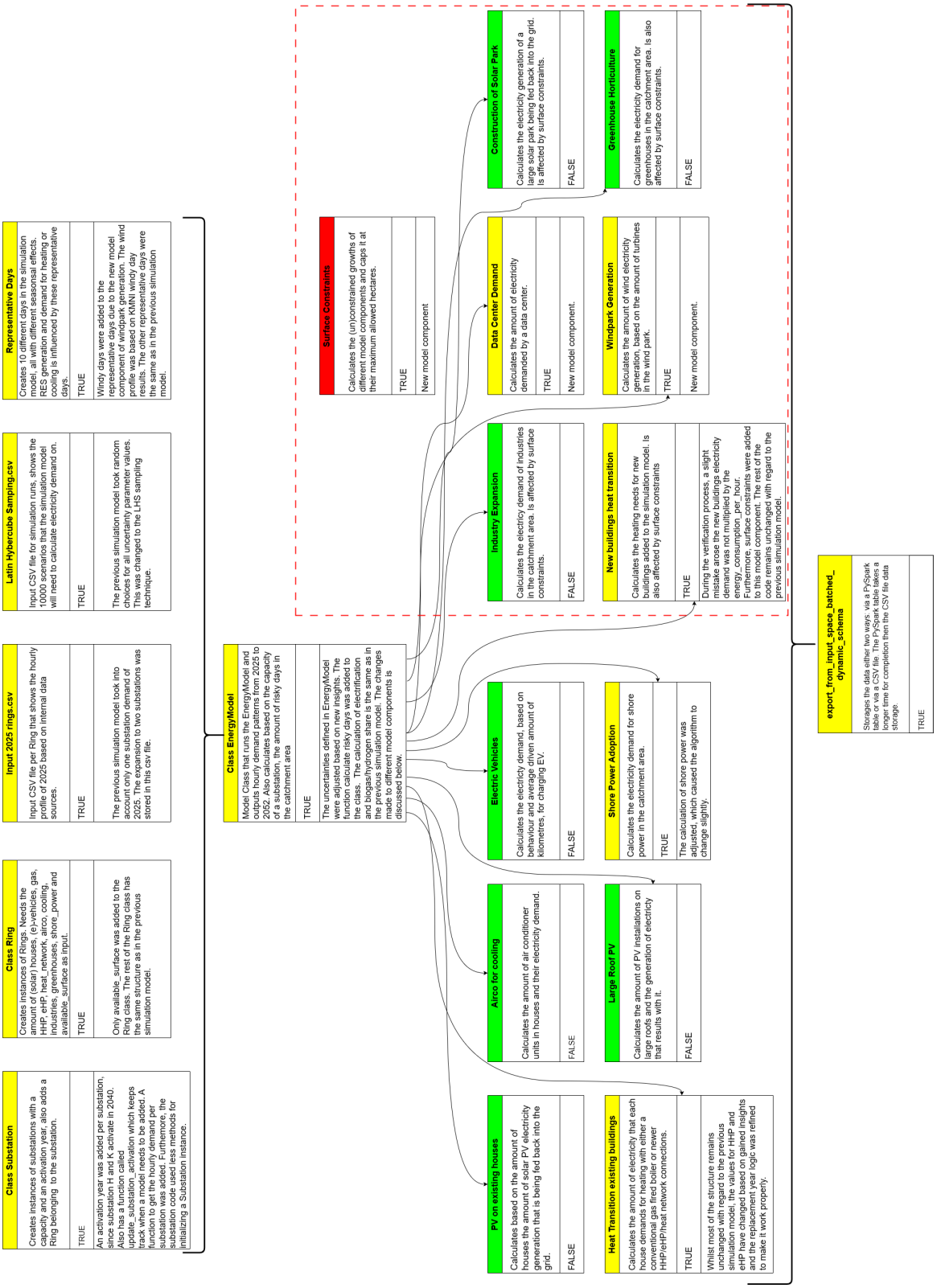

Figure D.32: *Quasi UML diagram of Simulation and Adjustments made to the simulation model*

E Appendix Results

In this section, one can get more analyses of the results as well as gain deeper insights into some analysis techniques.

E.1 Candidate Investment Plan

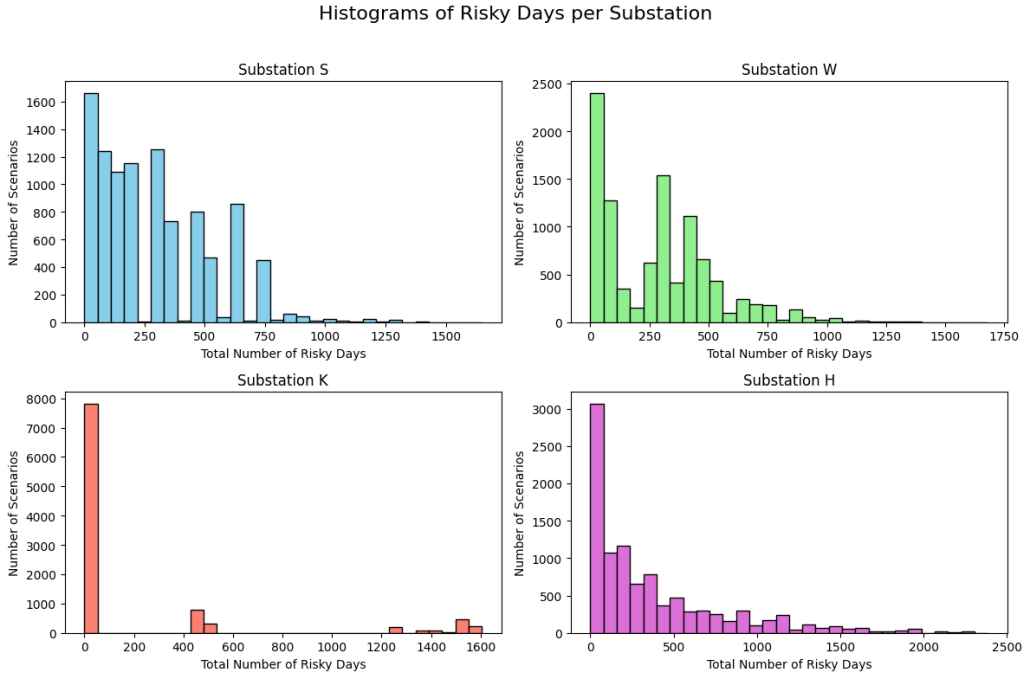

Figure E.33: *Risky days per substation of 10000 simulation runs*

Figure *E.33* presents the distribution of the number of risky days per substation across 10.001 simulated scenarios. For substation S, W, and H the distribution are roughly similar in shape. For those substations, the bulk of the scenario's experience between 1 and 750 risky days. However, a more limited number of scenario's exhibit higher numbers of risky days, as evident by their longer right tails in the distribution.

Substation H has the longest tail with several scenarios experiencing more than 2.000 risky days, a pattern that is not observed for the other substations. This pronounced right tail may be related to the fact that substation H inherits the ring from substation W, with the most amount of residential houses. This might indicate that the heating transition of the built environment or installation of residential PV's could contribute to the increased occurrence of risky days on substation H. In contrast, substation K exhibits a limited amount of scenarios with risky days compared to the other substations. This difference can be contributed to the higher capacity limits for substation K.

E.2 Feature Scoring Unexpected Outcomes

While some features can be easily explained, others need a more in depth explanation. For instance, an inconsistency arises from the fact that uncertainty value C exhibits higher feature importance then value B, despite representing a slower replacement of HHPs. Further investigation of the coincidence counts in Table *17* clarifies this inconsistency. Uncertainty value A coincides most frequently with risky days, while uncertainty value C has the fewest

coincidences, and value B lying between the other two. As a result, the RF model is trained on fewer observations for uncertainty value C, which reduces the reliability of its estimated feature importance. In contrast, uncertainty value B and A have more coincidences and are therefore more reliable then uncertainty value C. Consequently, the feature lifespan of HHPs is considered an important driver of capacity risks, with the notion that uncertainty value C may be less reliable due to data quantity. The same logic applies when looking at substation W heat transition C, which represents a slow replacement of gas boilers. Logically, this uncertainty value should cause less risky days because of the longer use of gas boilers and the subsequent postponement of electric heating options, like HHPs or eHPs.

Finally, substations S and W exhibit high feature importance for mix distribution uncertainty value B, which corresponds to the highest share of eHPs in the model. The more eHPs in the model, the higher the electricity demand on the substations which subsequently leads to more risky days. In addition, surface mix uncertainty value B for substation H, represents a residential housing focus where houses are allowed to grow more than other scenarios. This result is consistent with the substantial contribution residential houses have on the overall electricity load of a substation.

Uncertainty value	A	B	C
lifespan_hybrid_ = 1 ∧ risky_days_S = 1	111.920	68.600	43.100
lifespan_hybrid_ = 1 ∧ risky_days_H = 1	119.540	72.300	47.620
heat_transition_ = 1 ∧ risky_days_W = 1	63.890	58.050	19.600

Table 17: *Coincidence counts per uncertainty value*

F Appendix PRIM Analysis

This appendix shows the key drivers of capacity risks per year per substation. Furthermore, it explains in more detail why sometimes no high PRIM boxes are found, and it explains some unexpected drivers of capacity risks.

F.1 Key Drivers of Capacity Risks per Substation per Year

F.1.1 Key Drivers Substation S

2040

For substation S, risky days first appear in 2040. Showcasing that in the short-term the current candidate investment plan is sufficient enough. Although this year contains 612 cases of interest, no boxes can be found that match the density threshold criteria. Distinct PRIM boxes appear for the first time in 2043. In this year, box 3 (density = 0.809 and coverage = 0.719) is selected. This box contains in total 2538 cases of interest, and indicates that the combined effect of medium-to-high EV growth and the short lifespan of HHPs cause risky days to occur in 2043.

2043

Keep in mind that in all scenarios substation S has transferred one ring to substation K, leaving one residential and one industrial ring. Consequently, key drivers of risky days are expected to be associated with the electrification of both houses and industries. This logic is confirmed by the key drivers of risky days in 2043. The growth value for EVs is associated with fast and medium adoption of EVs, which increases electricity demand from EV users. This key driver is particularly plausible for the residential ring because vehicle ownership is high on residential

rings. Add to that the growing share of these vehicles becoming electric over the simulation horizon, this key driver is in line with logical reasoning.

The other key driver of risky days is lifespan of HHPs which is set to 10 years. After this period, the model assumes that households replace HHPs with eHPs, which require an additional 3 kW of electricity load, as discussed in *7.1.3*. When both key drivers are temporarily set to zero, no high density boxes can be found in the second iteration of PRIM for 2043.

2046
In 2046, the lifespan of HHPs continues to be a key driver for risky days, with 4266 interesting cases. The EV growth parameter, however, no longer appears as a driver. For a detailed description as to why this happens, see *F.2*. Risky days in 2046 are therefore primarily linked to the transition away from gas-fired boilers and increasing electrification of household heating systems. The second PRIM iteration yielded no high density boxes.

2049 & 2052
In 2049, the HHP lifespan again emerges as a key driver, underscoring the continued influence of residential heating electrification on substation electricity load. One additional driver also appears, the share of gas-fired boilers that are replaced by an eHP. The PRIM results show that 30% to 40% cause capacity risks in that year. The second PRIM iteration identified three key drivers. The HHP lifespan remains important, now with uncertainty values of 10 to 15 years. The eHP share remains an important driver as well, with values ranging between 20% to 30% which cause risky days. Combining the first and second PRIM iterations shows that, because the parameter value for eHP-share in the model ranges between 20% and 40%, this driver, together with other key drivers, consistently contributes to the occurrence of risky days. Lastly, in 2052, with 8334 interesting cases, the growth of EVs once again becomes an important driver of risky days.

F.1.2 Key Drivers Substation W

2028 & 2031
Substation W first starts to experiences risky days in 2028. In that year 157 cases are of interest but no high density boxes can be found. Indicating that the outcomes do not cluster enough for the PRIM algorithm to detect high density boxes. In 2031, the number of interesting cases increase sharply to 6615. A single high density box is identified, with the key driver in this year being the heat transition value. This uncertainty represents the share of HHPs replacing gas fired boilers. Risky days start occurring when the uncertainty parameter value ranges between 0.5 and 0.8. corresponding to medium-to-high HHP adoption levels. This result aligns with earlier findings showing that residential transitioning away from gas-fired boilers causes significant additional electricity loads and thus capacity risks.

Substation W is the only substation experiencing short-term capacity risks. Because substations cannot be expanded or built rapidly, short-term mitigation measures such as diesel or gas generators for large industrial consumers may temporarily relieve peak demand in 2031. Prior to 2032, substation W has two residential and one industrial rings. After 2032 one residential ring is transferred to substation H. This reduction in electricity demand is reflected in the PRIM results, from 2031 until 2040 no risky scenarios emerge. Moreover, the early emergence of risky days demonstrates that substations that serve multiple large residential rings may be more

vulnerable to early capacity risks then other substations.

2040–2046
For the years 2040, 2043 and 2046 there are 17, 452 and 1042 cases of interest, respectively. None of which yield high enough density boxes. This indicates that for those years the cases of interest are either too diversely spread across the uncertainty space or that there is no subset of the uncertainty space where cases of interest cluster for PRIM to notice.

2049
In 2049, four distinctive PRIM boxes arise from 2039 cases of interest. The uncertainties driving risky days that year are: the total vehicle growth (0.9-1.1), EV growth (0.57-0.9), the share of eHPs replacing gas-fired boilers (0.3-0.4) and the lifespan of HHPs (10-15). Collectively, these key drivers underscore how an increase of electric mobility together with the residential heating transition will amplify electricity loads of substation W. More specifically, risky days occur when total vehicle numbers either decrease by 10% or increase by 10%, combined with 57% to 90% EV growth and a high eHP share (30% - 40%) replacing gas-fired boilers. The second iteration of PRIM does not reveal additional high density boxes, which suggests further that these key drivers dominate the occurrence of risky days.

2052
In 2052, the key drivers persist: total vehicle growth (0.9-1.2), EV growth (0.62-0.99) and the share of eHPs replacing gas-fired boilers (0.3-0.4). Although the values slightly differ from the previous year it does show that electric mobility and residential heating transition are consistent key drivers of capacity risks on substation W.
The second iteration of PRIM yielded five high density boxes. Three key drivers are already extensively discussed, relating to total (electric) vehicle growth and the amount of eHPs that replace gas-fired boilers. Two new key drivers are the amount of ev_mix_cars (0.5-0.65) and new_industry_mix_no_industry(0.1-0.15). The former is intuitive, more electric passenger vehicles increase charging demand. The latter is not immediately interpretable. However, this factor is associated with uncertainty parameter value A and C, which assume 60% and 30% electrification of the industry. Mainly uncertainty parameter A exerts significant pressure on substation W. Therefore, the no industry uncertainty serves as a proxy for high electrification scenarios. A more detailed description of this and other counter-intuitive drivers, is provided in *Explaining Unexpected Drivers of PRIM Analysis*.

F.1.3 Key Drivers Substation H

2037 & 2040
Substation H becomes active in 2032, where it adopts one residential ring of substation W. For substation H risky days start to appear in 2037, though no high density boxes are found. For 2040, which has 1292 cases of interest also no high density boxes are found by the PRIM algorithm.

2043
In 2043, two key drivers of capacity risk emerge: the share of eHPs replacing gas-fired boilers and the lifespan of HHPs. The second PRIM iteration adds EV growth and surface mix solar parks as additional drivers. While the influence of EV growth aligns with the findings on other substations, the solar surface factors appears counter-intuitive because substation H is a mere residential ring which houses no solar park. However, this parameter serves as a proxy for the amount of available land that residential houses can expand on, as demonstrated in *Explaining*

Unexpected Drivers of PRIM Analysis. As shown in Table *5*, Ring IV has the second largest available surface for growth potentials in the model. Thus, allowing more residential houses to grow on substation H, which will get either hybrid, full-electric or a connection to the heating network increases the electricity load on substation H. In other words, if residential houses are allowed to grow more, combined with the other key drivers, causes risky days to appear more on residential rings.

This insight also carries broader policy relevance. Proposals to address the current housing shortage in the Netherlands, include building 10 new cities (AD, 2025a). However, under the current modelling assumptions, the PRIM analysis hints at the fact that building such new cities in the catchment area of this research will cause capacity risks.

2046
In 2046, risky days are again driven by EV growth (0.53-0.85) and the lifespan of HHPs (10) are key drivers of capacity risks. The second iteration of PRIM reidentifies lifespan of HHPs (15) and the surface mix solar parks proxy (0.06-0.068) as key drivers of risky days. The third PRIM iteration yielded no high density boxes. The results confirm again that residential heating transitions combined with more available surface for the growth residential houses cause risky days.

2049
In 2049, a total of 6767 scenarios cause risky days. The primary drivers remain the share of eHPs which replace gas-fired boilers (0.3-0.4) and the lifespan of HHPs (10-15). The second iteration of PRIM shows four key drivers, the first two drivers are the same as in the first iteration of PRIM, though with slight parameter value changes. The other two key drivers are vehicle growth (0.9-1.1) and EV growth (0.57-0.9) highlighting again that electric mobility and residential heating transition are key drivers for risky days. The third iteration of PRIM yielded three key drivers, of which two already discussed in the previous iterations, the additional key driver is again the allowed growth of residential houses. The fourth iteration of PRIM yielded no high density boxes.

2052
By 2052, a total of 8262 scenarios cause risky days. The first PRIM iteration identifies the share of eHPs that replace gas-fired boilers (0.3-0.4) as the most dominant key driver. The second iteration, despite temporarily excluding nearly 4000 risky cases, again highlights the same drivers albeit with slightly different parameter ranges: share of eHPs (0.2-0.3) and EV growth (0.62-0.99). The persistence of both uncertainties demonstrates the influence that heatpump adoption and electric mobility have on substations that house large residential areas. A thrid PRIM iteration adds the solar surface proxy as an additional factor.

F.1.4 Key Drivers Substation K

Remember that substation K is a predominantly rural area with a small village. In 2040 both a solar park as well as a datacenter will become operational on substation K. These developments cause risky days to appear on substation K only on the long-term for both 2049 and 2052

2049
In 2049, a total of 1088 scenarios generate risky days. Two key drivers dominate: datacenter

growth (3-4) and the datacenter PUE value (1.5-1.7). These results indicate that rapid datacenter growth, which scales linearly with electricity demand, combined with inefficient power usage by datacenters, places significant pressure on substation K. Although the substation was intentionally designed to serve as a buffer for future electricity developments, the PRIM analysis shows that constructing a large datacenter (> 30 MVA) will nullify substation K serving as a buffer.The second iteration of PRIM yielded no boxes.

2052
The PRIM results for 2052 confirm the above described logic. With 2177 cases of interest, the same drivers appear: datacenter growth (3.8-5) and data center PUE (1.2-1.7). These results demonstrate that once datacenter expansion reaches a scale of approximately four to five times its original value, risky days arise regardless of the effectiveness of power usage by the datacenter. Noting all of this, it seems imperative for Stedin to acknowledge that with the current candidate investment plan cannot facilitate datacenters that demand more then 30 MVA.

F.2 Deeper Understanding of PRIM Results

When looking at the PRIM results of substation S, the year 2043 identifies ev_growth_value and lifespan_hybrid_value as key drivers of risky days. In the following year, only lifespan_hybrid_value remains, while ev_growth_value reappears only in 2052. This pattern can be explained by the inner workings of the PRIM algorithm.

PRIM removes data along a single dimension at each iteration, and selects the slice that most increases the mean outcome of the remaining box (Kwakkel & Jaxa-Rozen, 2015). Consequently, if an uncertainty does not improve the mean outcome of the remaining box enough, the algorithm will not peel along that dimension a.k.a. uncertainty. Meaning that if, in a given year, a different uncertainty explains risky cases more strongly, then PRIM will peel along that uncertainty and subsequently ignoring the other uncertainties. Returning to the example, for the year 2043 the ev growth uncertainty best improves the mean outcome of the remaining box, whereas in 2046 the lifespan of HHPs provides stronger improvement of the mean outcome of the remaining box. Which causes the PRIM algorithm to ignore ev_growth_value, because a better dimension to peel along has been found in lifespan_hybrid.

A second explanation relates to the increasing number of scenarios exhibiting risky days over time. The more this number grows, the more the distribution of interesting cases can become too dispersed across the entire uncertainty space. If the interesting cases are spread too widely, PRIM can no longer find slices of the uncertainty space that increase density resulting in no high density boxes that are found by the algorithm. In other words, in the higher dimensional uncertainty space no subsets of that space can be found where risky cases cluster. Both explanations provide insights into why no high density boxes can be found and to why some uncertainties disappear in one year and reappear in another.

F.3 Explaining Unexpected Drivers of PRIM Analysis

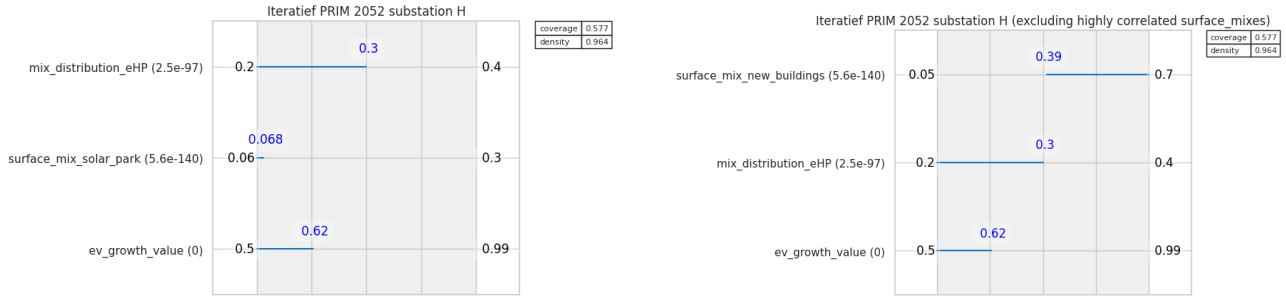

(a) Initial PRIM result

(b) PRIM result with exclusion of all other surface mixes

Figure F.34: *PRIM results for substation H (2052): side-by-side comparison*

The emergence of surface_mix_solar_park as a driver in the second PRIM iteration for substation H in the year 2052, is not in line with logic. Substation H does not have any solar parks and thus this uncertainty cannot contribute to more risky days. The surface remains constant throughout the simulation, and sum up to 1. The surface mix uncertainties allocate fixed shares of available land to different uses, such as solar parks, wind parks, and new buildings, and therefore exhibit strong correlations.

Specifically, surface_mix_solar_park is negatively correlated with surface_mix_new_buildings, which directly influences electricity demand through residential expansion and associated heat transitions. The PRIM algorithm identifies boxes in the uncertainty space that cluster risky days, and in this instance, the interval of 6–6.8% for solar share corresponds to Scenario B, characterized by a 70% surface allocation to new buildings (see *Uncertainty space for scenario creation.csv*). Consequently, surface_mix_solar_park functions as a proxy for high residential development rather than a causal factor. When all other surface mix uncertainties are excluded, PRIM correctly highlights surface_mix_new_buildings as the dominant driver, confirming that this surface mix uncertainty is the dominant driver of risky days rather than the surface_mix_solar_park. The same logic applies to new_industry_mix_no_industry, this uncertainty points towards the scenario parameter value where 60% of the industry is being electrified.

G Appendix Costs of Adaptive Measures and Investment Plans

This appendix provides an overview of how the costs are calculated for each adaptive measure and investment plans. Each adaptive measure has assumptions which will be clearly described in this Section. In the second paragraph, the total investment costs of the worst case, current investment plan and the adaptive investment plan will be calculated.

G.1 Costs of Adaptive Measures

The costs of each individual component are based on papers or open source databases of (CBS, 2025c; Netbeheer Nederland et al., 2019). The costs assumptions of each grid network component are:

- Cost of new HV/MV substation = €25.000.000
- Cost of new TV/MV substation = €10.000.000

- Cost of HV cables = 5000 [€/m]
- Cost of TV and MV cables = 1000 [€/m]
- Land acquisition costs = 1256 [€/m^2]
- Building a 150/50 kV transformer = €6.800.000 (Liander, 2024)

The first adaptive measure is reallocating rings. The cable length that will be needed to reallocate the industrial rings is approximately 4.5 km. With TS cables costing 1000 [€/m], the total cost per ring reallocation is: 1000 [€/m] $\cdot$ 4.5 [km] = € 4.500.000.

The second adaptive measure is the construction of substation X. To accomodate, substation X which has a 70 MVA capacity, an additional 150/50 kV transformer must be installed upstream to ensure adequate grid capacity. The total costs for building substation X equal: € 10.000.000 + 1256 [€/m2] $\cdot$ 10.000 [m2] + 1000 [€/m] $\cdot$ 8.6 [km] = € 31.160.000.
The additional 150/50 kV transformer requires expansion of the existing substation, including new land, a new building and cables. The total costs of such a operation amounts to: € 6.800.000 + 30 [ha] $\cdot$ 1256 [€/m2] + € 25.000.000 + 1.9 [km] $\cdot$ 5000 [€/m] = € 97.820.000. The 30 ha assumption is based on the average hectares needed for HV/MV station, which can be found in the same source as the costs are found in.
Combined, the construction of substation X and associated additional 150/50 kV transformer amounts to € 128.980.000.

The third adaptive measure is the developing substation H as a 21 kV station and not as a 13 kV station. Although the transformers for a 21 kV station will be slightly more expensive, these are not considered by this research since building substation H will happen no matter what. However, when substation H becomes a 21 kV station, the existing electricity cables will need to be replaced by cables that can handle 21 kV. This requires 55km of cables, resulting in total costs of: 55 [km] replaced cables $\times$ 1000 [€/m] = € 55.000.000.

The final adaptive measure, focuses on short-term capacity relief by installing diesel or gas generators for bulk consumers. One diesel generator which costs € 250.000 can deliver 1700 kVA (*Caterpillar PM1360*, n.d.). The peak of substation W is 83 MVA, which is a 38 MVA capacity deficit relative to its maximum capacity. Fully satisfying this capacity deficit would require: $\frac{38}{1.7} = 23$ generators. The total costs are then: $23 \cdot$ € 250.000 = 5.750.000.

G.2 Costs of Investment Plans

Three investment plans are evaluated in this thesis: the worst case, the candidate investment plan and the adaptive investment plan.

Firstly, the worst case represents a network configuration that is built to withstand the most extreme future scenario. This net configuration is the same as the candidate investment plan plus an additional substation X with an upstream 150/50 kV transformer. It causes 125 MVA extra capacity for the entire catchment area. This net configuration ensures that no scenario exceeds the grids capacity, although it is the most expensive option.

The candidate investment plan or investment option A reflects the baseline plan currently under consideration by Stedin and serves as the configuration which is stress-tested in the first iteration

of the simulation model.

The adaptive investment plan, is the network configuration of investment plan B. In contrast to the worst case, this adaptive investment plan allows adaptive measures to be implemented once ATPs showcase that the future electricity demand is heading towards high demand scenarios. In scenarios were the electricity demand remains moderate, these adaptive measures are not triggered, enabling cost savings compared to the worst case configuration.

Investment Components	***Worst case***	***Candidate Investment Plan***	***Adaptive Investment Plan***	***Length [m] or surface*** $[m^2]$	***Costs [€]***
1 new 150/50 kV trafo	True + 1 extra	True	False	–	6.800.000
2 new 150 kV cables	True + 1 cable extra	True	False	1720	17.200.000
1 new 21 kV station	True	True	True	–	10.000.000
Land acq. 21 kV station	True	True	True	10000	13.750.000
cables 21 kV station with 50 kV W	True	True	True	4300	4.300.000
1 new 13 kV station	True	True	True	–	10.000.000
Land acq. 13 kV station	True	True	True	10000	12.500.000
Cable 13 kV station	True	True	True	3400	3.400.000
3 direct 150/50 kV trafo's	False	False	True	–	13.500.000
3 new 150 kV cables	False	False	True	1720	25.800.000
Expansion 50 kV W land acq. direct connection	False	False	True	30000	37.500.000
Adaptive measure 1 (rings reallocation, per ring)	True	False	Depends on scenario	–	4.500.000
Adaptive measure 2 (new substation)	True	False	Depends on scenario	–	128.980.000
Adaptive measure 3 (H becomes 21 kV)	True	False	Depends on scenario	–	55.000.000
Additional upstream 150/50 kV trafo	True	False	True	–	6.800.000
Total Costs without adaptive measures	€ 93.350.000	€ 77.950.000	€ 130.750.000	–	–
Total Investment plan costs	€ 292.080.000	€ 83.700.000	€ 235.231.483	–	–

Table 18: *Total Costs of Investment Plans*

G.3 Elaboration on Comparison of Investment Plans

This Appendix will go into detail about the adaptive investment plan and a possible way to compare different investment plans based on min-max normalisation.

G.3.1 Worst Case Configuration

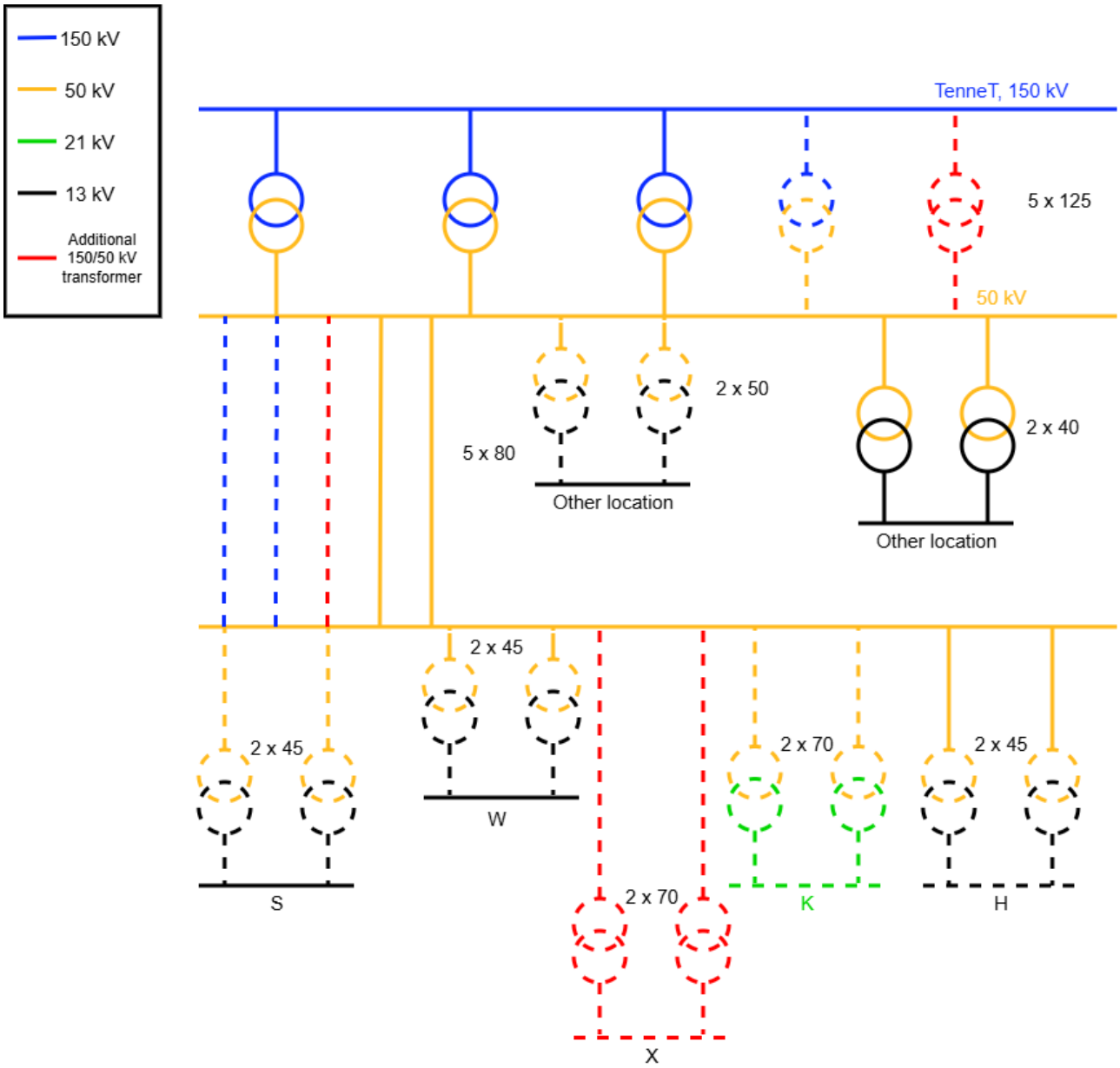

Figure G.35: *Worst Case Investment Plan*

G.3.2 Multi-Criteria Analysis Example

In order to compare the three decision criteria which all have different units, normalised scores are calculated using min-max normalisation as discussed by (De Haan & De Heer, 2015).

$$\mathrm{NS}_{i,j} = \frac{\max(x_j) - x_{i,j}}{\max(x_j) - \min(x_j)}$$

where: $x_{i,j}$ = denotes the value of decision criterion j for investment plan i. Note that since the capacity risks have four rows, the normalised value for each row is multiplied by $\frac{1}{4}$. This is done to prevent capacity risks from dominating the cost decision criterion table. All decision criteria are weighted equally, alternative weighting factors can also be applied if Stedin were to favour one decision criterion over the other. For this thesis however, this qualitative discussion is out of scope.

Decision Criteria \ Plans		**Worst case**	**Candidate Investment Plan**	**Adaptive Investment Plan**
Cap. Risks (ST)	**S**	0%	6%	1%
	W	0%	66%	0%*
	H	0%	13%	0%
	K	0%	0	0%
	NS	*1.00*	*0.25*	*0.94*
Cap. Risks (LT)	**S**	0%	83%	18%
	W	0%	38%	6%
	H	0%	83%	0%
	K	0%	22%	4%
	NS	*1.00*	*0.00*	*0.86*
Total Costs		€292.080.000	€83.700.000	€235.231.483
NS total costs		*0*	*1*	*0.27*
$\sum$NS scores		*2.00*	*1.25*	*2.07*
Unsupported scenarios		All scenarios can be supported	Scenarios with medium-to-fast heating transition in residential houses, medium-to-fast electric mobility, large datacenter scenarios, scenarios with a residential housing focus and scenarios with high electrification of the industry	Most scenarios can be supported. The remaining unsupported scenarios likely share the same key drivers of capacity risks as the candidate investment plan. However, these drivers are not fully captured by the current set of adaptive measures

Table 19: *Decision table with multiple criteria per investment plan MCA*

The results show that the adaptive investment plan has the highest sum of normalised scores. This indicates that this investment plan best satisfies Stedin's objectives under deep uncertainty. It substantially reduces both short and long-term capacity risks while also avoiding overinvestment like in the worst case investment plan. Although the difference between both investment options in terms of normalised score is relatively small, the adaptive plan implements only when triggered by scenario specific conditions. The categorical structure of the uncertainty space leads to some adaptive measures being implemented more frequently then strictly necessary. For instance, although only 22% of scenarios cause capacity risks at substation K in 2052, the construction of substation X is triggered in one-third of all scenarios. As a result, the costs for adaptive plan B are significantly higher than strictly necessary, subsequently decreasing the normalised score for total costs. Thus, the difference between worst case and adaptive investment plan seems small but can in fact be a larger difference. Despite this limitation, the adaptive plan still outperforms the other investment plans.

H Pseudo-Code of Adaptive Measures

This appendix provides the pseudocode for the adaptive measures within the second iteration of the simulation model. The adaptive measures are created using the insights of the PRIM analysis and the subsequent storylines per substation. The adaptive rules evaluate each scenarios categorical input and determine whether the scenario satisfies the if-statement conditions. When a scenario meets the conditions, the adaptive measure is implemented in the scenario run.
It is important to note that the implementation of the adaptive measures occur instantaneously

once the relevant year-threshold is reached. Given that capacity risks generally show themselves from 2040 onwards across nearly all scenarios, this year is used as a trigger point for the adaptive rule to be implemented. The sole exception being the heat_transition_value which is a short term adaptive measure for substation W.

```
# Rules for reallocating industrial ring S to substation K

if ev_growth in {A, B, C} and lifespan_hybrid == A:
    reallocate industrial ring S to substation K (year = 2040)
    industry_S_reallocated = True

if mix_distribution == B and lifespan_hybrid in {A, B}:
    reallocate industrial ring S to substation K (year = 2040)
    industry_S_reallocated = True

if ev_growth in {A, B} and lifespan_hybrid in {A, B} and mix_distribution in {A, C}:
    reallocate industrial ring S to substation K (year = 2040)
    industry_S_reallocated = True

if vehicle_growth in {A, B, C} and mix_distribution in {A, B, C} and new_industry_mix == A:
    reallocate industrial ring S to substation K (year = 2040)
    industry_S_reallocated = True


# Rules for reallocating industrial ring W to substation K

if heat_transition in {A, B}:
    reallocate industrial ring W to substation K (year = 2034)
    industry_W_reallocated = True

if vehicle_growth in {A, B, C} and ev_growth in {A, B}
   and mix_distribution == B and lifespan_hybrid in {A, B}:
    reallocate industrial ring W to substation K (year = 2040)
    industry_W_reallocated = True

if vehicle_growth in {A, B, C} and ev_growth == A and new_industry_mix == A
   and ev_mix in {B, C} and mix_distribution in {A, C}:
    reallocate industrial ring W to substation K (year = 2040)
    industry_W_reallocated = True


# Rule for building Substation X (high datacenter growth pathway)

if data_center_growth == A and data_center_PUE in {A, B, C}:
    substation X is built and takes over half of the electricity loads of K (year = 2042)
    substation_X = True
```

Four independent rules trigger the reallocation of the industrial ring of substation S. Each of these triggers is derived from the ATPs identified through PRIM. For example, PRIM shows that riksy days occur when EV growth lies between 0.47 and 0.8 and the lifespan of HHP is 10 years. When mapped back to the categorical input space, these conditions correspond to uncertainty parameters A and B for EV growth and parameter value A for lifespan of HHPs. Although one point for uncertainty parameter C (in 2052) overlaps with the ATP range, this uncertainty parameter is excluded from the adaptive rule because it spans a substantially lower

numerical range for all other years apart from 2052. The next simulated year 2046, shows the lifespan HHPs of 10 years again being an important driver of risky days. However, an independent rule has not been made for this uncertainty since it already coincides with a lot of other uncertainties.

Similarly, the 2049 PRIM results of substation S identify an eHP share of 30% to 40% (A) combined with an HHP lifespan of 10 to 15 years (A and B) leads to capacity risks. Altough these ATPs are achieved in 2049, the adaptive measure is applied in 2040. This year represents the earliest consistent onset of risky days across all substation, apart from the short term peak on substation W, making it an anticipatory trigger year. Implementing the measures at the earliest warning threshold aligns with the DAPP logic of intervening before system failure (capacity risks).

The same anticipatory reasoning applies to substation W. Although PRIM identifies four long-term key drivers in 2049, scenarios that cause risky days already emerge in 2040. Next to this, substation W has one short-term key driver of heat transition 50% to 80%, which maps mainly with uncertainty parameter values A and B. Uncertainty value C represents a slower transition and includes more values outside the PRIM identified range than within it. Therefore, uncertainty parameters A and B are used as trigger for reallocating the industrial ring of W. While short term measures of gas and diesel generators are assumed to always take effect, the year 2034 is used as an activation trigger for scenarios with medium to high heat transition values.

The above described choices ensure that ATPs derived from the PRIM analysis are translated to actionable measures for Stedin to use. While other configurations of adaptive measures are thinkable, the eight adaptive rules cover almost all PRIM derived ATPs.